**Analytical Methods for the Study of Opioid Peptides**

By

Abdullah M. Al-Hossaini

Submitted to the graduate degree program in Pharmaceutical Chemistry and the Graduate Faculty of the University of Kansas in partial fulfillment of the requirements for the degree of Doctor of Philosophy.

_____

Chair: Dr. Susan M. Lunte

_____

Dr. John F. Stobaugh

_____

Dr. Teruna J. Siahaan

_____

Dr. Michael Zhuo Wang

_____

Dr. Krzysztof Kuczera

Date Defended: 18 August 2017

The Dissertation Committee for Abdullah M. Al-Hossaini
certifies that this is the approved version of the following dissertation:

**Analytical Methods for the Study of Opioid Peptides**

_____

Chair: Dr. Susan M. Lunte

Date Approved: 18 August 2017

**Analytical Methods for the Study of Opioid Peptides**

Abdullah M. Al-Hossaini

The University of Kansas, 2017

Abstract

Dynorphin A 1-17 [Tyr-Gly-Gly-Phe-Leu-Arg-Arg-Ile-Arg-Pro-Lys-Leu-Lys-Trp-Asp-Asn-Gln] is an endogenous opioid peptide. It is widely distributed in blood and CNS tissue and exhibits a high affinity to the kappa (κ) opioid receptors and binds with less affinity to both delta (δ) and mu (μ) opioid receptors. This peptide has been found to show both antinociceptive and analgesic effects within the central nervous system. Dyn A is also involved in the body's immune response, in addition to control of heart rate, blood pressure, body temperature and feeding behavior. However, upregulation of Dyn A due to disease states has been shown to cause nonopioid activity such as hyperalgesia, allodynia, and excitotoxicity. In addition, altered levels of the neuropeptide have been linked to neurological disorders, including Alzheimer's and Parkinson's disease. Capillary electrophoresis is a powerful technique that can achieve high-efficiency separations of charged analytes. However, CE has limited use for the analysis of basic proteins and peptides, due to their adsorption onto the inner surface of the fused silica at pHs below their pI. This adsorption can lead to a loss of efficiency, irreproducibility of migration times, and peak tailing. This thesis describes the separation of dynorphin A 1-17 and its key metabolites using fused silica capillaries coated with positively charged polydiallyldimethylammonium chloride (pDDA) and pDDA stabilized gold nanoparticles modified capillaries. The coating material minimized unwanted adsorption of the positively charged peptides onto the surface of the fused-silica capillary.

The studies with capillary electrophoresis were performed using UV detection at 214 nm. However, the detection limits are too high to determine endogenous concentrations of these bioactive peptides in brain microdialysis samples. To improve the detection limits, while still maintaining small sample volume requirements, the development of glass and glass/polydimethylsiloxane microchip electrophoresis (ME) system with fluorescence detection is described. Several fluorescence tags were evaluated including the fluorescent probe, fluorescein isothiocyanate, and the fluorogenic probe, naphthalene-2,3-dicarboxaldehyde with sodium cyanide, which produces a fluorescent 1-cyanobenz[f]isoindole (CBI) derivative. The ME-LIF system was shown to separate CBI-peptides of derivatized fragments of dynorphin A.

## Acknowledgements

I must express my sincere gratitude to my Ph.D. advisor Professor Susan M. Lunte for her guidance, motivation, and patience through my Ph.D. graduate study. Even with your busy schedule you always try to find time to meet and discuss my research, always encourage me to give talks and posters to present my work both on and off campus. Professor Lunte, you have been an incredible mentor for me, and I cannot imagine having a better advisor for my Ph.D. graduate work. I am extremely thankful for all you have done.

I would also like to thank my committee members Dr. John F. Stobaugh, Dr. Teruna J Siahaan, and Dr. Michael Zhuo Wang and Dr. Krzysztof Kuczera for their valuable suggestions to my thesis.

I want to thank Dr. Siahaan again, for allowing me to perform my experiments in his lab and for his helpful comments and recommendations.

Thank also to Dr. Siahaan lab group members especially Paul Kiptoo for his help with animal experiments. I must also thank the members of the Susan Lunte groups that I had the pleasure of working with for the past six years. I am especially thankful for the present lab members Manjula Wijesinghe and Shamal Gunawardhana who taught me how to make and run PDMS microchips. Thanks to Nate Oborny for showing me the best way to make a glass microchip, and also, I want to thank Dr. Rachel Saylor with reading my abstracts over the years and Dr. Leena Suntornsuk, a visiting scientist in our lab for her suggestions.

Finally, I need to thank my parents and all my family members for their encouragement and support over the years.

## Table of Contents

# Chapter 1

## Thesis Objective and Chapter Summaries

## 1.1 Introduction

The endogenous opioid peptide dynorphin A (Dyn A) is a 17-amino acid polypeptide [Tyr - Gly - Gly - Phe - Leu - Arg - Arg - Ile - Arg - Pro - Lys - Leu - Lys - Trp - Asp - Asn - Gln]. The peptide was first isolated from porcine pituitary by Goldstein and co-workers[1]. It is widely distributed in blood and CNS tissue and exhibits a high affinity to the kappa (κ) opioid receptors. It also binds with less affinity to both delta (δ) and mu (μ) opioid receptors. Dyn A has been reported to show both antinociceptive and analgesic effects within the CNS. It is involved in the body's immune response as well as control of heart rate, blood pressure, body temperature and feeding behavior. However, upregulation of Dyn A due to pathophysiological states has been shown to cause nonopioid activity such as hyperalgesia, allodynia, and excitotoxicity. In addition, altered levels of the neuropeptide have been linked to neurological disorders, including Alzheimer's and Parkinson's disease.

This thesis explores the use of various electrophoresis separation methods, mainly capillary electrochromatography and microchip electrophoresis, for the separation of Dyn A (1-17) and its metabolites.

## 1.2 Chapter summaries

### 1.2.1 Chapter two

This chapter provides an overview of the classification of opioid peptides and their receptors. It also provides a more detailed look at the CNS distribution of the opioid peptide Dyn A and its metabolism. In addition, this chapter provides a general summary of some of the

pharmacological effects of Dyn A and a description of reported pathophysiological effects that are caused by abnormal levels of the neuropeptide.

A review of some of the different analytical methods that have been reported for the separation and detection of Dyn A and its metabolites are also provided in this chapter, including liquid chromatography, micellar electrokinetic chromatography (MEKC) aqueous capillary electrophoresis (CE) and nonaqueous CE, that are coupled with different detection methods such as ultraviolet (UV), fluorescence and mass spectrometry (MS).

### 1.2.2 Chapter three

Chapter three is a review of approaches and strategies reported for the separation of protein and peptides by CE, microchip electrophoresis and capillary electrochromatography (CEC). The primary focus of the chapter is on the theory, classification, and materials used for CEC separation and applications of these techniques to protein and peptides, to improve both resolution and efficiency of protein and peptides analysis.

### 1.2.3 Chapter four

This chapter describes the development of a polydiallyldimethylammonium chloride-stabilized gold nanoparticle-coated (pDDA-GNPs) capillary for an electrochromatography based separation of the basic peptide Dyn A (1-17) and seven of its fragments. The pDDA-GNPs coated capillary was used to minimize undesirable adsorption of positively charged peptides onto the surface of ionized fused-silica capillary. A range of CEC separation parameters including capillary

length, applied electric field strength and concentration of background electrolyte were evaluated for the peptide separation of fragments of Dyn A. Finally, the CEC pDDA-GNPs coated capillary was applied for separation of tryptic peptide fragments of dynorphin A 1-17.

### 1.2.4 Chapter five

Dynorphin A and its metabolites are found at very low concentrations. CE-UV can be used to provide quantitive data for higher concentration samples of these opioid peptides. However, in order to achieve the limits of detection necessary for the detection of dynorphin and its metabolites in microdialysis samples, a more sensitive method, such as fluorescence, must be employed. Therefore the compounds were derivatized with naphthalene-2,3-dicarboxaldehyde and sodium cyanide to produce fluorescent 1-cyanobenzoic[f]isoindole derivatives. The products were separated and detected by CEC and ME with laser-induced fluorescent detection (LIF). Chapter five provides the results of the development of a capillary and microchip LIF system for the separation of dynorphins.

### 1.2.5 Chapter six

This chapter summarizes the research presented in this thesis, and provides a discussion of future directions for the determination of dynorphin A and other neuropeptides in biological samples as potential disease biomarkers.

### 1.2.6 Appendix

The appendix provides the result of *in situ* perfusion studies that were carried out on Sprague Dawley® rats for investigating the activity of Dyn A(1-6) on the blood brain barrier. It was previously observed that this peptide increased the permeability of the BBB using a cell culture model. In these studies, the effect of Dyn (1-6) on the permeability of $^{14}$C-mannitol at the blood-brain barriers (BBB) *in situ* was investigated. The *in situ* perfusion was used to compare the effect of opioid peptide Dyn A(1-6) to control, and to that of a scrambled peptide (GLYRFG). A hypothesis for the activity of Dyn A(1-6) for changes in BBB permeability is also provided.

## 1.3 References

1. Goldstein, A.; Fischli, W.; Lowney, L. I.; Hunkapiller, M.; Hood, L., Porcine pituitary dynorphin: complete amino acid sequence of the biologically active heptadecapeptide. Proc. Natl. Acad. Sci. U. S. A. 1981, 78 (11), 7219-23.

# Chapter 2

# The Endogenous Opioid Peptide Dynorphin A

## 2.1 Introduction

The opioid system is composed of several peptides and various types of receptors. Both opioid peptides and their receptors are widely distributed in the central (CNS) and peripheral nervous systems (PNS)[1-2]. They act as neurotransmitters and neuromodulators[3]. They also regulate main physiological states that include cardiovascular [4] and endocrine balance[5].

### 2.1.1 Opioid peptide

Opioid peptides are formed by proteolytic cleavage of three protein precursors. The protein proopiomelanocortin (POMC) is the precursor of β-endorphin, preproenkephalin (PENK) is the precursor of Met-enkephalin (Met-ENK) and Leu-enkephalin (Leu-ENK), and preprodynorphin (PDYN) is the precursor of dynorphin A, dynorphin B and neoendorphin[6] [Figure 1]. Opioid peptides range in length from 5-31 amino acids. They share a common N-terminal tetrapeptide sequence of Tyr-Gly-Gly-Phe that is essential for binding to the opioid receptor's "message domain". However, these peptides differ in the C-terminal residues or "address domain" [Figure 2]. This effects the affinity of these peptides to the opioid receptor and their subtypes[7]. For example, the neuropeptide, nociceptin, (orphanin FQ) is produced from the precursor pronocicptin (PNOC) and lacks the N-terminal Tyr. Thus, it has a very low affinity to opioid receptors and acts on a different receptor[8]. Opioid peptides, such as enkephalins and dynorphins, are found in various regions of the brain such as the hypothalamus, posterior pituitary, striatum, substantia nigra, hippocampus, and amygdala[9]. Dynorphins, in addition to being in the brain, are also present in high amounts in the interneurons of the spinal cord[10-11]. Opioid peptides are also produced in nonneuronal cells, such as the immune and endocrine cells[12]. Endogenous opioid peptides help

regulate (balance) the body's homeostasis, by acting as neurotransmitters and hormones, as they influence several physiological and pathological states.

### 2.1.2. Opioid receptors

The family of opioid receptors includes the μ, δ, and κ receptors. These are all considered part of what is known as the "classical" opioid receptors, based on the classification of the antagonist effect of naloxone on opioid receptors. Nociceptin receptors (NOR) show activity to nociceptin and are classified as a non-opioid member of the opioid receptors family. This classification is based on the shared structural similarities and location of NOR to the classical opioid receptors but the difference in the activity of naloxone to the NOR (inactive)[13]. Subtypes of classical opioid receptors have been identified based on their pharmacological response; this includes the $\mu_1$, $\mu_2$ and $\mu_3$ for μ opioid receptors, $\delta_1$ and $\delta_2$ for δ opioid receptors, and $\kappa_{1a}$, $\kappa_{1b}$, $\kappa_{2a}$, $\kappa_{2b}$, $\kappa_3$ for the κ opioid receptors [13-14].

The opioid receptors μ, δ, and κ all belong to a family of receptors called the G-protein-coupled receptors (GPCR) that are also known as the seven-transmembrane domain receptors. All three types of opioid receptors share high structural similarities, mainly at the transmembrane domains 2, 3, 7 and the 1st and 2nd intracellular loops of the GPCR[15]. This explains the ligand selectivity and high affinity to one type of opioid receptors and lower affinity to other types of opioid receptors. Ligands of the GPCR cause activation of the GPCR via coupling with $G_i/G_o$ proteins of receptors and which activation leads to inhibition of adenyl cyclase (AC), thereby reducing production of cyclic adenosine monophosphate (cAMP). This reduces calcium ion influx by inhibiting voltage-gated calcium channels and activation of potassium channels via

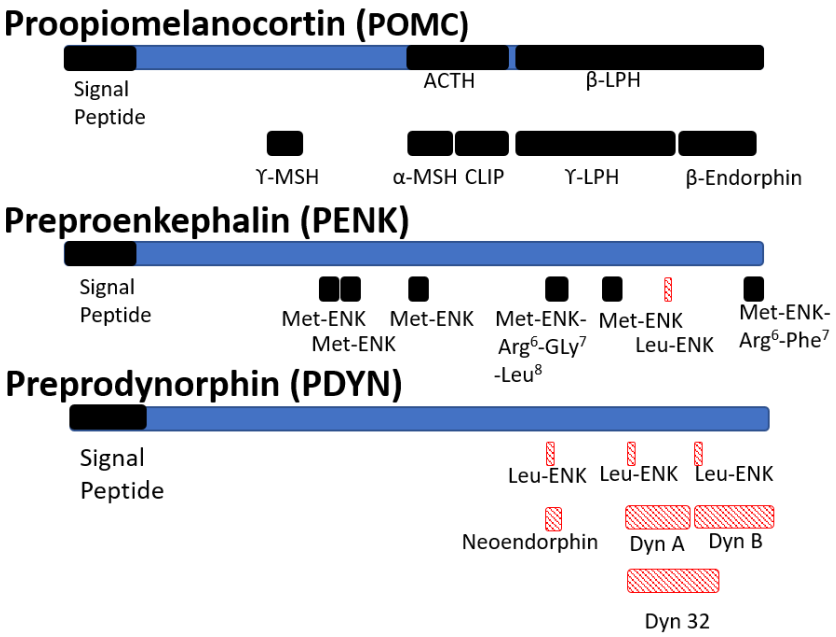


**Figure 1:** The opioid peptide precursors. Dyn: dynorphin, ENK: enkephalin.

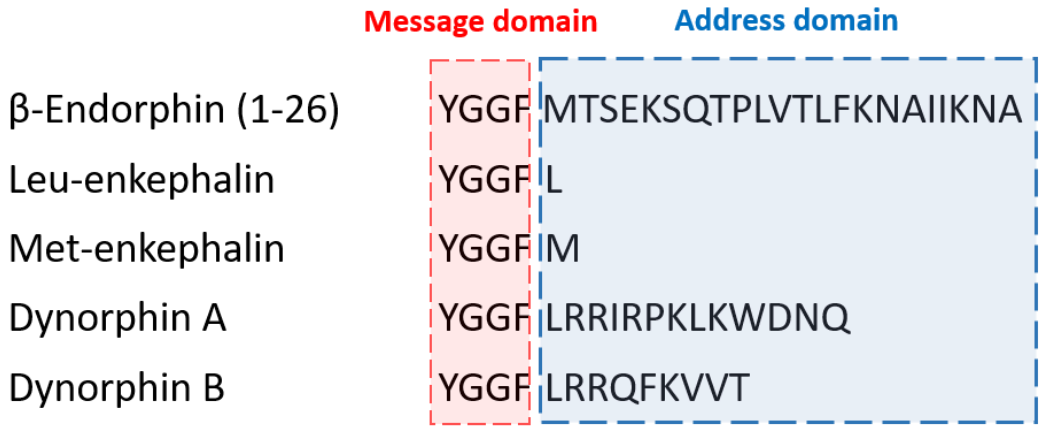


**Figure 2:** Amino acid sequences of message and address domains of different opioid peptides.

G protein-coupled inwardly-rectifying potassium channels (GIRK)[16] causing efflux of potassium ions. This induces membrane hyperpolarization of the neurons causing inhibition of neuronal release of excitatory neurotransmitter [Figure 3][17-18]. Table 1 shows a summary of the opioid receptors μ, δ, κ and NOR and their ligands.

| | μ | δ | κ | NOR |
|---|---|---|---|---|
| Nomenclature | MOR, MOP, $OP_3$ | DOR, DOP, $OP_1$ | KOR, KOP, $OP_2$ | $ORL_1$, $OP_4$ |
| Endogenous ligand | β-endorphin, endomorphin-1, endomorphin-2 [19] | Leu-enkephalin, Met-enkephalin | Dynorphin A | Nociceptin |
| Selective antagonist | CTAP, CTOP[20] | Naltrindole[21] | Nor-BNI [22] | LY2940094[23] |
| Antagonist effect of naloxone | Antagonist | Antagonist | Antagonist | Inactive |

**Table 1:** Summary of differences of opioid receptors and ligands. [CTAP: $^{D}$Phe-Cys-Tyr-$^{D}$Trp-Arg-Thr-Pen-Thr-$NH_2$, CTOP: $^{D}$Phe-Cys-Tyr-$^{D}$Trp-Orn-Thr-Pen-Thr-$NH_2$, nor-BNI: nor-binaltorphimine].

## 2.2 Dynorphin A

The opioid peptide dynorphin (Dyn) was named based on the prefix "Dyn" from the Greek word dynamic (power) and the suffix "orphin" indicating its opioid nature[24]. It was first isolated from the porcine pituitary in 1975[25]. After its discovery, further studies have shown that Dyn is widely distributed within the CNS, with the highest concentrations of the neuropeptide found the posterior lobe of the pituitary. This is followed by the hypothalamus then striatum, then midbrain,

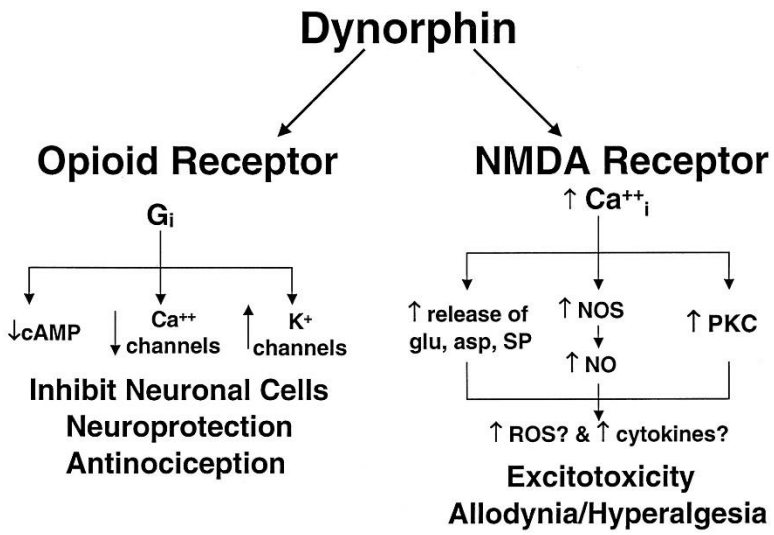


**Figure 3:** Effect of the opioid peptide on neuronal cells by acting on GPCR and NMDA receptors [PKC: protein kinase C, SP: substance P, ROS: reactive oxygen species].[26] *(Reprinted with permission)*

hippocampus, medulla-pons and spinal cord followed by cortex and then the cerebellum[27]. Dyn A (1-17) is composed of 17 amino acid residues Tyr[1]-Gly[2]-Gly[3]-Phe[4]-Leu[5]-Arg[6]-Arg[7]-Ile[8]-Arg[9]-Pro[10]-Lys[11]-Leu[12]-Lys[13]-Trp[14]-Asp[15]-Asn[16]-Gln[17]. The neuropeptide has the highest affinity to the κ opioid receptor and shows lower affinity to the δ, and a lesser extent to the μ receptors[28]. The primary structure of Dyn can be divided into two domains. The first is the messenger domain that corresponds to the N-terminal tetrapeptide of Dyn ($Y^1G^2G^3F^4$). These four amino acid residues are essential for binding to the opioid receptors. The second domain is the address domain that corresponds to the C-terminal[29]. The address domain affects the selectivity of the peptide to the κ opioid receptor.

The structural extension of the neuropeptide sequence Leu-ENK YGGFL[5] ($K_i$ μ:6.9 nM, δ:0.37 nM, κ: 93.65 nM) with the addition of an Arg residue YGGFLR[6], leads to a 30 fold increase in affinity to the κ receptors ($K_i$ κ: 2.88 nM) and a decrease in affinity to the δ opioid receptors ($K_i$ δ: 1.04 nM) compared to Leu-ENK[30]. Addition of another Arg residue at position seven has been reported to show a 14-fold further enhancement of the affinity of the Dyn peptides to the κ receptor ($K_i$ κ: 0.21 nM)[30-31]. Further structural extension of the C-terminal of the Dyn peptide did not distinctly improve affinity or selectivity to the κ receptors. Although longer chain fragments of the Dyn peptides such Dyn A (1-13) ($K_i$ κ: 0.23 nM) and Dyn A (1-17) ($K_i$ κ: 0.37 nM) provide extended activity, this may be due to the longer peptide chain show longer stability [30-32]. Table 2 shows the *in vitro* experimental $K_i$ values to the opioid receptors (μ, δ, and κ) of various ligands. Aside from opioid receptors, Dyns and their fragments have been reported to bind to non-opioid receptors such as orphanin receptors, the N-methyl-D-aspartate (NMDA) receptors, and the melanocortin receptors[33].

| | Opioid receptor (Ki values) | | |
|---|---|---|---|
| | μ (nM) | δ (nM) | κ (nM) |
| Leu-ENK | 6.19 | 0.37 | 93.65 |
| Met-ENK | 1.8 | 0.45 | 47.44 |
| Dyn A (1-6) | 1.88 | 1.04 | 2.88 |
| Dyn A (1-7) | 1.80 | 2.71 | 0.21 |
| Dyn A (1-8) | 2.56 | 1.17 | 0.45 |
| Dyn A (1-9) | 2.62 | 1.47 | 0.13 |
| Dyn A (1-13) | 4.14 | 5.56 | 0.23 |
| Dyn A (1-17) | 2.64 | 1.29 | 0.37 |
| Dyn A (1-32) | 6.87 | 3.34 | 3.08 |
| β-Endorphin (1-27) | 5.31 | 6.17 | 39.82 |
| β-Endorphin (1-31) | 3.37 | 5.02 | 32.70 |
| Morphine | 7.48 | 302.15 | 52.65 |
| Naloxone | 0.92 | 18.76 | 2.09 |

**Table 2:** Ligands and opioid receptors Ki values. Table from Mansour et. al [30]

### 2.2.1 Dynorphin metabolism

Dyn A can undergo metabolism by various proteolytic enzymes in the brain, spinal cord, cerebrospinal fluid (CSF) and blood. Enzymatic cleavage of Dyn A and its fragments can produce metabolites that can also be active at opioid receptors or produce fragments that may not bind to

the opioid receptors but may bind to various other types of receptors within the body. Aminopeptidase is known to cleave the N-terminal Tyr group of Dyn, producing a des-tyrosyl fragment that shows a low affinity for the opioid receptors, but shows a high affinity to other receptors (mainly the NMDA receptor). C-terminal enzymatic cleavage of the peptide amino acid chain by carboxypeptidase has also been shown in both blood and CSF[34-35]. Other enzymes that have been reported to act on Dyn A by cleaving peptide bond at different regions of the peptide chain include angiotensin converting enzyme ($Phe^4$-$Leu^5$), dynorphin A-processing enzyme ($Arg^6$-$Arg^7$ and $Ile^8$-$Arg^9$)[36], and finally, dynorphin A-converting enzyme that has been described to convert Dyn A(1-17) to dynorphin A(1-6) and Leu-ENK in the human spinal cord[37].

*In vitro* studies on the metabolism of the dynorphin A (1-13) in blood have shown that the peptide has an extremely short half-life ($t_{1/2}$) of less than 1 minute[34, 38] compared that of Dyn A (1-17), with a $t_{1/2}$ of approximately 180 minutes[35]. The longer stability of Dyn A (1-17) is believed to be due to the C-terminal amino acid residues that protect the peptide from enzymatic degradation.

Chou et.al.[35] investigated the biotransformation of both Dyn A(1-17) and Dyn A(1-13) in human blood using matrix-assisted laser desorption/ionization (MALDI) mass spectrometry (MS). The peptides were incubated in a human blood, and at various time points, small portions of the sample mixture were collected and analyzed. Chou reported major metabolites of Dyn A (1-17) in blood include Dyn A (2-17), Dyn A (7-17), Dyn A (8-17) and Dyn A (9-17). The major metabolites of Dyn A (1-13) include Dyn A (1-12) and Dyn A (2-12) and Dyn A (4-12). Table 3 presents a summary of some of the enzymes that have been reported for the metabolism of Dyn A.

| Primary Dyn fragment observed | Enzyme | Cleavage site | Reference |
|---|---|---|---|
| Dyn A (2-17)<br>Dyn A (2-12) | Aminopeptidase M | $Tyr^{1}$-$Gly^{2}$ | [39]<br>[34] |
| Dyn A (1-12) | Carboxypeptidase | $Leu^{12}$-$Lys^{13}$ | [34-35] |
| Dyn A (1-6) | Dynorphin converting enzymes | $Arg^{6}$-$Arg^{7}$ | [37] |
| Dyn A (1-10) | Angiotensin converting enzyme | $Pro^{10}$-$Lys^{11}$ | [38] |
| Dyn A (1-8) | Dynorphin processing enzymes | $Ile^{8}$-$Arg^{9}$ | [36] |
| Dyn A (1-4) | Angiotensin converting enzyme | $Phe^{4}$-$Leu^{5}$ | [34] |
| Dyn A (1-8) | Carboxypeptidase E | $Ile^{8}$-$Arg^{9}$ | [40] |

**Table 3**: Summary of produced fragments of Dyn A by enzymatic cleavage.

### 2.2.2 Pharmacological effects of dynorphin

The pharmacological effects of Dyn and its metabolites are not fully understood. This could be due low endogenous levels and the rapid metabolism of the neuropeptides by a wide range of enzymes in the CNS and plasma[34]. Besides its effect on the nervous system, several of these peptides have been found to serve multiple regulatory functions such as cardiovascular regulation, temperature regulation, and hormonal balance.

#### 2.2.2.1 Analgesic effects

Similar to the classic example of an opioid receptor agonist, animals studies have shown the analgesic property of Dyn [41-42]. Several research groups have reported that low-dose intrathecal injections (IT) of Dyn A (1-13) in human cancer patients as well as rat and mice models, produced

an analgesic effect with a potency effect similar to morphine[42-45]. However, high doses of Dyn given IT to rats have been shown to produce neurotoxic effects that include hindlimb paralysis and enhanced sensitivity to sensory stimuli[46-48]. The neurotoxic effects are suggested to be due to the non-opioid activity at other receptors, since the same adverse effects occur with an IT injection of Dyn derivatives that lack the N-terminus Tyr residue. Nerve injury and peripheral inflammation have been found to lead to an upregulation of spinal Dyn A production and are associated with chronic neuropathic pain[11]. The effect of Dyn in the brain has been reported to be opposite to that in the spinal cord. Intracerebroventricular injection (icv) of Dyn in the brain of mammalian animal models has produced no analgesic effect.

#### 2.2.2.2. Interaction of dynorphin with nonopioid receptors

Several research articles have reported that under physiological concentrations, dynorphin binds with high affinity to the κ opioid receptors. However high levels of Dyn production due to pathophysiological states, such as trauma or spinal injuries, cause the peptide to act on nonopioid receptors such as NMDA and AMPA leading to neurotoxic effects[49]. Hauser et.al [50] performed *in vitro* toxicity studies of fragments of Dyn A by looking at their interaction with expressed κ opioid and NMDA receptors on mouse spinal cord neurons. They found that concentrations of Dyn of 1mM or greater led to significant neuronal loss. Neuronal loss was also reported for dynorphin fragments. Dyn A (1-17) was found to be the most toxic, this was followed by Dyn A(1-13), and then Dyn A(2-13) and Dyn A(13-17). In contrast, Dyn A (1-11) and Leu-ENK were found not to cause neuronal death. The toxic effects of the Dyn neuropeptides is believed to be mediated by NMDA receptors[51].

#### 2.2.2.3 Cardiovascular effects

The effect of the Dyn A on both blood pressure and heart rate has been investigated by several research groups[52-54]. The effect is seen in both the CNS and PNS, and affects both opioid and nonopioid receptors[32, 55]. Studies have shown that the effect of the neuropeptides on the cardiovascular system (CVS) appear to depend on the site of administration and the state of consciousness of the animal model studied. Injections of Dyn A into specific regions of the brain in anesthetized rats was reported to cause both hypotension and bradycardia. These effects were blocked by the naloxone, indicating that the activity of Dyn is mediated by opioid receptors[27, 52]. Stimulation of opioid receptors at the presynaptic nerve terminal could lead to inhibition of norepinephrine release and cause the observed CVS effects. However, with the IV administration of Dyn to awake animals, this has been reported to induced a hypertensives effect, due to stimulation of the nonopioid receptors, that can cause a blockade of norepinephrine reuptake[27, 32, 56].

#### 2.2.2.4 Temperature and hormonal effects

Dyn has been found to cause a small hyperthermic effect when administered alone. However, when it was administered after an IV injection of morphine, the Dyn was found to potentiate the hypothermic effect of morphine[57]. The concentrations of the Dyn within different regions of the brain was found to be altered by body temperature. Morley et.al. [58] found lower levels of Dyn in the hypothalamus of rats that were subjected to a two-hour exposure to a temperature of 4°C. Thus suggesting that the peptide has a neuromodulatory effect, by acting as a feedback system for controlling body temperature[57].

Dyn has been reported to affect the level of several hormones, such as prolactin[59-60] and luteinizing hormone[61]. It has also been reported to suppress the release of oxytocin in lactating rats[62].

### 2.2.3 Dynorphin and neurodegenerative disorders

At normal concentrations in the body, Dyn is involved in multiple regulatory functions. However, abnormal levels of the neuropeptide are believed to be linked to various neurological disorders. Dyn is thought to be related to the pathology of Alzheimer disease. In rodents, it was found that Dyn production is upregulated with age, and the neuropeptide induces neurodegeneration and cognitive impairment[63]. Postmortem brain samples of human patients that have shown symptoms of Alzheimer disease, exhibit elevated Dyn levels[64]. It is proposed that one of the contributions to the disease may be elevated levels of Dyn acting through nonopioid receptors[64].

### 2.2.4 Dynorphin effect on the reward pathway

It has been reported that the administration of drugs of abuse (e.g. cocaine), leads to an increase in dopamine levels in the brain. The κ opioid receptors can be found in the presynaptic terminal of the synapses of the mesolimbic dopamine neurons [65-66]. The activation of the κ opioid receptors by Dyn or synthetic agonists such as U-69593 and bremazocine can inhibit dopamine release in the striatum[67]. In contrast, the κ opioid receptors antagonists such as nor-binaltorphimine (nor-BNI) cause stimulation of dopamine release[68]. Chronic administration of drugs of abuse can lead to upregulation of Dyn production in the brain, were the neuropeptide has a neuroprotective

effect from drug-induced high levels of dopamine[69]. Zang et.al. [70] investigated the effect of Dyn A(1-17) on the cocaine-induced increase in dopamine levels in the caudate putamen of mice. They were able to show that there was a decrease in dopamine levels when Dyn A(1-17) was directly infused into the caudate-putamen in the animal. They also showed that pre-injection of mice with nor-BNI blocked the effect of Dyn and increased dopamine levels. These results supported the hypothesis that the activation of the κ opioid receptors can modulate the effect of cocaine.

### 2.3. Analytical methods for determination of dynorphin

#### 2.3.1 Chromatographic methods

##### 2.3.1.1 Liquid chromatography (LC) with ultraviolet absorbance detection

One of the oldest articles describing the use LC for analysis and separation of Dyn A(1-17) was by Seyfried and Tobler[71]. They developed a chromatographic method for the separation of some of the N- and C-terminal fragments of Dyn A(1-17) produced by the incubation with homogenized striatum and spinal cord of Wistar rats. The LC methods involve the use of a C-8 column with 5µm particles (25 cm × 4.66 mm i.d.). Samples were analyzed with one of the following two gradients. Gradient elution method I ( phase A: 60% acetonitrile): t = 0−21 min (0−34% B), then t = 21−31 min (34% B), and finally t= 31−60 min (100% B). Gradient method II was performed for higher resolution of short non-Tyr containing fragments, the following mobile phase gradient was used (gradient elution method II): t = 0−12 min (0 – 22% B), then t = 12−22 min (22% B), and finally t = 22−60 min (100% B). With both methods, the flow rate was constant at 1 mL/min. Ultraviolet (UV) absorbance detection was used to detect the eluted neuropeptides at 210 nm.

### 2.3.1.2 LC with fluorescence detection

Fluorescence detection can provide a more sensitive method for the determination of Dyns and other neuropeptides. Kai, M et.al.[72] reported a pre-column fluorescence derivatization method for selectively derivatized peptides containing tryptophan residue at the N-terminus of the peptide. The N-terminal primary amine of a Trp-containing peptide can react with glyoxal [Figure 4] if the mixture is heated to 100 °C for 30 min. The fluorescent product was detected at an excitation wavelength ($\lambda_{Ex}$) of 275 nm and an emission wavelength ($\lambda_{Em}$) of 465 nm [Figure 5]. One example that shows an application of this derivatization method was the LC analysis of the tryptic digest of Dyn A(1-17). The tryptic digest produced several N- and C-terminus products that can be detected with LC/UV. However, only one peptide fragment (Trp-Asp-Asn-Gln) was detected after sample derivatization with glyoxal by the LC/fluorescent detection system because of the selectivity of the fluorescence reagent for the N-terminus Trp. The chromatographic method used a 5µm particle size TSKgel ODS-80Tm column (15 cm × 4.6 mm i.d.). An isocratic mobile phase that consisted of 60% 20 mM phosphate, 23% acetonitrile and 17% methanol was employed at a flow rate of 0.8 mL/min.

Another LC/fluorescence method was reported for the determination of the concentration of various N-terminal tyrosine peptides including Leu-ENK, Met-ENK, Dyn A(1-6), Tyr-Gly-Gly-Phe and Tyr-Arg. This approach involved pre-column fluorescent derivatization of the N-terminal tyrosine residue with a borate solution (pH 8.5) containing hydroxylamine and cobalt(II) ions. Analytes were separated on a reverse phase 5µm particle size TSKgel ODS-120T (15 cm × 4.6 mm i.d) colum. The gradient elution was from 2-26% of ACN in an aqueous solution of tetrabutylammonium chloride. The fluorescent products (structure unknown) were detected at $\lambda_{Ex}$

of 330 nm and $\lambda_{Em}$ of 440 nm. The method was reported to be both sensitive and selective for the tested peptides, however the estimated yield for fluorescent derivatization of the two neuropeptides Leu-ENK, Met-ENK was 55%. They reported a limit of detection (LOD) of 1.5 pmol based on a signal-to-noise ratio of 2 [73].

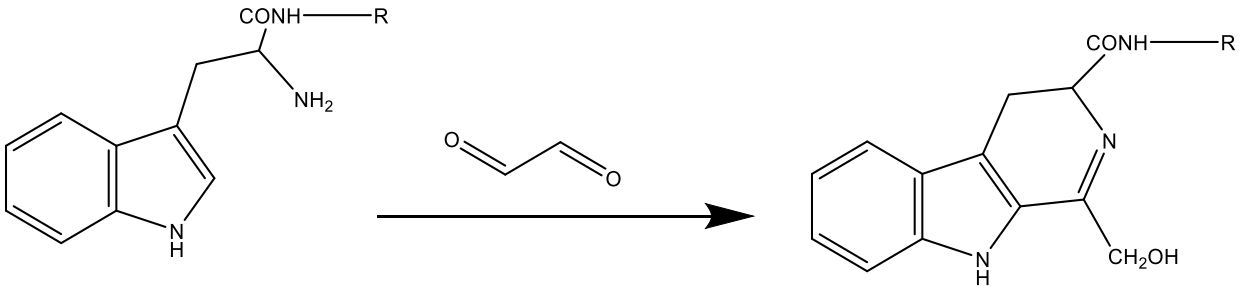


**Figure 4:** The reaction of N-terminal Trp-containing peptide reaction with glyoxal forming fluorophore product.

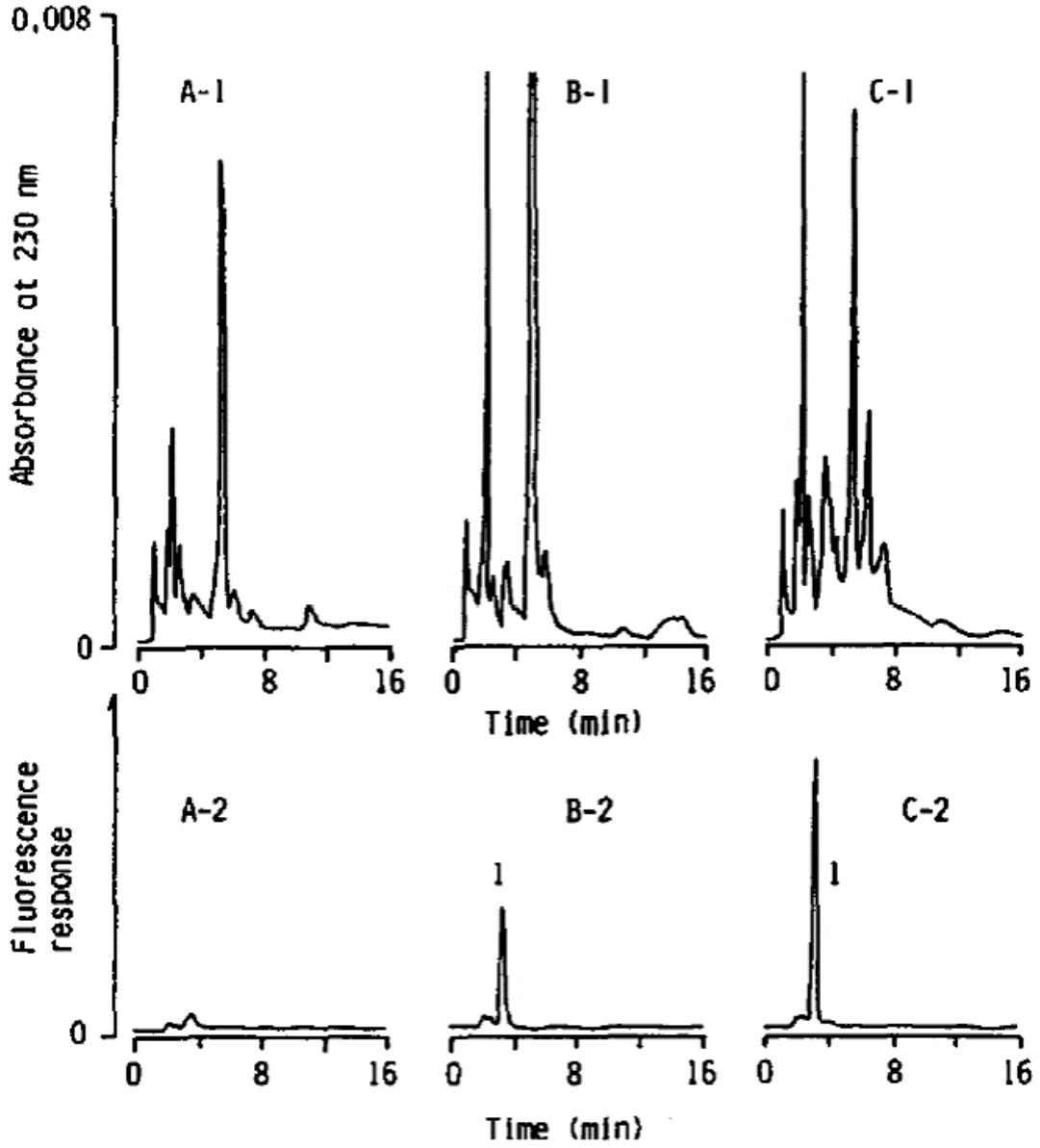


**Figure 5:** LC/UV (TOP) and LC/ Fluorescence detection of the peptide fragments produced by tryptic digestion of dynorphin A. Incubated for (A) 0, (B) 5 and (C) 30 min.[72] *(Reprinted with permission)*

#### 2.3.1.3 LC with radioimmunoassay (RIA)

Quantitation of peptides and proteins by immunoassay methods is a highly specific method. The main principle of RIA assays is a competitive binding between a known amount of a radio-labelled analyte and the unlabelled analyte in the biological sample to a highly specific antibody. This is followed by the separation of the antigen-antibody complex and unbound labeled fraction[74]. One method reported by Müller et.al.[75] combines an LC separation method with radioimmunoassay (RIA) for an analytical method that can be used to determine the three main metabolites of Dyn A(1-13), (Dyn A(2-13), Dyn A(1-12), and Dyn A(2-12)) in blood samples. By combining a chromatographic method with RIA, the research group was able to detect very low concentrations of the neuropeptides. The LOD that was reached was 0.07 ng/mL for Dyn A(1-13), Dyn A(2-13), Dyn A(1-12), and 0.21 ng/mL for Dyn A(2-12). This method was then used for the determination of the concentrations of Dyn A(1-13) and its metabolites in blood samples obtained from two human subjects that received I.V. infusion of either 250 µg or 1000 µg/kg of Dyn A(1-13) over 10 minutes. Compared to *in vitro* samples, the *in vivo* human blood samples showed a more rapid metabolism of Dyn A(1-13) and a shorter $t_{1/2}$ than what was estimated from previously performed *in vitro* experiments by the same research group. This may be due to the involvement of blood vessels and other organs in the clearance of the neuropeptides. Although, RIA is a sensitive and selective method for the analysis of proteins and peptides in biological samples, there are some disadvantages of this approach. Among these are the difficulty in preparing the radiolabeled antigens and highly specific antibodies use for the RIA assay and the high cost of disposal of radioactive materials used for the assay.

#### 2.3.1.4 LC with mass spectrometry (MS):

LC coupled to MS is one of the most reported methods used for the study of the activity and metabolism of Dyn A(1-17) and its metabolites, both *in vivo* and *in vitro*. Reed et.al [76] studied the metabolism of Dyn A(1-17) in the striatum of freely moving Fisher rats. Dyn A(1-17) was infused to the rats at a rate of 0.1µL/min for over 20 minutes, via a microdialysis probe, and the dialysate fractions were then collected at specific time points. Once the microdialysis samples were collected, they were analyzed by a MALDI time-of-flight analyzer and MALDI ion trap mass spectrometer for tandem mass experiments. In addition to MALDI, other mass spectrometry methods such as electrospray ionization (ESI) have been used for the study of Dyn.

Beaudry et. al[77] reported the use of LC coupled to a quadrupole ion trap mass spectrometer for the identification and quantification of three peptides that are involved in neuropathic pain (substance P, calcitonin gene-related peptide (CGRP) and Dyn A) in homogenized rat spinal cord samples. Our lab[78] has previously performed LC-MS/MS using a triple quadrupole mass spectrometer to investigate the metabolism of Dyn A (1-17) by brain and spinal cord slices from Winster rats. Various fragments of Dyn A (1-17) were detected, including Dyn A (1-6), which is one of the major metabolites of the parent neuropeptide. In addition to this, our group has used LC-MS to investigate the transport of the peptide Dyn A(1-6) across a monolayer of bovine brain microvascular endothelial cells (BBMEC) as an *in vitro* model of the blood brain barrier[79] [Figure 6].

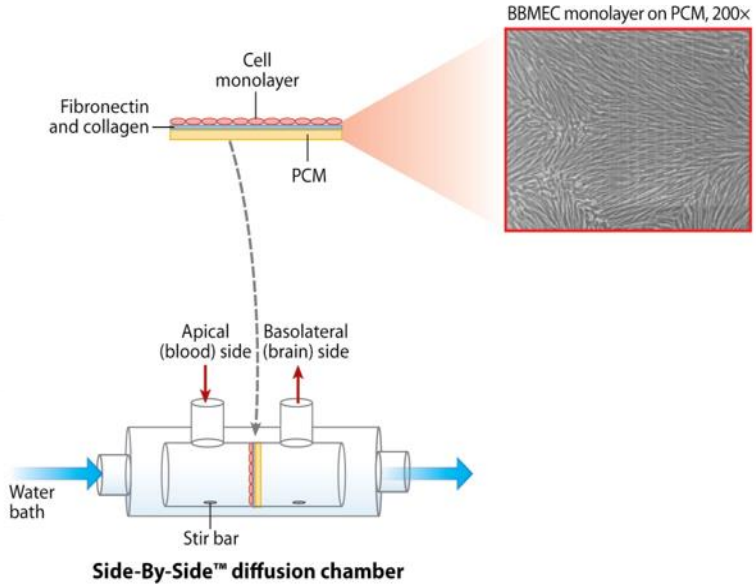


**Figure 6**: Side-by-Side® diffusion chamber used for monitoring *in-vitro* transport of Dyn A(1-6) across the BBMECs.[80] *(Reprinted with permission)*

### 2.3.2 Electrophoresis methods

Dynorphin A(1-17) and most of its metabolites are charged peptides. This makes it possible to separate them by different electrophoretic methods such as capillary electrophoresis (CE). A limitation of the use CE in the determination of Dyn A and its metabolites is mainly due to electrostatic adsorption of the positvely charged peptides to the capillary walls. A more detailed explanation of the forces causing the adsorption and some of the strategies reported to decrease the undesirable peptide-wall interaction are described in chapter three.

#### 2.3.2.1 Capillary electrophoresis (CE)

##### 2.3.2.1.1 Capillary electrophoresis

*In vitro* studies of the metabolism of Dyn A in human blood and rat brain tissue using CE was first reported by our lab [81]. Dyn A(1-17) and four of its metabolites were separated by CE method that involved on-capillary complexation of copper (II) with nitrogens atoms of the peptide backbone [Figure 7]. Complexation of copper ion with peptides was found to improve UV detection and effect resolution of peptide separation. In addition, the complex exhibits selectivity for peptides in the presence of amino acids because a minimum of three amino acids residues is needed to form the complex. The copper-Dyn complexation was reported to increase both peak height and area of the Dyn A(1-17) and its fragments using UV detection. The adsorption of the basic peptides to the inner surface of the capillary wall was decreased by adding 25 mM phytic acid to the background electrolyte (BGE). The polyanionic molecules act as an ion pairing agent with positively charged amino acids residues, shielding them from the negatively charged silanol groups of the capillary wall[81].

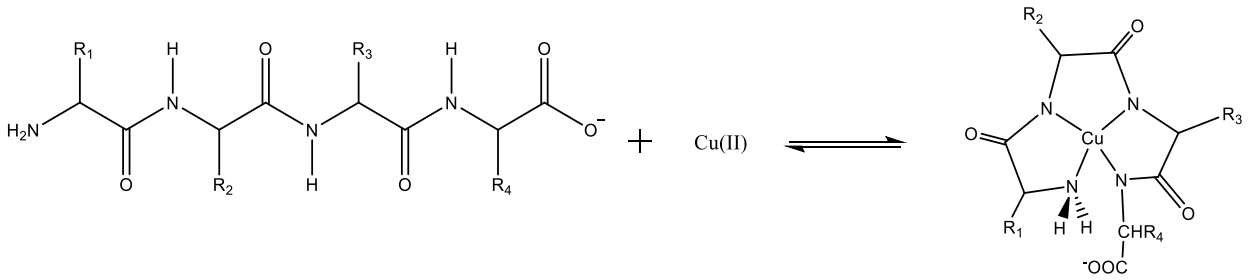


**Figure 7:** Complexation of Cu(II) with peptides.

#### 2.3.2.1.2 Nonaqueous capillary electrophoresis

Several benefits have been reported concerning the use of nonaqueous CE (NACE) compared to aqueous CE methods. These include the increased solubility of many nonpolar compounds in organic solvents[82] and reduced aggregation of large nonpolar compounds[83]. This makes it possible for NACE systems to separate analytes that have similar electrophoretic mobility in aqueous BGEs[84]. It also has better compatibility with a wide range of solvents to MS.

The separation of the opioid peptides, Leu-ENK, and Met-ENK, was investigated by Psurek et al. [84] using NACE. The BGE consisted of 10 mM ammonium acetate in ACN/methanol (3:1). Capillaries utilized for the separation had an effective length ($L_D$) of 60 cm and a total length ($L_T$) of 67 cm with a 75 µm inner diameter (i.d.). The applied voltage was +25 kV. Detection was accomplished by both UV (215 nm) and electrochemical detection (60 µm Pt microdisk and a detection potential +0.65). Electrochemical detection showed a lower LODs (0.3 µM) by a factor of 10 compared to UV detection (~ 3.2 µM).

### 2.3.2.2 Micellar electrokinetic chromatography (MEKC)

Surfactants added to the BGE solution at concentrations above its critical micelle concentration (CMC) can form micelles. Micellar electrokinetic chromatography (MEKC) is a modification of capillary electrophoresis. MEKC separation is based on the partition of an analyte between the mobile phase (the bulk solution) and a pseudostainary phase (micelle) under an applied electrical field[85-86]. An attempt of the separation of a series of Dyn analogs by MEKC was reported by Fürtös-matel et.al [87] since the mixture could not be separated by RP-LC. The analogs shared 18 amino acid residues (FNXEDLRKQAKRYGGFLR) but differed only the position of

one residue (X=alanine) within their sequence. Three different surfactants were evaluated including sodium dodecyl sulfate (SDS) as an anionic surfactant, cetrimonium bromide (CTAB) as a cationic surfactant, and 3-[(3-cholamidopropyl)dimethylammonio]-1-propanesulfonate (CHAPS) as a zwitterionic surfactant. The capillaries used for the MEKC separation were 50 µm i.d. with a $L_D$ of 61.2 cm and $L_T$ of 69.7 cm. UV detection was performed at λs of 200 and 235 nm. Among the three surfactants used for MEKC separation of the 13 Dyn analogs, CHAPS showed the best separation. The BGE used for the final MEKC separation consisted of 100 mM sodium phosphate (pH 3.5) and 35 mM CHAPS with an applied field strength of +360 V/cm. The addition of CHAPS within the BGE improved the separation compared to the addition of CTAB, due to the differences in the way the two surfactants form aggregates within the BGE solution, and CHAPS showed a much lower affinity to the Dyn analogs.

## 2.4 Summary

The chapter gives a general overview opioid peptides, and their receptors, with a more detailed look at dynorphins distribution within CNS, its metabolism, in addition to, the pharmacological and pathophysiological effects of elevated levels of the neuropeptides due to different diseases states such as spinal injury.

The chapter also covered different analytical methods used for the investigation of Dyn's metabolism and pathophysiological effect caused by up normal levels of the peptide within animal models. The most widely reported method utilized for the investigation of Dyn A and metabolites has been chromatographic methods. Although LC methods are the most widely used techniques, they can require large volumes of sample and mobile phase. Reported articles that use CE

techniques for the analysis of Dyn are limited. The fact that CE requires small (submicroliter) sample volumes, and provides high separation efficiencies, as well as the ability to couple CE with microdialysis sampling (including the microfluidic platform), makes it an attractive separation technique for neuropeptides.

Mass spectrometry and UV detection are the most widely used detection methods paired with LC and CE for the detection of dynorphins. Other sensitivity and selectivity detection methods have been used such as fluorescence detection. This chapter briefly covered some of the fluorescent derivatization methods used for the fluorescent detection of the neuropeptide.

## 2.5 References


1. Whiteside, G. T.; Boulet, J. M.; Walker, K., The role of central and peripheral mu opioid receptors in inflammatory pain and edema: a study using morphine and DiPOA ([8-(3,3-diphenyl-propyl)-4-oxo-1-phenyl-1,3,8-triaza-spiro[4.5]dec-3-yl]-acetic acid). *J. Pharmacol. Exp. Ther.* **2005,** *314* (3), 1234-40.

2. Lefebvre, R. A., Opioid peptides and their receptors. In *Comparative Veterinary Pharmacology, Toxicology and Theraphy: Proceedings of the 3rd Congress of the European Association for Veterinary Pharmacology and Toxicology, August 25–29 1985, Ghent, Belgium Part II, Invited Lectures*, Van Miert, A. S. J. P. A. M.; Bogaert, M. G.; Debackere, M., Eds. Springer Netherlands: Dordrecht, 1986; pp 447-453.

3. Mulder, A. H.; Wardeh, G.; Hogenboom, F.; Frankhuyzen, A. L., Selectivity of various opioid peptides towards delta-, kappa; and MU-opioid receptors mediating presynaptic inhibition of neurotransmitter release in the brain. *Neuropeptides* **1989,** *14* (2), 99-104.

4. Johnson, M. W.; Mitch, W. E.; Wilcox, C. S., The cardiovascular actions of morphine and the endogenous opioid peptides. *Prog. Cardiovasc. Dis.* **1985,** *27* (6), 435-450.

5. Morley, J. E., The endocrinology of the opiates and opioid peptides. *Metabolism* **1981,** *30* (2), 195-209.

6. Benarroch, E. E., Endogenous opioid systems: Current concepts and clinical correlations. *Neurology* **2012,** *79* (8), 807-814.

7. Simon, E. J., Opioid receptors and endogenous opioid peptides. *Med. Res. Rev.* **1991,** *11* (4), 357-374.

8. Zaveri, N. T., The Nociceptin/Orphanin FQ Receptor (NOP) as a Target for Drug Abuse Medications. *Curr. Top. Med. Chem.* **2011,** *11* (9), 1151-1156.

9. Fallon, J. H.; Leslie, F. M., Distribution of dynorphin and enkephalin peptides in the rat brain. *The Journal of Comparative Neurology* **1986,** *249* (3), 293-336.

10. Akil, H.; Watson, S. J.; Young, E.; Lewis, M. E.; Khachaturian, H.; Walker, J. M., Endogenous opioids: biology and function. *Annu. Rev. Neurosci.* **1984,** *7* (1), 223-255.

11. Podvin, S.; Yaksh, T.; Hook, V., The Emerging Role of Spinal Dynorphin in Chronic Pain: A Therapeutic Perspective. *Annu. Rev. Pharmacol. Toxicol.* **2016,** *56*, 511-33.

12. Hallberg, M., Neuropeptides: metabolism to bioactive fragments and the pharmacology of their receptors. *Med. Res. Rev.* **2015,** *35* (3), 464-519.

13. McDonald, J.; Lambert, D., Opioid receptors. *BJA Education* **2015,** *15* (5), 219-224.

14. Dietis, N.; Rowbotham, D. J.; Lambert, D. G., Opioid receptor subtypes: fact or artifact? *BJA: British Journal of Anaesthesia* **2011,** *107* (1), 8-18.

15. McNally, G. P.; Akil, H., *Chapter 3: Opioid Peptides And Their Receptors: Overview And Function In Pain Modulation* Lippincott, Williams and Wilkins: Philadelphia, PA, 2002; Vol. 17.

16. Al-Hasani, R.; Bruchas, M. R., Molecular Mechanisms of Opioid Receptor-Dependent Signaling and Behavior. *Anesthesiology* **2011,** *115* (6), 1363-1381.

17. Ikeda, K.; Yoshii, M.; Sora, I.; Kobayashi, T., Opioid Receptor Coupling to GIRK Channels. In *Opioid Research: Methods and Protocols*, Pan, Z. Z., Ed. Humana Press: Totowa, NJ, 2003; pp 53-64.

18. Shirayama, Y.; Ishida, H.; Iwata, M.; Hazama, G.-i.; Kawahara, R.; Duman, R. S., Stress increases dynorphin immunoreactivity in limbic brain regions and dynorphin antagonism produces antidepressant-like effects. *J. Neurochem.* **2004,** *90* (5), 1258-1268.

19. Horvath, G., Endomorphin-1 and endomorphin-2: pharmacology of the selective endogenous mu-opioid receptor agonists. *Pharmacol. Ther.* **2000,** *88* (3), 437-63.

20. Chieng, B.; Connor, M.; Christie, M. J., The mu-opioid receptor antagonist D-Phe-Cys-Tyr-D-Trp-Orn-Thr-Pen-Thr-NH2 (CTOP) [but not D-Phe-Cys-Tyr-D-Trp-Arg-Thr-Pen-Thr-NH2 (CTAP)] produces a nonopioid receptor-mediated increase in K+ conductance of rat locus ceruleus neurons. *Mol. Pharmacol.* **1996,** *50* (3), 650-5.

21. Crook, T. J.; Kitchen, I.; Hill, R. G., Effects of the delta-opioid receptor antagonist naltrindole on antinociceptive responses to selective delta-agonists in post-weanling rats. *Br. J. Pharmacol.* **1992,** *107* (2), 573-576.

22. Takemori, A. E.; Ho, B. Y.; Naeseth, J. S.; Portoghese, P. S., Nor-binaltorphimine, a highly selective kappa-opioid antagonist in analgesic and receptor binding assays. *J. Pharmacol. Exp. Ther.* **1988,** *246* (1), 255-8.

23. Post, A.; Smart, T. S.; Krikke-Workel, J.; Dawson, G. R.; Harmer, C. J.; Browning, M.; Jackson, K.; Kakar, R.; Mohs, R.; Statnick, M.; Wafford, K.; McCarthy, A.; Barth, V.; Witkin, J. M., A Selective Nociceptin Receptor Antagonist to Treat Depression: Evidence from Preclinical and Clinical Studies. *Neuropsychopharmacology* **2016,** *41* (7), 1803-1812.

24. Schwarzer, C., 30 Years of Dynorphins – New Insights on Their Functions in Neuropsychiatric Diseases. *Pharmacol. Ther.* **2009,** *123* (3), 353-370.

25. Cox, B. M.; Opheim, K. E.; Teschemacher, H.; Goldstein, A., Purification and properties. *Life Sci.* **1975,** *16* (12), 1777-1782.

26. Laughlin, T. M.; Larson, A. A.; Wilcox, G. L., Mechanisms of Induction of Persistent Nociception by Dynorphin. *J. Pharmacol. Exp. Ther.* **2001,** *299* (1), 6-11.

27. Dumont, M.; Lemaire, S., Opioid and nonopioid cardiovascular effects of dynorphins. *Adv. Pharmacol.* **1997,** *37*, 1-33.

28. Zhang, S.; Tong, Y.; Tian, M.; Dehaven, R. N.; Cortesburgos, L.; Mansson, E.; Simonin, F.; Kieffer, B.; Yu, L., Dynorphin A as a Potential Endogenous Ligand for Four Members of the Opioid Receptor Gene Family. *J. Pharmacol. Exp. Ther.* **1998,** *286* (1), 136-141.

29. O'Connor, C.; White, K. L.; Doncescu, N.; Didenko, T.; Roth, B. L.; Czaplicki, G.; Stevens, R. C.; Wuthrich, K.; Milon, A., NMR structure and dynamics of the agonist dynorphin peptide bound to the human kappa opioid receptor. *Proc. Natl. Acad. Sci. U. S. A.* **2015,** *112* (38), 11852-7.

30. Mansour, A.; Hoversten, M. T.; Taylor, L. P.; Watson, S. J.; Akil, H., The cloned μ, δ and κ receptors and their endogenous ligands: Evidence for two opioid peptide recognition cores. *Brain Res.* **1995,** *700* (1–2), 89-98.

31. Chavkin, C.; Goldstein, A., Specific receptor for the opioid peptide dynorphin: structure--activity relationships. *Proc. Natl. Acad. Sci. U. S. A.* **1981,** *78* (10), 6543-6547.

32. Naqvi, T.; Haq, W.; Mathur, K. B., Structure–activity relationship studies of dynorphin A and related peptides. *Peptides* **1998,** *19* (7), 1277-1292.

33. Quillan, J. M.; Sadee, W., Dynorphin peptides: antagonists of melanocortin receptors. *Pharm. Res.* **1997,** *14* (6), 713-9.

34. Brugos, B.; Hochhaus, G., Metabolism of dynorphin A(1-13). *Pharmazie* **2004,** *59* (5), 339-43.

35. Chou, J. Z.; Chait, B. T.; Wang, R.; Kreek, M. J., Differential biotransformation of dynorphin A (1-17) and dynorphin A (1-13) peptides in human blood, ex vivo. *Peptides* **1996,** *17* (6), 983-90.

36. Berman, Y.; Ageyeva, L.; Veksler, B.; Wood, D.; Devi, L. A., Dynorphin A processing enzyme: tissue distribution, isolation, and characterization. *J. Biochem.* **1999,** *125* (3), 641-7.

37. Silberring, J.; Castello, M. E.; Nyberg, F., Characterization of dynorphin A-converting enzyme in human spinal cord. An endoprotease related to a distinct conversion pathway for the opioid heptadecapeptide? *J. Biol. Chem.* **1992,** *267* (30), 21324-21328.

38. Muller, S.; Hochhaus, G., Metabolism of dynorphin A 1-13 in human blood and plasma. *Pharm. Res.* **1995,** *12* (8), 1165-70.

39. Young, E. A.; Walker, J. M.; Houghten, R.; Akil, H., The degradation of dynorphin A in brain tissue in vivo and in vitro. *Peptides* **1987,** *8* (4), 701-7.

40. Day, R.; Lazure, C.; Basak, A.; Boudreault, A.; Limperis, P.; Dong, W.; Lindberg, I., Prodynorphin processing by proprotein convertase 2. Cleavage at single basic residues and enhanced processing in the presence of carboxypeptidase activity. J. Biol. Chem. 1998, 273 (2), 829-36.41. Chavkin, C., Dynorphin–Still an Extraordinarily Potent Opioid Peptide. *Mol. Pharmacol.* **2013,** *83* (4), 729-736.

42. Nakazawa, T.; Ikeda, M.; Kaneko, T.; Yamatsu, K., Analgesic effects of dynorphin-A and morphine in mice. *Peptides* **1985,** *6* (1), 75-78.

43. Han, J. S.; Xie, C. W., Dynorphin: potent analgesic effect in spinal cord of the rat. *Life Sci.* **1982,** *31* (16-17), 1781-4.

44. Wen, H. L.; Mehal, Z. D.; Ong, B. H.; Ho, W. K.; Wen, D. Y., Intrathecal administration of beta-endorphin and dynorphin-(1-13) for the treatment of intractable pain. *Life Sci.* **1985,** *37* (13), 1213-20.

45. Wen, H. L.; Mehal, Z. D.; Ong, B. H.; Ho, W. K., Treatment of pain in cancer patients by intrathecal administration of dynorphin. *Peptides* **1987,** *8* (1), 191-3.

46. Lai, J.; Ossipov, M. H.; Vanderah, T. W.; Malan, T. P., Jr.; Porreca, F., Neuropathic pain: the paradox of dynorphin. *Mol. Interv.* **2001,** *1* (3), 160-7.

47. Long, J. B.; Kinney, R. C.; Malcolm, D. S.; Graeber, G. M.; Holaday, J. W., Intrathecal dynorphin A (1-13) and (3-13) reduce spinal cord blood flow by non-opioid mechanisms. *NIDA Res. Monogr.* **1986,** *75*, 524-6.

48. Long, J. B.; Petras, J. M.; Mobley, W. C.; Holaday, J. W., Neurological dysfunction after intrathecal injection of dynorphin A (1-13) in the rat. II. Nonopioid mechanisms mediate loss of motor, sensory and autonomic function. *J. Pharmacol. Exp. Ther.* **1988,** *246* (3), 1167-74.

49. Kurt, F. H.; Pamela, E. K.; Tatiana, Y.; Dineke, S. V.; Georgy, B., Dynorphins in Central Nervous System Pathology. In *Neuropeptides in Neuroprotection and Neuroregeneration*, CRC Press: 2012.

50. Hauser, K. F.; Knapp, P. E.; Turbek, C. S., Structure–Activity Analysis of Dynorphin A Toxicity in Spinal Cord Neurons: Intrinsic Neurotoxicity of Dynorphin A and Its Carboxyl-Terminal, Nonopioid Metabolites. *Exp. Neurol.* **2001,** *168* (1), 78-87.

51. Tan-No, K.; Cebers, G.; Yakovleva, T.; Hoon Goh, B.; Gileva, I.; Reznikov, K.; Aguilar-Santelises, M.; Hauser, K. F.; Terenius, L.; Bakalkin, G., Cytotoxic Effects of Dynorphins through Nonopioid Intracellular Mechanisms. *Exp. Cell Res.* **2001,** *269* (1), 54-63.

52. Laurent, S.; Schmitt, H., Central cardiovascular effects of κ agonists dynorphin-(1–13) and ethylketocyclazocine in the anaesthetized rat. *Eur. J. Pharmacol.* **1983,** *96* (1), 165-169.

53. Rabkin, S. W., Comparative effects on blood pressure and heart rate of dynorphin A(1-13) in anterior hypothalamic area, posterior hypothalamic area, nucleus tractus solitarius, and lateral cerebral ventricle in the rat. *Peptides* **1993,** *14* (6), 1253-8.

54. Fan, L.; McIntosh, T. K., Cardiovascular effects of microinjection of dynorphin fragments into the nucleus of the solitary tract (NTS) are mediated by non-opioid mechanisms. *Brain Res.* **1993,** *623* (1), 110-6.

55. van den Berg, M. H.; van Giersbergen, P. L.; Cox-van Put, J.; de Jong, W., Endogenous opioid peptides and blood pressure regulation during controlled, stepwise hemorrhagic hypotension. *Circ. Shock* **1991,** *35* (2), 102-8.

56. Dumont, M.; Lemaire, S., Inhibitory Effects of Dynorphin-A on Norepinephrine Uptake by Cardiac Synaptosomal-Mitochondrial Fractions. *J. Cardiovasc. Pharmacol.* **1995,** *25* (4), 518-523.

57. Smith, A. P.; Lee, N. M., Pharmacology of dynorphin. *Annu. Rev. Pharmacol. Toxicol.* **1988,** *28*, 123-40.

58. Morley, J. E.; Elson, M. K.; Levine, A. S.; Shafer, R. B., The effects of stress on central nervous system concentrations of the opioid peptide, dynorphin. *Peptides* **1982,** *3* (6), 901-906.

59. Kreek, M. J.; Schluger, J.; Borg, L.; Gunduz, M.; Ho, A., Dynorphin A1-13 causes elevation of serum levels of prolactin through an opioid receptor mechanism in humans: gender differences and implications for modulation of dopaminergic tone in the treatment of addictions. *J. Pharmacol. Exp. Ther.* **1999,** *288* (1), 260-9.

60. Kato, Y.; Matsuhita, N.; Katakami, H.; Shimatsu, A.; Imura, H., Stimulation by dynorphin of prolactin and growth hormone secretion in the rat. *Eur. J. Pharmacol.* **1981,** *73* (4), 353-355.

61. Kinoshita, F.; Nakai, Y.; Katakami, H.; Imura, H., Suppressive effect of dynorphin-(1-13) on luteinizing hormone release in conscious castrated rats. *Life Sci.* **1982,** *30* (22), 1915-9.

62. Wright, D. M.; Pill, C. E. J.; Clarke, G., Effect of ACTH on opiate inhibition of oxytocin release. *Life Sci.* **1983,** *33*, 495-498.

63. Ménard, C.; Herzog, H.; Schwarzer, C.; Quirion, R., Possible Role of Dynorphins in Alzheimer's Disease and Age-Related Cognitive Deficits. *Neuro - Degenerative Diseases* **2014,** *13* (2-3), 82-5.

64. Yakovleva, T.; Marinova, Z.; Kuzmin, A.; Seidah, N. G.; Haroutunian, V.; Terenius, L.; Bakalkin, G., Dysregulation of dynorphins in Alzheimer disease. *Neurobiol. Aging* **2007,** *28* (11), 1700-1708.

65. Shippenberg, T. S.; Zapata, A.; Chefer, V. I., Dynorphin and the pathophysiology of drug addiction. *Pharmacol. Ther.* **2007,** *116* (2), 306-321.

66. Aldrich, J. V.; McLaughlin, J. P., Peptide Kappa Opioid Receptor Ligands: Potential for Drug Development. *The AAPS Journal* **2009,** *11* (2), 312-322.

67. Spanagel, R.; Herz, A.; Shippenberg, T. S., Opposing tonically active endogenous opioid systems modulate the mesolimbic dopaminergic pathway. *Proc. Natl. Acad. Sci. U. S. A.* **1992,** *89* (6), 2046-50.

68. Lalanne, L.; Ayranci, G.; Kieffer, B. L.; Lutz, P.-E., The Kappa Opioid Receptor: From Addiction to Depression, and Back. *Frontiers in Psychiatry* **2014,** *5*, 170.

69. Bruijnzeel, A. W., Kappa-opioid receptor signaling and brain reward function. *Brain Res. Rev.* **2009,** *62* (1), 127-146.

70. Zhang, Y.; Butelman, E. R.; Schlussman, S. D.; Ho, A.; Kreek, M. J., Effect of the endogenous κ opioid agonist dynorphin A(1–17) on cocaine-evoked increases in striatal dopamine levels and cocaine-induced place preference in C57BL/6J mice. *Psychopharmacology* **2004,** *172* (4), 422-429.

71. Seyfried, C. A.; Tobler, P., High-performance liquid chromatographic system for the separation of dynorphin A (1-17) fragments and its application in enzymolysis studies with rat nerve terminal membranes. *J. Chromatogr.* **1990,** *529* (1), 43-54.

72. Kai, M.; Kojima, E.; Ohkura, Y.; Iwasaki, M., High-performance liquid chromatography of N-terminal tryptophan-containing peptides with precolumn fluorescence derivatization with glyoxal. *J. Chromatogr.* **1993,** *653* (2), 235-240.

73. Nakano, M.; Kai, M.; Ohno, M.; Ohkura, Y., High-performance liquid chromatography of N-terminal tyrosine-containing oligopeptides by pre-column fluorescence derivatization with hydroxylamine, cobalt (II) and borate reagents. *J. Chromatogr.* **1987,** *411*, 305-11.

74. Sandrini, M.; Romualdi, P.; Vitale, G.; Morelli, G.; Capobianco, A.; Pini, L. A.; Candeletti, S., The effect of a paracetamol and morphine combination on dynorphin A levels in the rat brain4. *Biochem. Pharmacol.* **2001,** *61* (11), 1409-1416.

75. Muller, S.; Ho, B.; Gambus, P.; Millard, W.; Hochhaus, G., An HPLC/RIA method for dynorphin A1-13 and its main metabolites in human blood. *J. Pharm. Biomed. Anal.* **1997,** *16* (1), 101-9.

76. Reed, B.; Zhang, Y.; Chait, B. T.; Kreek, M. J., Dynorphin A(1–17) biotransformation in striatum of freely moving rats using microdialysis and matrix-assisted laser desorption/ionization mass spectrometry. *J. Neurochem.* **2003,** *86* (4), 815-823.

77. Beaudry, F.; Ferland, C. E.; Vachon, P., Identification, characterization and quantification of specific neuropeptides in rat spinal cord by liquid chromatography electrospray quadrupole ion trap mass spectrometry. *Biomed. Chromatogr.* **2009,** *23* (9), 940-50.

78. Sloan, C. D. K. The Development of Analytical Methods for Investigations of Dynorphin A 1-17 Metabolism in the Central Nervous System and Peripheral Tissues and Transport

at the Blood Brain Barrier (Doctoral dissertation). Doctoral dissertation, University of Kansas, 2011.

79. Sloan, C. D. K.; Audus, K. L.; Aldrich, J. V.; Lunte, S. M., The permeation of dynorphin A 1–6 across the blood brain barrier and its effect on bovine brain microvessel endothelial cell monolayer permeability. *Peptides* **2012,** *38* (2), 414-417.

80. Kuhnline Sloan, C. D.; Nandi, P.; Linz, T. H.; Aldrich, J. V.; Audus, K. L.; Lunte, S. M., Analytical and biological methods for probing the blood-brain barrier. *Annu. Rev. Anal. Chem. (Palo Alto Calif.)* **2012,** *5*, 505-31.

81. Kuhnline, C. D.; Lunte, S. M., Evaluation of an on-capillary copper complexation methodology for the investigation of in vitro metabolism of dynorphin A 1–17. *J. Sep. Sci.* **2010,** *33* (16), 2506-2514.

82. Steiner, F.; Hassel, M., Nonaqueous capillary electrophoresis: a versatile completion of electrophoretic separation techniques. *Electrophoresis* **2000,** *21* (18), 3994-4016.

83. Yang, Q.; Benson, L. M.; L. Johnson, K.; Naylor, S., Analysis of lipophilic peptides and therapeutic drugs: on-line-nonaqueous capillary electrophoresis–mass spectrometry. *J. Biochem. Biophys. Methods* **1999,** *38* (2), 103-121.

84. Psurek, A.; Matysik, F.-M.; Scriba, G. K. E., Determination of enkephalin peptides by nonaqueous capillary electrophoresis with electrochemical detection. *Electrophoresis* **2006,** *27* (5-6), 1199-1208.

85. Terabe, S., Capillary separation: micellar electrokinetic chromatography. *Annu. Rev. Anal. Chem. (Palo Alto Calif.)* **2009,** *2*, 99-120.

86. Hancu, G.; Simon, B.; Rusu, A.; Mircia, E.; Gyéresi, Á., Principles of Micellar Electrokinetic Capillary Chromatography Applied in Pharmaceutical Analysis. *Advanced Pharmaceutical Bulletin* **2013,** *3* (1), 1-8.

87. Fürtös-Matei, A.; Day, R.; St-Pierre, S. A.; St-Pierre, L. G.; Waldron, K. C., Micellar electrokinetic chromatography separations of dynorphin peptide analogs. *Electrophoresis* **2000,** *21* (4), 715-723.

# Chapter 3

# Capillary Electrophoresis and Electrochromatography Methods for the Separation of Proteins and Peptides

## 3.1 Introduction

### 3.1.1 Capillary electrophoresis

Capillary electrophoresis (CE) is a separation method that is based on the migration of charged species in a background electrolyte solution (BGE) within a narrow capillary under the influence of an applied electric field [Figure 1].

Some of the advantages of CE over other separation techniques, such as liquid chromatography (LC) includes higher separation efficiencies. This is due to the flat plug flow profile of CE in contrast to the parabolic profile of pressure driven flow systems. CE also requires low sample volumes (pL to nL vs. µL), small amounts of BGE (< 20 µL), short analysis times, and has a low cost of operation and instrument maintenance. As the separated analytes move through the capillary, various detection methods can be used such as ultraviolet (UV), laser induced fluorescence (LIF), mass spectrometry (MS), amperometric and conductivity detection.

#### 3.1.1.1 Theory of CE

The velocity ($v$) at which an ion travels within the capillary can be expressed as:

$$v = \mu_e E \qquad (1)$$

where (E) is the electric field strength and ($\mu_e$) is the ion's electrophoretic mobility. The electrophoretic mobility of an ion is proportional to the charge of the ion ($q$) and inversely proportional to the ions radius ($r$) and the viscosity of the BGE.

$$\mu_e = {}^{q}/_{6\pi\eta r} \qquad (2)$$

Equation (2) shows that highly charged small ions have higher electrophoretic mobilities, compared to larger ions of the same charge. Another important feature of CE is that under the influence of applied electric field, there is a bulk flow of the BGE within the capillary due to electroosmosis, termed electroosmotic flow (EOF) [Figure 2]. When a capillary is filled with an electrolyte solution, positivity charged ions of the buffer are attracted to the negatively charged silanol groups of a fused-silica capillary, creating an electrical double layer and a potential difference at the capillary wall (zeta potential (ξ)).

$$\mu_{eo} = (\varepsilon_o \varepsilon_r \xi)/\eta \qquad (3)$$

$$\xi = (\sigma\delta)/(\varepsilon_o \varepsilon) \qquad (4)$$

where $\mu_{eo}$ is the EOF mobility, ($\varepsilon_o$) is permittivity of a vacuum, ($\varepsilon_r$) is relative permittivity of medium (dielectric constant) and where δ is the thickness of the electrical double layer. The EOF is dependent on a number of factors that includes pH and the ionic strength of the BGE. From equation (3) we can see that $\mu_{eo}$ is proportional to the zeta potential at the surface.

The overall migration time of an ion under an applied electrical field is related to both the $\mu_e$ and $\mu_{eo}$ :

$$v_{app} = (\mu_e + \mu_{eo})\, E = (\mu_e + \mu_{eo})\, (V/L) \qquad (5)$$

where ($v_{app}$) is the apparent velocity, and E is a function of the applied voltage (V) and (L) is the length of the capillary. From equation (5) we find that small highly charged cations show the fastest velocity, followed by larger size cations of the same charge, then all the neutral molecules migrate togther in a single zone, and then large anions follow and then finally small highly charged anions [Figuer 2].

Although CE has been shown to provide high-efficiency separations of many analytes, unfortunately there are some sources of band broadening found in CE. They include Joule heating due to the resistance of the BGE to the flow of current that leads to an insufficient dispersion of heat across the capillary [1-2]. Joule heating can be minimized by using narrow inner diameter (i.d.) capillaries, which dissipate heat more effectively. However, smaller i.d. capillaries also shorten the optical path length and increase the limits of detection for CE-UV compared to LC-UV. Other sources of band broadening in CE includes the nonspecific adsorption of analytes onto the inner walls of capillaries, which may require additives to the BGE or modification of the capillary wall.

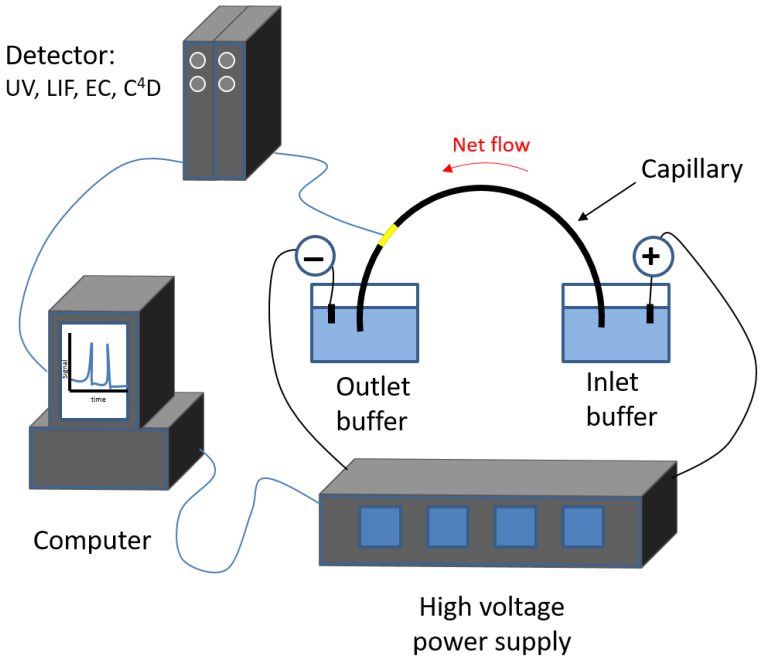


**Figure 1:** General schematic of CE instrument.

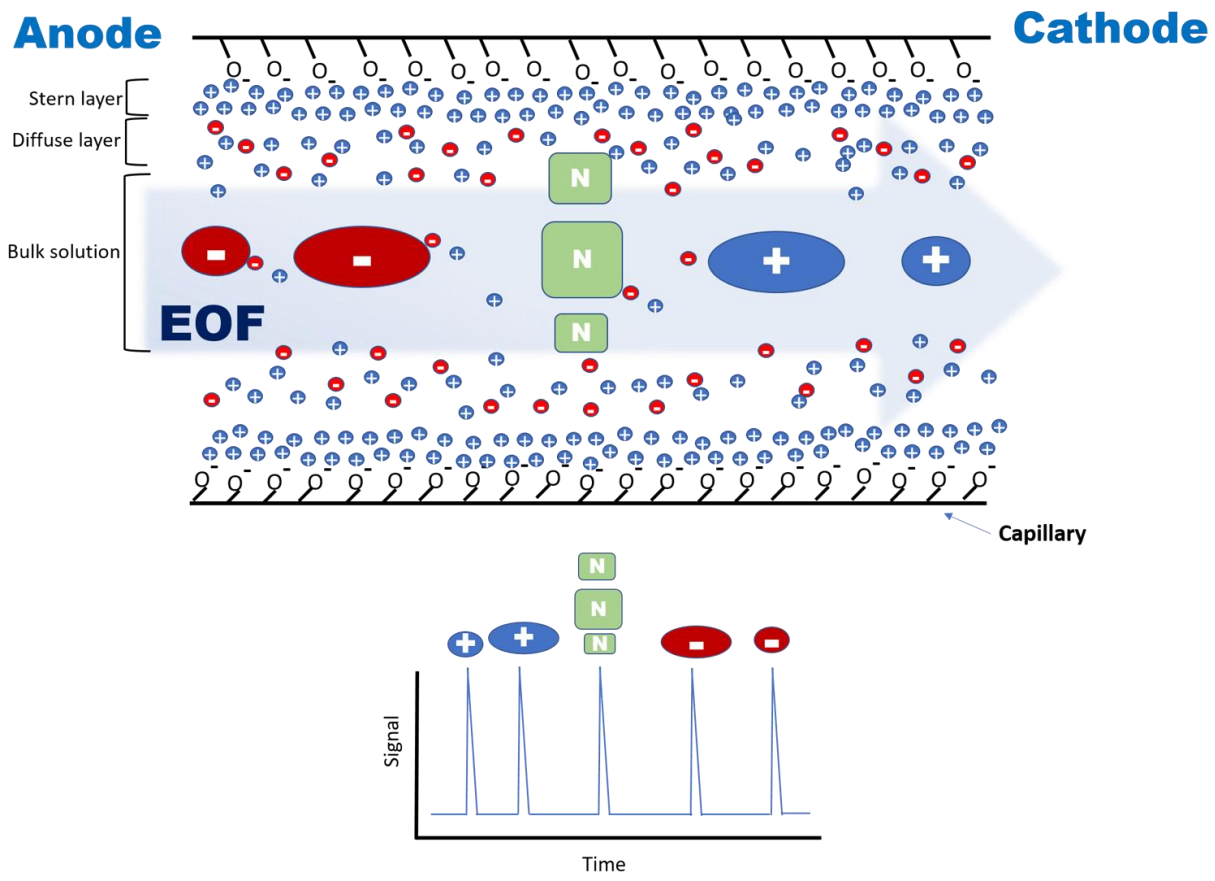


**Figure 2:** Schematic of the separation mechanism for capillary and microchip electrophoresis.

### 3.1.2 Microchip electrophoresis

Microchip electrophoresis (ME) is a miniaturized version of CE and operates under the same separation mechanism. ME is a separation system that has the potential to assay multiple samples within minutes[3] (high throughput). The microchip design can include sample preparation, derivatization, injection, separation, and detection all in a single microfluidic platform[4]. ME has minimal sample requirements (as low as picoliters) and uses short separation channels along with high field strengths to produce rapid separations[5]. This makes microchip electrophoresis an attractive method for high throughput analysis of protein/ peptide samples.

Microchannels in ME are most commonly fabricated either by photolithographic or micromolding methods. To perform a separation by ME, the BGE and sample are loaded onto the chip, and the sample is introduced into the separation channel electrokinetically through the application of a high voltage at the sample and buffer reservoirs. The analytes can then be detected by laser induced fluorescence (LIF)[6-9], electrochemistry[10], conductivity[11], or mass spectrometry(MS)[12-13].

### 3.1.2.1 Microfabrication methods and materials

Microchannels in ME typically have a channel width of less than 200 µm and depth of less than 50 µm. The most commonly used material for fabrication of ME devices is glass (soda lime, borofloat, or high-quality quartz)[14-15]. Glass substrates are not only known for their excellent optical properties[16] but also their well-understood surface chemistry, compatibility with most solvents and well-developed fabrication procedures. Other materials that are commonly used in ME are polymers such as polymethylmethacrylate (PMMA), polydimethylsiloxane (PDMS), polyvinyl chloride (PVC)[17], polyimide (PI), and cyclic olefin copolymer[18-19]. The advantages of using polymers for ME are the simplicity of fabrication and low cost of the produced microchips. This makes it possible to produce disposable MC devices[15, 20]. Table 1 shows some of the properties of glass and various polymers used in ME.

| | Glass | PDMS | PMMA | PI |
|---|---|---|---|---|
| Useful temperature range (ºC) | < 500 | −40 to 50 | −70 to 100 | −73 to 240 |
| Thermal conductivity (W/mK) | 1.2 | 0.17 to 0.3 | 0.186 | 0.2 |
| Visible transmittance (%) | > 90 | 91 | 92 | 87 |
| Surface charge (native) | Yes | Weak | Yes | No |
| Acid resistance | Excellent | Fair-good | Good | Fair-good |
| Base resistance | Excellent | Poor-fair | Excellent | Fair-good |
| Solvent resistance | Excellent | Poor | Poor | Fair |

**Table 1:** Comparison of glass and various polymers used ME. PMMA: polymethylmethacrylate, PDMS: polydimethylsiloxane, and PI: polyimide. [Table from L.A. Legendre, et.al.][21]

#### 3.1.2.1.1 Glass chip fabrication procedures

Standard photolithography followed by wet etching is the most commonly used method for glass chip fabrication [22]. This technique requires a glass substrate coated with two layers; the first is a chromium layer that functions as a sacrificial etching mask. The second is a photoresist layer that functions to provide the chip design and helps protects the substrate from chemical etching. The photoresist is placed over the glass-chromium substrate by spin coating. The photoresist most commonly used is a positive photoresist (soluble in the developer after light exposure) although, a

negative photoresist can also be used (insoluble in the developer after light exposure). The choice of which photoresist is used for fabrication will depend on the design of an opaque film with a defined transparent pattern (photomask) that is placed over the photoresist.

The photoresist coated substrate is then exposed to UV light through a microchip design pattern that is defined by a photomask. The UV exposure time mostly depends on the power of the UV source and the thickness and type of photoresist. The UV exposed photoresist is then removed using a developer solution (containing approximately 2% tetramethylammonium hydroxide in an aqueous solution). The Cr layer is then removed by a Cr etchant solution consisting of a mixture of perchloric acid ($HClO_4$), and ceric ammoniumnitrate $(NH_4)_2[Ce(NO_3)_6]$ to reveal the underlying glass. The exposed glass is then etched using a concentrated $HF/HNO_3$ solution. The rate of etching depends on the type of glass being etched and the concentration of HF used. The etching rate is controlled by maintaining a constant temperature [23]. Once the desired channel depth is reached, the acidic etching solution is neutralized by washing the chip with a $CaCO_3$ suspension, and the remaining photoresist and Cr are removed by immersing the glass substrate first with acetone followed by Cr etchant solution. Access holes are then drilled to generate reservoirs at the end of each of microfluidic channels, and finally, the substrate is bonded to a coverplate [Figure 3].

The most frequently used bonding procedure is thermal bonding. In this case, two glass plates are brought to close contact by applying vertical pressure to the surface and then subjected to a high temperature (550-650 °C) for several hours. It should be noted that both glass surfaces must be extremely clean to avoid dust particles affecting the glass bonding and this required condition is found in a cleanroom environment [24-25]. Other, less frequently, used methods for chip bonding include chemically activation. In this case, a small volume of 1% HF solution is placed between the two glass substrates and kept at room temperature while applying perpendicular

pressure over the glass chip using weights for 24 hours[26]. Anodic bonding is another method that can be used for bonding of a glass/glass or glass/silicon microchips. With anodic bonding the two substrates are clamped together under temperatures of approximately 400°C and placed between two metal electrodes and an external voltage of 1 kV is applied. An irreversible chemical bond between the two substrates occurs. The bonding is due to the migration of the $Na^+$ ions of one substrate to the negative electrode, producing a strong electrostatic attraction to the second substrate layer [27-28]. Other methods include adhesive bonding, where glue guide channels are fabricated along the microchip channels and reservoirs of the glass substrate. The glue guide channels then are filled with UV-curable glue, and the glass coverplate is then placed over the etched plate. Finally, the chip exposure to a UV light for 30 min, bonding the two glass substrates together [25, 29].

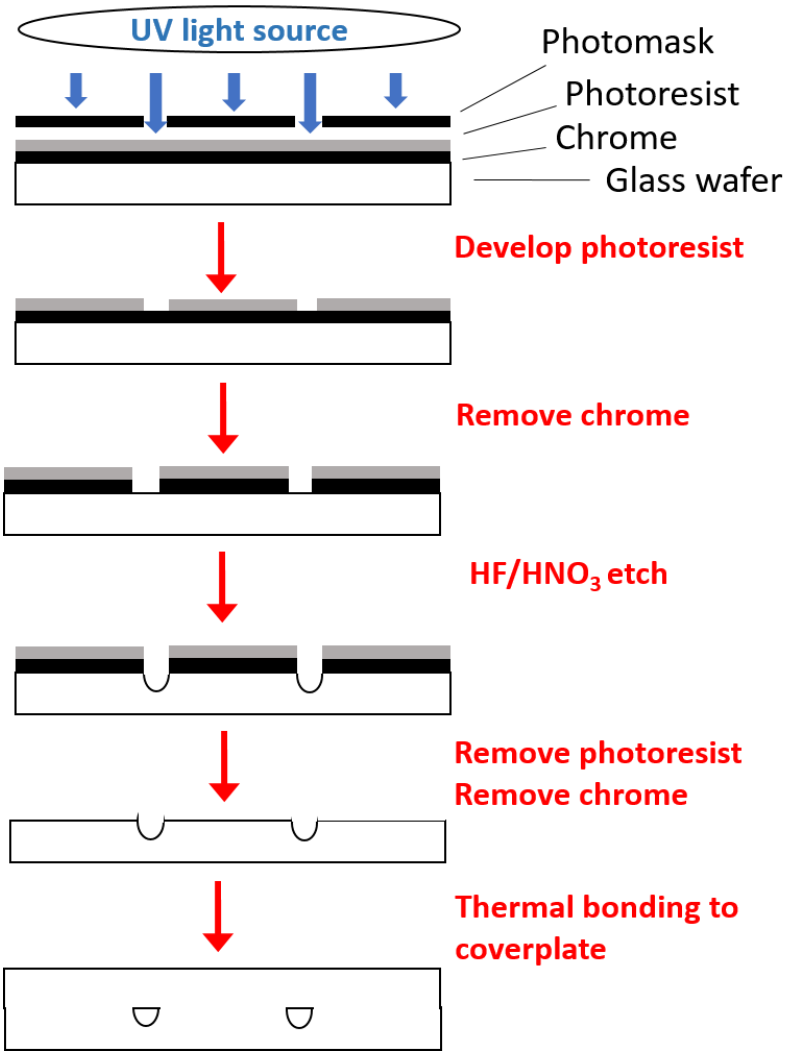


**Figure 3:** General scheme showing glass microchip fabrication steps

#### 3.1.2.1.2 Polymer material fabrication procedure

##### 3.1.2.1.2.1 ME fabrication by laser ablation

The approaches used for the fabrication of polymer microchips are mostly controlled by the nature of the polymer materials used. One method involves the breakdown of covalent bonds of long chain polymer materials using a short wavelength laser to form the ME channels. The

position of the laser is controlled by an X-Y stage. Some of the materials used to make ME devices with this method include polycarbonate, PMMA [30], and PDMS [31]. A method was described by Fogarty et.al. [31] using a $CO_2$ laser for the ablation of microchannel within a PDMS substrate. A standard hole puncher was then used to make the reservoir holes at the ends of the ablated channels. This procedure had the advantages of being rapid and relatively inexpensive. The ME chips produced using this approach were used for the separation and detection of fluorescent cyano[f]benzoisoindole (CBI) derivatized neurotransmitters (glutamate and aspartate) by LIF detection.

**3.1.2.1.2.2 Injection molding and casting fabrication procedures for polymer microchips**

Both injection molding and casting microchannel fabrication share two initial steps, the first step is the fabrication of a mold or a master. The second step is the transfer of the channel design of the mold onto the polymer material or substrate. Injection molding is a high-throughput production method for the fabrication of microfluidic devices and has a low production cost. In this approach, acrylic substrates are initially melted and then injected into a reusable master [32].

The casting method is an alternative and more simple and popular method used for ME fabrication. Polymer materials, for example, PDMS, are mixed with a curing agent and poured onto a master e.g. silicon master. The polymer is then cured at room temperature. The polymerization reaction can also be accelerated at higher temperatures [33-34] [Figure 4]. The surface chemistry of the PDMS polymer can be controlled by changing the monomer-curing agent ratio. Once the PDMS polymer is cured, the PDMS is peeled off from the master, and reservoir access holes are made at each end of the microfluidic chip using a standard hole puncher or biopsy

punches. The final step involves the bonding of the PDMS substrate containing the channels to a cover layer (e.g. glass or PDMS). The bonding strength of the two layers may be a weak bond (Van der Waals forces), that allows a reversible seal of the chip, or a stronger irreversible seal can be produced by exposing both surfaces to an oxygen plasma.

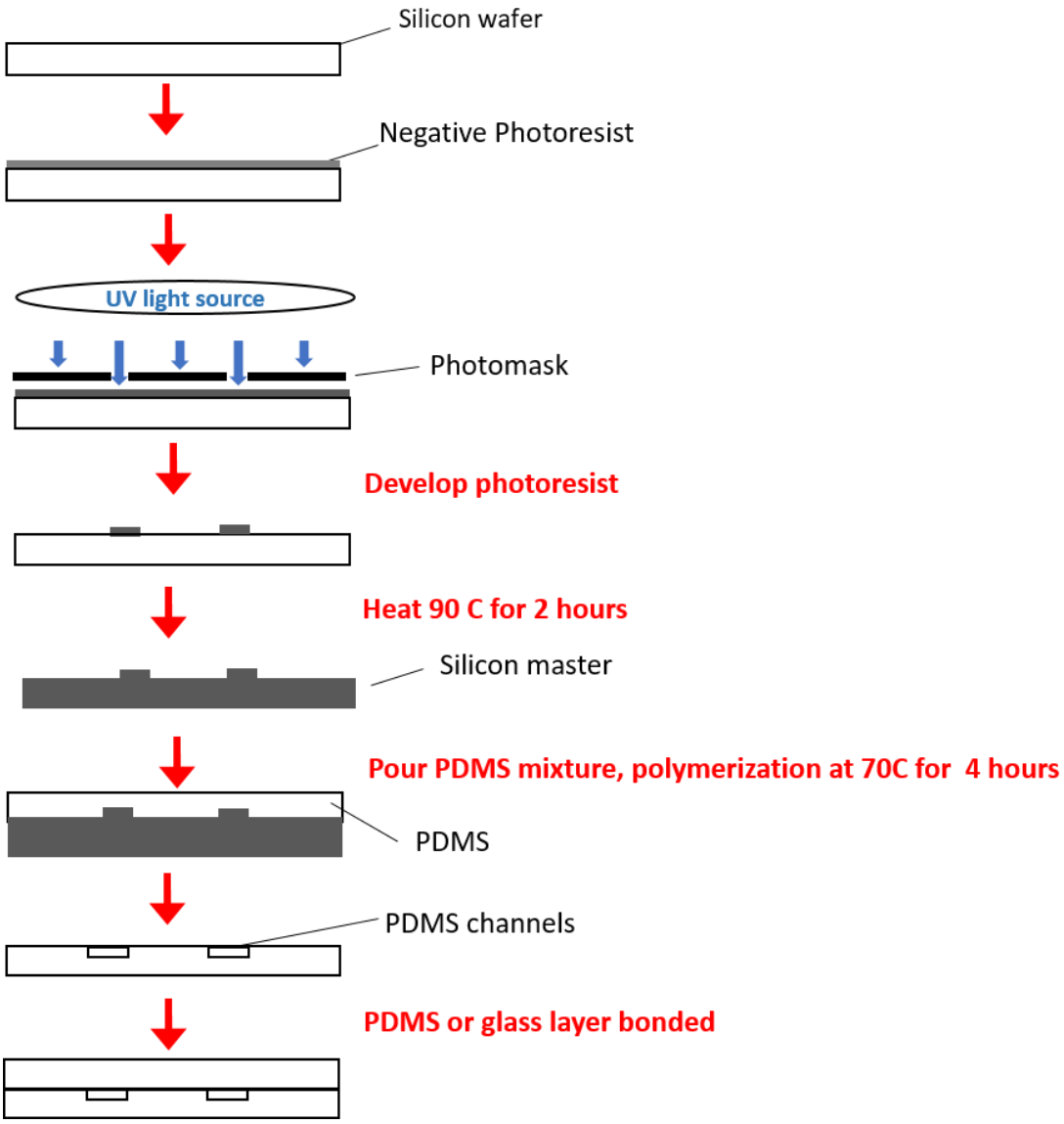


**Figure 4:** General scheme showing polydimethylsiloxane (PDMS) microchip fabrication steps

### 3.1.2.2 Microchip design and sample injection

Various microchip designs have been used for ME, from a simple channel to a complex design with multiple channels within the microfluidic chip. The sample can be introduced into the ME separation channel by several different methods. They are based on the ME chip design and injection requirements. For ME devices with a simple t-design, the three most popular methods are floated, pinched and gated injections.

Floating injection [Figure 5A] can be performed by using a single power supply [35]. The sample is injected electrokinetically by applying a high voltage (HV) to the sample (S), with the buffer waste (BW) reservoirs, and the sample waste (SW) reservoirs kept at ground, and the buffer (B) reservoir left floating for 1-5 seconds. This causes the sample to be introduced into the separation channel. In the dispensing step, a HV is applied to the (B) with the (BW) kept at ground and the (S) and (SW) floating. A disadvantage of the floating injection method is the irreproducibility of the injection volumes and a large sample plug that is due to the absence of pushback flow from the (S) and (SW) [36-37].

Pinched injections [Figure 5B] require power supplies that are connected to each of the four reservoirs. A sample is loaded by applying a HV to the (S), (B) and (BW) with the (SW) kept at ground for a given moment. Once the tee is filled with the sample, the sample plug is injected into the separation channel by applying a HV to (B), and at the same time, a fraction of the HV is applied to the both the (S) and (SW) reservoirs. The advantage of this method is the plug shape is controlled.

The third injection method used in ME is the gated injection method. This injection method requires a minimum of two power supplies. Unlike the first two methods, the sample is first placed in the top reservoir and the BGE is placed in one of the side channel reservoirs of the ME [Figure 5C]. In the loading step, a high voltage is applied to the (B), and a fraction of the high voltage is applied to the (S). With both the (SW) and (BW) kept at ground causing a gated to form. The sample is then introduced into the separation channel by floating the (B) voltage (less than 5 seconds), and a plug is formed within the separation channel. This is followed by restoring the applied voltages causing the sample plug to flow to the (BW). The amount of voltage applied to both (B) and (S) are determined based on the field strength required for the separation. This is calculated based on the junction voltage at the ME intersection and calculated using Kirchoff's Laws. The gated injection method can be utilized for continuous sampling but suffers from electrokinetic bias [38].

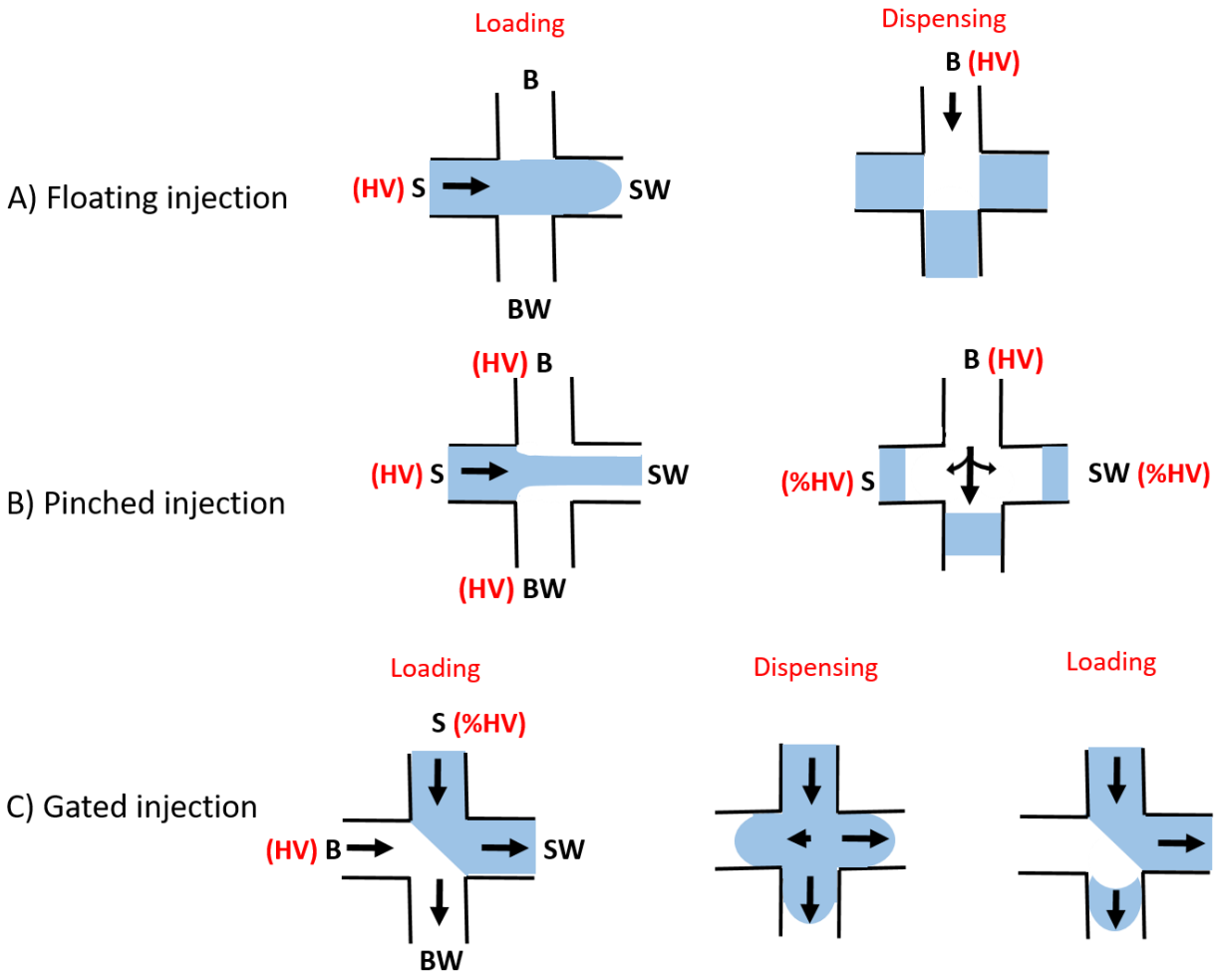


**Figure 5:** Sample injection methods in electrophoresis microchip. A) Floating injection, B) Pinched injection, C) Gated injection. S: sample, B: buffer, SW: sample waste, BW: buffer waste.

### 3.2 Limitations of CE and ME for protein/ peptide analysis

Protein and peptide analysis by CE or ME can be limited by irreversible adsorption of these substances onto the inner walls of the fused silica capillaries or glass substrates normally used for separations. This is especially a problem with basic proteins and peptides [Figure 6]. Protonation of the amino group at the N-terminal or basic amino acid residues, such as arginine and lysine of a protein/peptide, may affect the CE separation of a protein/peptide due to electrostatic interactions with the silanol surface. Analyte adsorption can lead to peak tailing, poor efficiency, loss of analyte, lack of reproducibility of migration time[39] or instability of baseline. Therefore CE or ME may not always be the best option for protein/ peptide analysis [40].

Proteins are high molecular weight molecules, composed of simple amino acids linked together by peptide bonds, forming long polypeptide chains that are known as the primary structure. Several polypeptide chains, each with its specific sequence of amino acid residues, can form secondary structures (α-helix or β-sheets) through H-bonding. Also, the polypeptides chains can fold to form more complicated and unique tertiary structures through hydrogen bonding, polar interactions, nonpolar interactions, disulfide bonds and/or salt bridges. Finally, a more complex protein structure can also occur through intermolecular interactions between two or more tertiary structures causing the formation of the protein quaternary structure. Also, many proteins may also contain other components such as saccharides, lipids or metals. The complexity of a proteins structures can lead to a protein having several different surface chemistries. The same protein can possess nonpolar, polar, cationic and anionic properties on different parts of the protein surface. In addition, the properties of a protein can be sensitive to changes in the overall environment in which the proteins are placed, such as pH, ionic strength, temperature or solvent composition. It should be noted that not every interaction of the protein with the surface (e.g. inner surface of a

fused silica capillary) will result in adsorption. It will occur only when the protein is in the correct orientation [41-42]. One example is a negatively charged

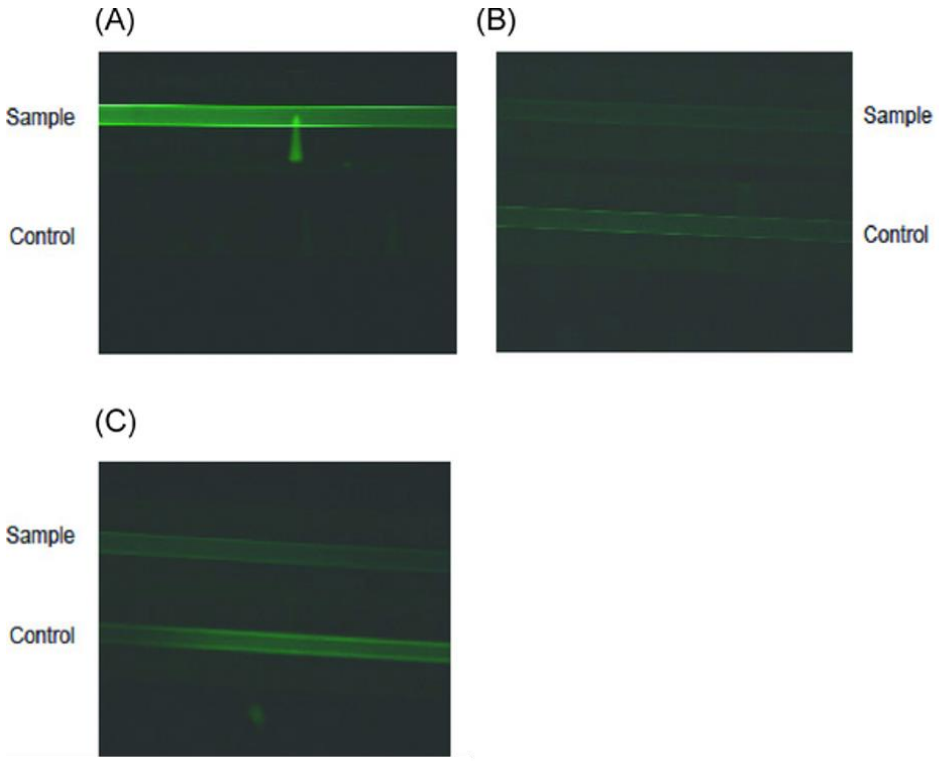


**Figure 6:** Image of fluorescence labeled protein adsorption onto fused silica capillary. FITC-anti-human-β2gpI in pretreated capillaries with (A) BGE (50 mM phosphate buffer pH 7.4), (B) HCl, and (C) NaOH. Note: FITC-anti-human-$\beta_2$gpI was incubated for one hour at room temperature. [43] *(Reprinted with permission)*

protein may not always be electrostatically repelled by the negatively charged silanol groups of a capillary wall. A possible explanation may be that, although the overall charge of the protein is negative, positive patches of the protein in a specific orientation can be electrostatically adsorbed onto the negatively charged capillary wall and result in protein adsorption [44].

One model used to explain adsorption of proteins/ peptides onto the surface of a fused silica capillary is shown in figure 7 [45]. The first step involves the transfer of the protein/ peptide to the surface. The second step is the interaction and adsorption of the protein/ peptide at the surface. From the model, it shows that based on the protein/ peptide, medium, and the residence time of these molecules on the surface, the adsorption in some cases may be reversible [46]. Graf et. al. [47] investigated the strength of the protein adsorption to fused silica capillaries in CE as a function of pH and buffer constituents. Model proteins were used in the study, which included cytochrome c (pI 9.6) as a basic protein, myoglobin (pI 6.8-7.4) as a neutral reference and β-lactoglobulin (pI 5.4) as an acidic protein. The research group studied the protein adsorption to the capillary due to different CE conditions and their effect on the reproducibility of the EOF. One major parameter that was investigated was the pH dependence of protein adsorption. They found that myoglobin showed strong adsorption at pH values below its pI, and a negligible adsorption at pHs near or above its pI. The two proteins, cytochrome c and β-lactoglobulin, were reported to show less protein adsorption to the capillary at pHs above their pIs. The group also investigated the regeneration of the myoglobin adsorped onto the capillary by rinsing the capillary with sodium dodecyl sulfate (SDS) within the BGE after subsequent runs of a protein sample. Capillary regeneration was possible only when recently adsorbed myoglobin was rinsed with SDS. This was

accomplished by simply rinsing the capillary with buffers containing 200 mM SDS for 3 hours. Unfortunately, capillary regeneration with SDS was not successful for longer contact times (after a storage time of 24 h) of the protein within the capillary.

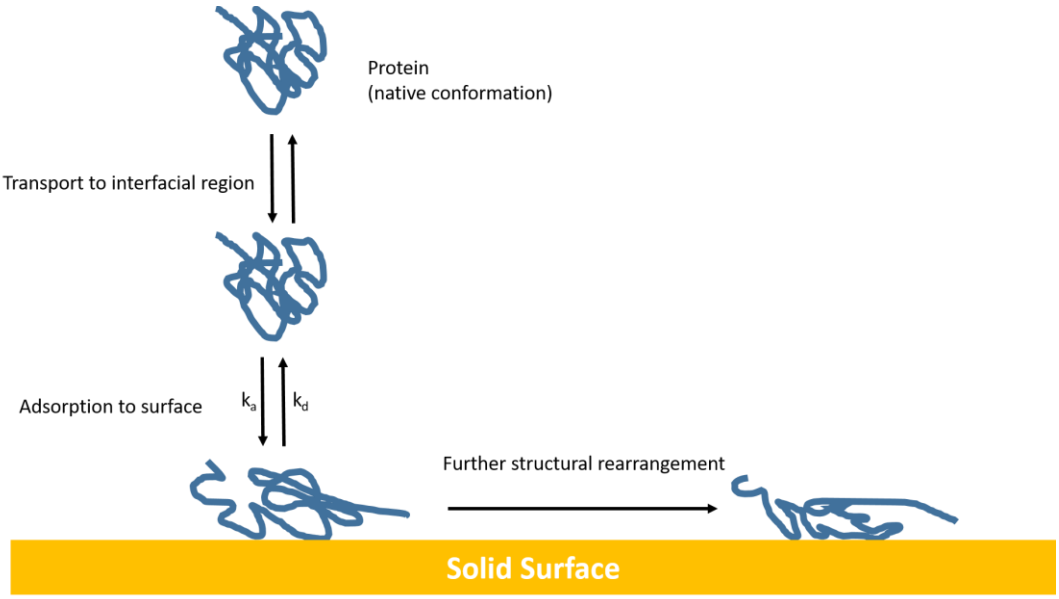


**Figure 7:** Protein adsorption model (*with adaptation*). [45]

### 3.3. Strategies for the separation of basic protein/ peptides by CE

Some of the strategies that haven been reported to improve efficiency and resolution of protein/ peptide CE separation include an adjustment in BGE strength, pH, or the addition of additives to BGE [47-49].

### 3.3.1 Adjustment of the ionic strength of BGE

Two methods used to enhance the separation efficiency of protein/ peptide CE separations are through the use of sample stacking and high ionic strength BGE [50]. Sample stacking is an on-column concentration technique that requires that the sample to have a lower conductivity than of the BGE. When a voltage is applied within the capillary, the differences in concentration of electrolytes (conductivity) between the sample plug and BGE, cause ions in the sample to experiences a higher electrical field then the rest of the capillary. Therefore, ions stack at the boundary between the sample region (high electrical field) and the BGE region (lower electrical field).

For example with cations, the high electrical field strength in the sample region causes positively charged analytes to migrate fast until they reach a low field strength of the BGE where they slow down and stack at the sample BGE region interface [Figure 8] [51]. This sample stacking techniques may provide higher peak efficiency and sensitivity enhancement in CE and can be beneficial for high sensitivity analysis of proteins/ peptides. One CE-MS investigation of the effect of sample stacking was performed by Yang et.al[52] on synthetic and bioactive peptides. They investigated the impact of the sample soloution properties such as acidity and conductivity on sample stacking. They reported better detection limits with a 3000-fold enhancement of sensitivity, with peptide detection of concentrations in low nano-molar range.

The use of a high ionic strength BGE can also reduce analyte adsorption by suppressing the ionic interactions between charged proteins/peptides and the ionized silanol groups of the capillary wall. However, some caution must be taken since high ionic strength BGEs can cause hydrolysis or denaturation of some proteins [50]. Also, a high concentration BGE within the CE system will alter the double layer thickness, leading to a decrease in the EOF and an increase the

migration times of analytes. Also, BGEs with very high ionic strengths may lead to Joule heating, thus requiring lowering the current by applying a lower voltage across the capillary.

### 3.3.2 Adjustment of BGE to basic pH

CE analysis of proteins and peptides at extremes of pH has been used to minimize analyte-wall adsorption in particular cases, but not as a general strategy for protein/peptide separations [44]. The adjustment of the pH of BGE to alkaline pHs will provide a faster EOF through increasing of the ionization of silanol groups at the surface of fused silica capillaries [Figure 9]. Most proteins/ peptides are zwitterionic molecules. Therefore, at basic pHs (pH 8-11), there is a reduction of the protonation of the N-terminus, and amino group residues, such as in lysine, and an increase in the ionization of the C-terminus and acidic residues of these molecules. For proteins or peptides with pI < pH of the BGE, alkaline conditions cause an increase in the number of ionized silanol groups on the surface of fused silica capillaries as well as increase the overall negative charge of the protein or peptide. This may cause an electrostatic repulsion to occur and lead to a decrease in protein/ peptide adsorption on the capillary surface[49], although the negatively charged species will favor to migrate to the anode, the stronger EOF drives the charged species to the cathode. This phenomenon has been reported by Lauer and McManigill [53] in the separation of several proteins with pIs ranging between 7 and 11.

It should be noted that, in some cases, an extreme increase in the pH of the BGE can result in damage or hydrolysis of the protein or peptide [54]. In addition, precipitation may occur when the pH of the BGE is approximately equal to the pI of the protein/peptide. The loss of protein/ peptide by precipitation may be minimized by the addition of a surfactant or organic solvents within the

BGE. It is advised not to run CE analyses at pHs above pH 11. This is because Joule heating is observed at these pHs due to high currents produced by BGE with pH >11. In addition dissolution of the silica can slowly start and causes change in the EOF over time [54].

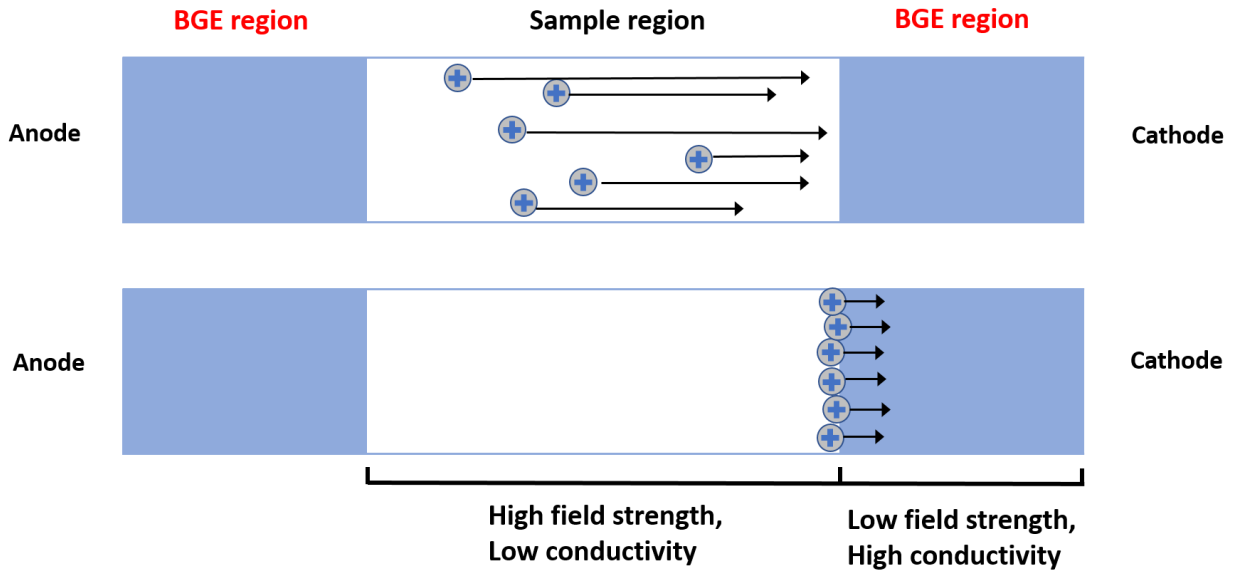


**Figure 8:** Diagram explaining the principle of sample stacking in CE

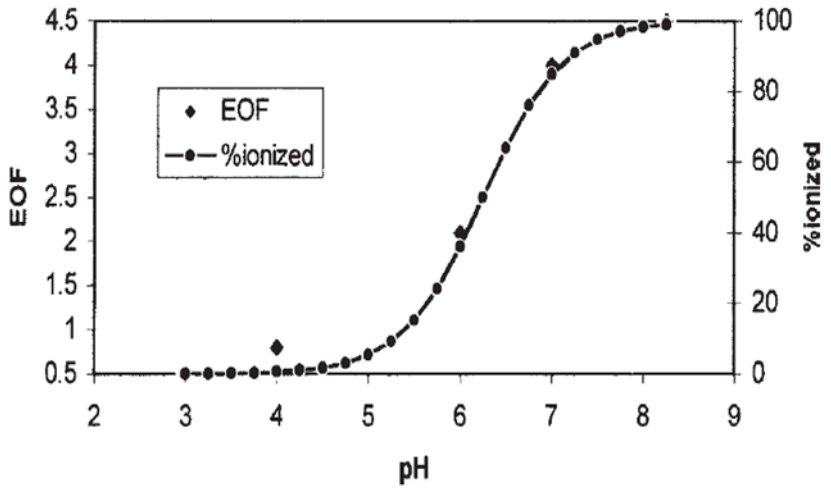


**Figure 9:** The effect of pH on EOF mobility for a fused silica capillary.[55] *(Reprinted with permission)*

### 3.3.3 Adjustment of BGE to acidic pH

A less popular approach to enhance protein/ peptide separation is by the adjustment of the BGE pHs to an acidic pH (2.5-5.0) [52, 54]. Lower pHs cause a lower number of ionized silanol groups on the capillary surface. This reduction of the number of activated silanol groups can enhance the separation efficiency by minimizing electrostatic attraction of positively charged protein/ peptide with the capillary wall, in addition to suppressing the EOF [56]. In addition; operating at pHs below the protein/peptide pIs will cause protonation of protein/ peptide and yield faster mobility of the analyte to the cathode and may affect the resolution of the separation.

McCormick [57] published one of the first papers on CE separations of protein mixtures using low pH phosphate buffers (pH 1.5 to 5.25). He found that at very low pH values, poor separations occurred due to the similarity of mobility of the proteins in the mixtures to be separated at pH 1.5.

However, when the proteins mixture was analyzed at a higher pH (4.0), the mobility differences between the proteins became larger and enhanced their separation. Further increases in BGE pH above 5.2 lead to worsening of both resolution and separation efficiency due to the increased EOF and peak tailing due to adsorption of the proteins.

### 3.3.4 Addition of background electrolyte additives

Dynamic coating of the inner wall of the capillary by physical adsorption of the coating material dissolved in the BGE, can reduce the undesirable adsorption of analytes and/or may reduce the EOF. The dynamic coating method is an attractive approach due to the simple and quick coating process. In addition, it is easy to remove of the coating material from the capillary walls using appropriate rinsing procedure. Surfactants are the most widely used BGE additives for dynamic coating. These include both ionic and nonionic surfactants. Other additives can also be used such as amines, short chain polymers and ionic liquids (IL) [58-59].

Cationic surfactants, such as dodecyltrimethylammonium bromide (DTAB), cetyltrimethylammonium bromide (CTAB) and didodecyldimethylammonium bromide (DDAB) [60-62], are frequently added to the BGE to reduces electrostatic adsorption of positively charged protein/ peptides with negativity charged silanol capillary walls and cause a reversal of the EOF due to the adsorbed cationic surfactants onto the inner capillary wall. Although, DTAB and CTAB are the most widely used cationic surfactants used for dynamic coating in protein /peptide CE separations, newer materials have been frequently tested. For example, the novel positively charged surfactant, N-dodecyl-N,N-dimethyl-(1,2-propandiol) ammonium chloride (DDPAC), was synthesized by Znaleziona et.al. [58] and used as a dynamic coating in CE. The cationic

surfactant caused reversal of the EOF and reduction of the electrostatic adsorption. It was then possible to separate a mixture of basic proteins that included ribonuclease A, myoglobin, lysozyme and cytochrome c. The best separation was achieved by using a BGE of 100 mM acetate (pH5) containing 10.0 mM DDPAC. The separation was then compared to one obtained using equal concentrations of DTAB or CTAB in 100 mM acetate (pH5). Separations using DDPAC as the BGE additive provided better resolution of the four proteins as well as separation efficiency compared with DTAB or CTAB.

The reported applications of ionic liquids (IL) to CE peptide/protein separations are limited. An example of the use of ionic liquids as a stationary phase using the dynamic coating method was described in the research article by Guo et.al [63]. N-methyl-2-pyrrolidonium methyl sulfonate was used as an additive within the BGE and increased the CE separation efficiency of several basic proteins such as lysozyme, cytochrome c, ribonuclease A, and α-chymotrypsinogen A. Under optimal separation conditions (pH 5), the protonated amine of the IL is electrostatically attracted to the negatively charged silanol groups of the capillary wall in addition to the formation of a hydrogen bond between the N−H of amine and the silanol groups of the capillary [Figure 10]. A fast baseline separation of the four proteins was obtained with the coated capillary (i.d. = 75 μm, $L_T$ = 50 cm, $L_D$ = 41cm), with the separation efficiency ranging from 209,000−448,000 plates/ m.

### 3.3.5 Capillary gel electrophoresis

The most popular and most widely used form of electrophoresis for the separation of proteins is sodium dodecyl sulfate-polyacrylamide gel electrophoresis (SDS-PAGE), where proteins are separated by differences in size of the produced SDS-proteins complex. This technique

is known to be a time consuming and labor intensive method that requires multiple steps (preparation of the gel, sample preparation, loading, and staining). Capillary gel electrophoresis (CGE) is the capillary version of slab gel electrophoresis. CGE has the advantage of having a high resolving power, on-column detection and protein quantification[64].

The major difference between CGE and CE is that with CGE the separation medium is a sieving matrix, whereas in CE the separation medium is the BGE. Different sieving matrixes have been used in CGE; these include linear and cross-linked polyacrylamide, polyethylene glycol, and dextran[65-66]. Mostly within CGE, proteins are treated with a detergent (most commonly SDS) causing the charge differences between proteins to be normalized (i.e. having the same charge-to-mass ratio, however this assumption may not always hold for positively charged and hydrophobic proteins). The EOF in CGE is mostly suppressed, and the separation of proteins are mainly based on the mobility of a SDS coated protein within the sieving matrix, with smaller size proteins having the greatest mobility. Differences between SDS-CGE and SDS-PAGE, include the ability to be automated with on-line detection and the fact that protein quantification can be accomplished in a shorter time, since higher field strengths can be applied.

The capillary format is the most common format for gel electrophoresis in both pharmaceutical and biological research laboratories, next to slab-gels. Microchip devices have also been used for gel electrophoresis of proteins [67]. A major advantage of performing capillary gel electrophoresis (MCGE) in microchannels is the fast separation time of microchips compared to capillaries. P. Schultz's (1999) 68 lab was one of the earliest research groups to transfer SDS-CGE based methods from capillaries to the microchip format, reporting the separation of a mixture of six proteins with a molecular weight ranging from 9 kDa to 116 kDa in less then 40 seconds. More recently Seyfried et. al. [69] reported the successful separation of PEGylated human serum albumin

(PEG-HSA). This method was used to determine the degree of PEGylation in a reaction sample of HSA with a 20 kDa branched PEG [Figure 11]. Compared to SDS-PAGE, Seyfried was able to combine the time consuming multi-step process of the conventional SDS-PAGE method into a one-step MCGE system.

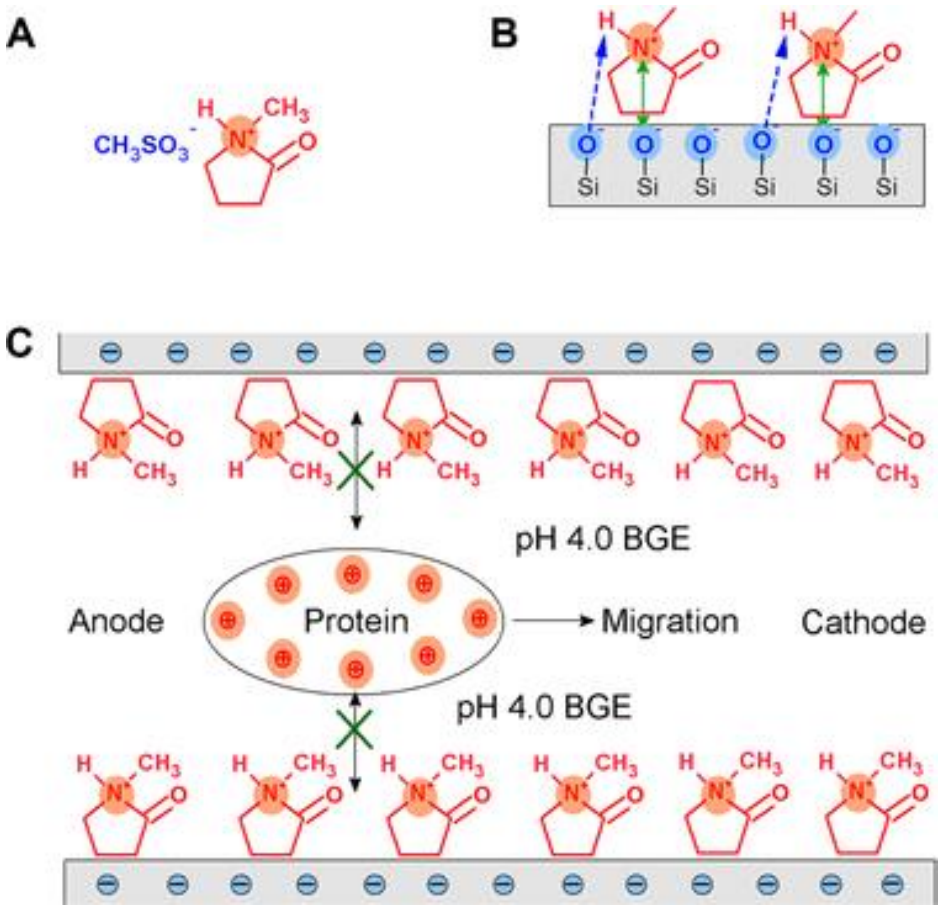


**Figure 10:** (A) The structure of $[NMP]^{+}CH_3SO_3^{-}$ (B) the interaction between $[NMP]^{+}CH_3SO_3^{-}$ and the silica capillary wall; (C) the mechanism of separation of proteins using $[NMP]^{+}CH_3SO_3^{-}$ as dynamic coating.[63] *(Reprinted with permission)*

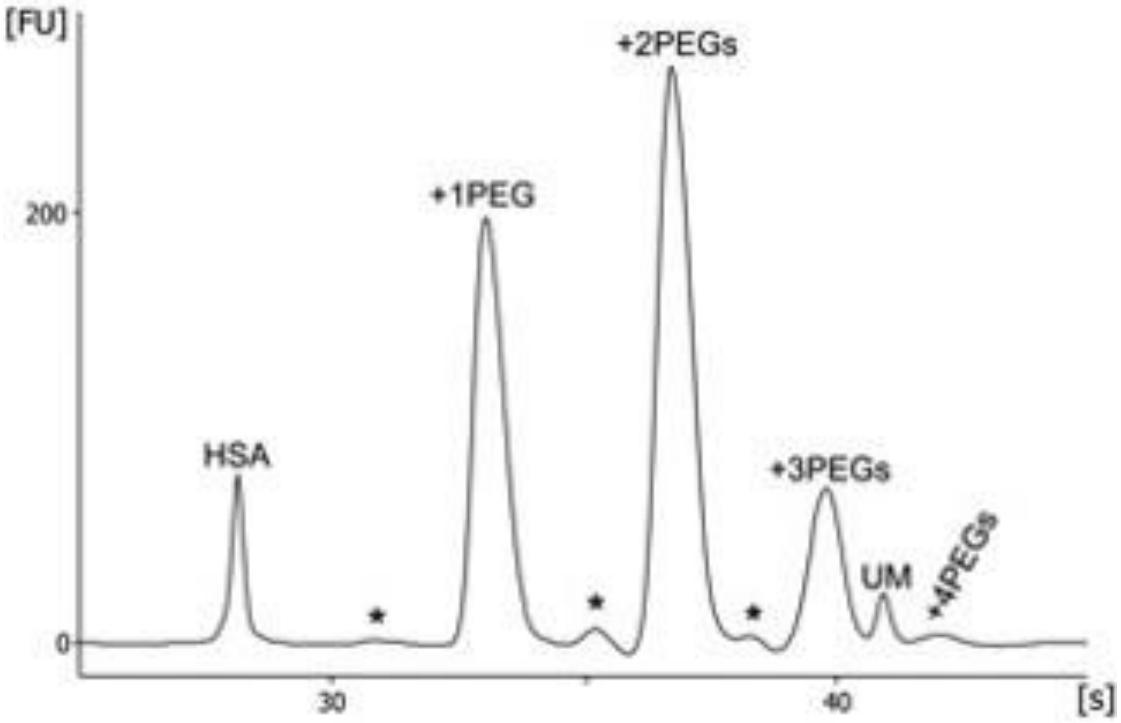


**Figure 11:** MCGE electropherogram of separation of a multiply PEGylated protein HSA sample.[69]

(*Reprinted with permission*)

### 3.4 Capillary electrochromatography

Capillary electrochromatography (CEC) is a technique that combines the principles of capillary electrophoresis (electroosmotic flow of bulk solution and electrophoretic mobility of the analyte) and principles of chromatography (distribution of the analyte between the stationary and mobile phases). The technique was first reported by Strain (1939) for the separation of a mixture of dyes using an applied electric field across a packed column[70]. According to F. Svec and other authors, the term electrochromatography was coined by Berraz in 1943[71-73]. Decades later, CEC has grown in popularity with applications in a broad number of areas including environmental, food and pharmaceutical analysis[74-75] in addition to, proteomic research[76], disease biomarkers, or pharmaceutical and biotechnology products[77]. Proteins/peptides differ from each other in charge, polarity, molecular mass and solubility among many other physical or chemical properties. As described above, CE separations of peptides and proteins are primarily based on the differences of the charge to hydrodynamic size. However, in CEC other parameters may influence the separation. The main one being differences in polarity causing adsorption/partitioning events to occur at the surface of the stationary phase. Other separation parameters that may influence resolution include pH and the type and fraction of nonaqueous solvents within the CEC BGE (mobile phase).

#### 3.4.1 Theory of CEC

The most frequently used classifications systems for CEC analysis of protein/ peptide are based on the capillary column format and the mode of separation. The first can be divided into packed partials columns, monolithic columns, and open-tubular capillary electrochromatography (OT−CEC) [Figure 12]. The mode of separation is based on differences in the stationary phase.

Examples include normal phase (NP), reverse-phase (RP), cationic or anionic ion-exchange, affinity or size exclusion separations.

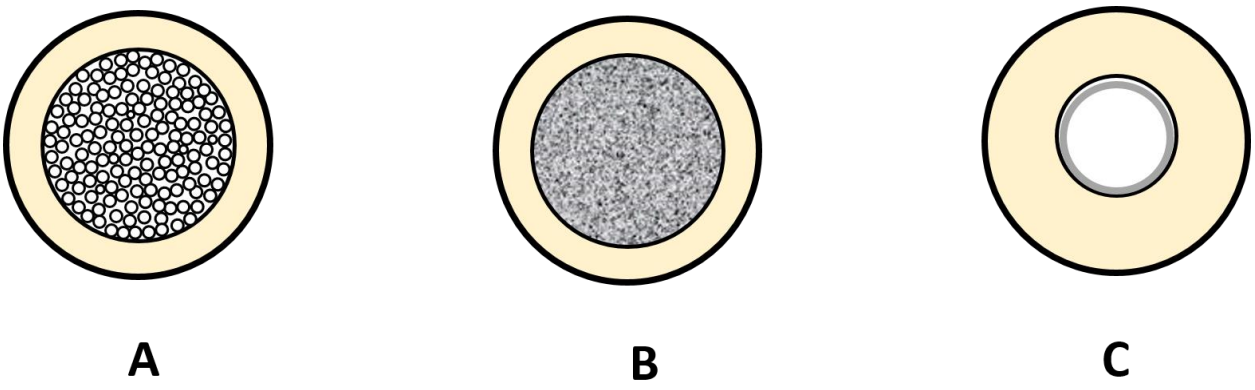


**Figure 12:** Classification of the packing state for columns for capillary electrochromatography: (A) packed stationary phase CEC column, (B) monolithic CEC column, (C) open-tubular CEC column.

Unlike LC, flow in CEC is generated by EOF, rather than pressure, because both the surface of the capillary wall and the stationary phase are charged. A plug-like flow profile is therefore produced inside the capillary[78]. Similar to CE, the magnitude of the EOF in CEC is proportional to the zeta potential of the electrical double layer at the surface of the stationary phase[78].

$$\mu_{eo} = (\varepsilon_o \varepsilon_r \xi)/\eta \qquad (3)$$

where ($\varepsilon_o$) is permittivity of a vacuum, ($\varepsilon_r$) is relative permittivity of medium (dielectric constant) and ($\eta$) is viscosity of the solvent.

In packed CEC, the surface area of the stationary phase is significantly larger than of the surface wall, and subsequently the contribution of the wall to the EOF is small, and the zeta potential is affected by the charge density at the surface ($\sigma$)[78].

$$\xi = (\sigma\delta)/(\varepsilon_o\varepsilon_r) \quad (4)$$

The liner velocity of the fluid in a EOF driven CEC system is proportional to the electrical field strength.

$$u_{eo} = \mu_{eo}E = (\mu_{eo}V)/L \quad (6)$$

From equation 6, it can be seen that higher field strengths cause an increase of the EOF. For a packed CEC column, the porosity of the packaging is considered to determine the mobility of the mobile phase. Also the CEC flow is affected by the physical characteristics of the mobile phase ($\varepsilon$ and $\eta$), its ionic strength, the surface charge (due to the pH and the stationary phase properties).

For a monovalent electrolyte, the thickness of the electrical double layer ($\delta$) is affected by molar concentration (c) of the electrolyte[79]:

$$\delta = [(\varepsilon_o\varepsilon_r RT)/(2cF^2)]^{0.5} \quad (7)$$

where T is absolute temperature, R is the universal gas constant (8.314 J/ mol. K) and F is Faraday constant ($9.65 \times 10^4$ C/mol.). From equation 7, we can see that the higher concentration of the BGE will decrease thickness of the double layer and that will lead to a decrease in the EOF.

CEC has the potential to provide high-efficiency separations of proteins/peptides since the flow in CEC is a plug like leading to less dispersion. The Van Deemter equation can be used to illustrate the effect of different factors on band broadening:

$$H = A + B/u + Cu \quad (8)$$

$$h = H/d_p \quad (9)$$

Where (H) is the plate height, (u) is the average linear velocity, h is reduced plate height, and $d_p$ is the CEC particle size. The term A, B, and C are eddy diffusion, longitudinal diffusion, and mass transfer terms respectively. The A, B, and C terms can be quantified, and equation (8) can be presented as[78]:

$$H = 2\lambda d_p + 2\gamma D_m + c(d_p^2/D_m) \quad (10)$$

Where ($\lambda$) is packing factor, ($\gamma$) is the stationary phase obstruction factor, ($D_m$) is the analyte diffusion coefficient. Unlike LC, in CEC the effect the A term is minimal, because of the plug flow profile of the EOF this lowers the multipath band dispersion [80]. Moreover, the C term is also reduced compared to LC due to intra-particle EOF through the porous particles that have a lower mass transfer resistance. The lower values of the A and C terms in equation (8) for CEC, explains the high efficiency obtained with CEC separation compared to LC. Also, due to plug flow of the EOF, the flow velocity is independent of particle size in CEC, and longer capillary columns with small particles can be used without worrying about back pressure[81].

### 3.4.2 Packed columns

CEC based packed columns were used in the earliest applications of CEC [82]. Typically, fused silica capillaries are used that have inner diameters of less than 100 µm with particle sizes between 1.5-5 µm[80]. The packing materials used for CEC are the same particles that are commonly

used for reverse phase or ion exchange liquid chromatography (LC). For example, most of the research that has been done concerning RP-CEC used C18-modifed silica particles (1.5-5 µm in diameter). Table 2 lists commonly used packing materials for RP-CEC [80]. The packing methods that are used for packing CEC columns are similar to those employed for LC columns. These methods include pressure packing of slurries of particles in LC solvents, supercritical $CO_2$, electrokinetic packing, using centripetal forces, or gravity[83-84]. A more detailed description of each of these methods can be found in the review by Colon et. al. 2000 [83].

| Packing material | Particle size (µm) |
|---|---|
| Hypersil C18 | 3, 5 |
| Spherisorb C18 | 3 |
| Nucleosil C18 | 3, 5 |
| Zorbax C18 | 6, 7 |
| Gromsil C18 | 3,5, 7 |
| Vydax C18 | 3, 5 |

**Table 2:** Commercially available reversed phase packing materials commonly used in CEC. [Table from Li.et.al. [80]]

### 3.4.2.1 Reversed phase CEC

The first separation of peptides using reversed phase CEC was reported by Schmeer et. al. 1995 [88-89]. They separated a mixture of enkephalin methylester and enkephalin amide, using a CEC column packed with 1.5 µm RP stationary phase coupled to mass spectrometry. More recently, a

number of other application for the analysis of protein/peptide have been reported, due to the advances in packing technology of CEC columns [88].

Liu et al. reported a rapid preparation method for capillary CEC columns. This method involves the use of the CEC mobile phase solution as the packing and conditioning solvent and allows for rapid preparation of capillary columns based on a single particle fritting technology. This led to a high throughput preparation of CEC columns (1 column/h) that included all the fritting, packing and conditioning steps, compared with a time-consuming multistep CEC column fabrication process − e.g. sinter-fritted columns − that may take up to a total of 12−24 hours to complete. These RP CEC columns showed a high efficiency (150,000 N/m) and a retention times reproducibility of less than 0.8% RSD with a standard peptides mixture (Gly-Tyr, Val-Tyr-Val, Met-enkephalin, Leu-enkephalin and angiotensin II) [90].

Other research groups have studied the separation performance of different packing materials within the CEC columns on the separation of a cytochrome c tryptic digest. The peptides were separated on C18 silica-based stationary phases of different properties and origin, in addition to a CEC capillary packed with cyanosilca particles. It was reported that both C18 and cyanosilca CEC columns obtained high separation efficiencies, in addition to short analysis times. Their work also showed that the cyanosilca particles CEC packed capillaries provided an overall better separation of a cytochrome c tryptic digest [91].

It should be noted that individual amino acids, charge, size, hydrophobicity, and sequence can impact the overall charge density and hydrophobicity of proteins/ peptides and affect their CEC elution behavior. One study investigated the effect of C18 CEC retention behavior of 10 immunogenic peptide analogs (pI: 3.7 − 10.1). One was a peptidomimetic related to an HIV-1 $gp_{120}$ epitope and the other nine were short synthetic analogs of the parent peptide. The study used

a packed fused silica capillary (i.d. 100 µm and a total length 33.5 cm, packed length 25 cm), containing 3 µm C18 particles. The impact of mobile phase composition on the separation of these peptides was investigated. It was shown that the mobile phase properties, such as pH, buffer concentration and the choice and concentration of the organic modifier, can be selected to favor either electrophoretic mobility or chromatographic retention. This makes it possible to effect the overall selectivity of CEC for the peptides by exploiting both separation mechanisms[92]. For example, at high pHs of the mobile phase, acidic peptides became more negatively charged and therefore migrated more rapidly to the anode, thus favoring an electrophoretic mobility separation mechanism. However, by adjusting the fraction of ACN within mobile phase, the hydrophobic interactions between the n-alkyl ligand of the stationary phase and hydrophobic peptides can be exploited. The hydrophobic peptides in the mixture were retained longer on the CEC column at lower percentages of ACN. The increase in the fraction of ACN in the mobile phase cause the hydrophobic interactions to decrease and thus the electrophoretic mobility of the peptide and the EOF becomes the most dominant effect for the migration of both acidic and basic peptides within the mixture.

#### 3.4.2.2 Ion-exchange CEC

##### 3.4.2.2.1 Capillary electrochromatography ion-exchange columns

Various ion exchange packed CEC columns, have been used for the separation of peptides/proteins including strong cation (SCX), strong anion ion-exchange (SAX) columns, weak cation exchange (WCX) and weak anion exchange (WAX) columns.

A CEC separation of insect oostatic peptides (IOP) was achieved using a capillary packed with a strong-cation-exchange stationary phase (3 µm propyl sulfonic acid modified silica particles)[93]. The effect of different experimental parameters (organic modifier, ionic strength, buffer pH, applied field strength, and temperature) on the resolution of the IOP peptides was evaluated. Baseline separation was achieved using a mobile phase that consisted of 100 mM $NaH_2PO_4$ buffer (pH 2.3) /$H_2O$/ACN (10:20:70%). The selection of the experimental parameters strongly affected the retention factor ($k'_{CEC}$), retention time and resolution of the analytes. For example, ACN content within the mobile phase is known to affect the viscosity, zeta potential, and dielectric constant of the mobile phase. By increasing the percentage of ACN within the mobile phase from 40 –80%, there was an increase in $k'_{CEC}$, and improved resolution. The increase in the percentage of ACN also enhanced the hydrophilic interactions of the peptides with both the free silanol of the fused-silica capillary and sulfonic groups of the stationary phase. On the other hand, a higher fraction of ACN enhanced the hydrogen bond interaction between the IOPs and sulfonic acid modified silica particles.

**3.4.2.2.2 Microchip ion-exchange electrochromatography**

Although most research articles on CEC that have been published deal with packed capillaries, there are a limited number of articles that focus on the packing and different applications of CEC with a microchip system [94-96]. This is mainly due in part to the difficulty of packing microfluidic channels with stationary phase materials [96]. Microfluidic chip-based bead-packed columns for electrochromatography have been used with several types of stationary phases such as silica colloidal beads [94] and octadecylsilane-coated silica beads[97]. One example is a fabrication of microchip electrochromatography chips with columns of only 2 mm in length. These

micro-fabricated devices were then used for the separation of FITC-labeled peptides by ion-exchange using a 488 nm Ar ion laser for LIF detection. A mixture of three FITC labeled peptides (FITC-dilysine, -trilysine, -tetralysine) was separated using strong cation-exchange beads (Pheno Sphere®SDX), and a BGE that consisted of 60 mM $KH_2PO_4$/ ACN/ tween 20 [60: 40: 0.025]. The peptides were baseline resolved with separation efficiencies of up to 400,000 N/m and run times of less than 40 s. The retention times of the three separated peptides were reproducible (RSD <3%) [95].

### 3.4.2.3 Specially packed CEC stationary phases

Enantioseparation of amino acids and dipeptides can be accomplished with a packed CEC column with silica-based ligand-exchange chiral stationary phases (CSPs) [98]. These CSP CEC column were prepared by two different approaches. The first involved a dynamic coated layer of the chiral selector N-decyl-L-4-hydroxyproline onto an RP packed capillary. The other approach involved chemically bonding L-4-hydroxyproline to 3 μm silica material. Better resolution for the enantioseparation of amino acids and dipeptides of enantiomer mixtures was obtained using a chemically bonding method compared to the dynamic coated method [98].

Liao et. al. [99] were able to develop a rapid one-step approach for the preparation of anti-voltage photonic crystals (PCs) as a stationary phase within a microchip channel. This is frequently a time-consuming method that requires many steps. The heat-accelerated one-step approach produced a crack-free and stable PCs stationary phase within the channels within 15 mins. Figure 13 illustrates the PC assembly process. By using these PCs and a BGE of 20 mM $NaB_4O_7$ (pH 10.02) and a field strength of 1000 V/cm, they were able to separate a mixture of three FITC

labeled amino acids in 4 s and a mixture of four FITC labeled oligoglycin peptides in 12 s [Figure 14]. This was accomplished using a microchip with a channel with an effective length ($L_D$) of 2.5 mm and total length ($L_T$) of 1cm. These separations exhibited good reproducibility of migration times (RSD 0.24%–0.35%) and peak heights (RSD 1.1%–3.1%).

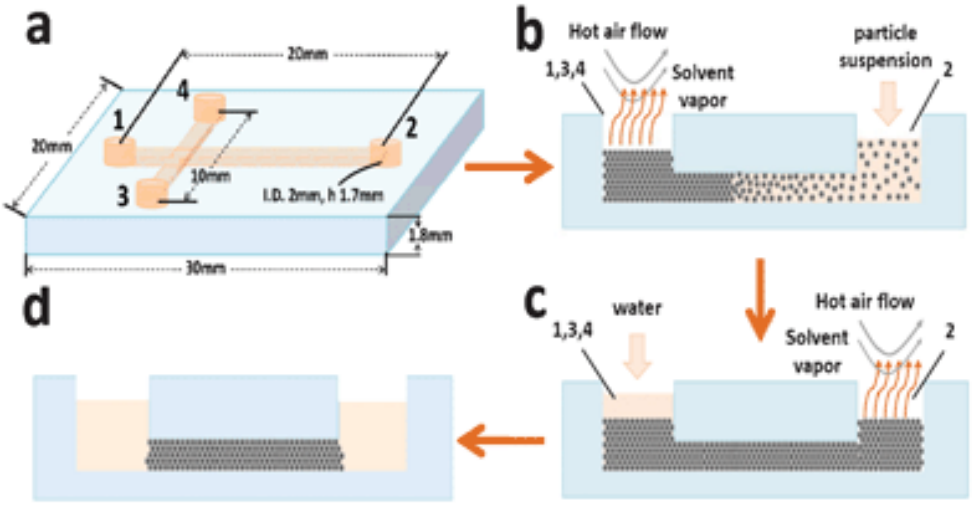


**Figure 13:** Flowchart showing (a) the assembly of stable PCs into glass MC channels by (b and c) heating with a hot air flow to accelerate the evaporation-induced assembly (b) and to fix the assembled ends (b and c). The fixed PCs was used after the removal of the particles in the reservoirs (d). [99] *(Reprinted with permission)*

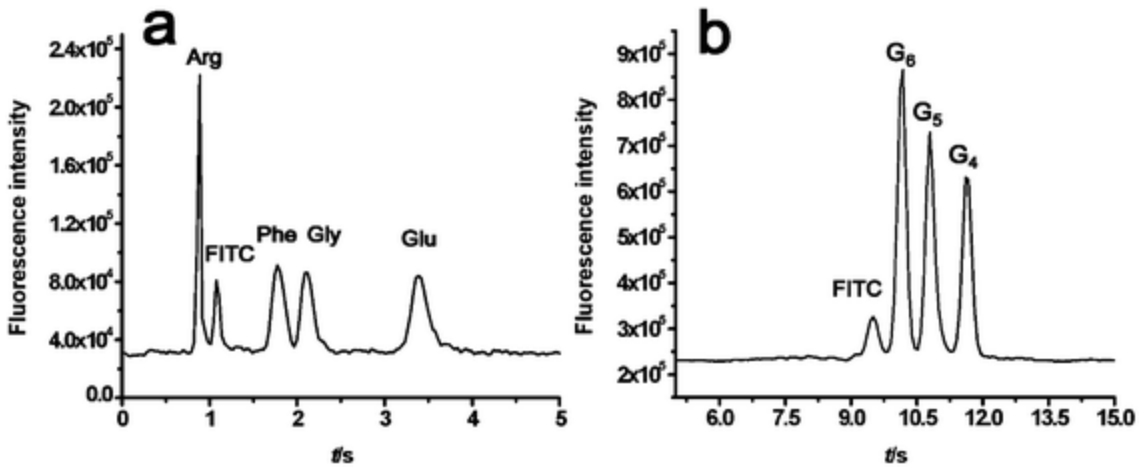


**Figure 14:** Separation of (a) FITC-labeled amino acids at 1200 V $cm^{-1}$ (b), FITC-labeled peptides at 1000 V $cm^{-1}$. BGE: 20 mM $Na_2B_4O_7$ at pH 10.02. The $L_D$ and $L_T$ were 2.5 mm and 1 cm, respectively[99]. *(Reprinted with permission)*

### 3.4.3 Porous polymer monolith CEC

Porous polymer monoliths (PPM) have rapidly grown in popularity as stationary phase materials for the separation of protein and peptides by CEC. A major reason for this is that the packing of narrow diameter capillaries with particles can be a multi-step process that requires considerable skill to obtain stable columns with reproducible properties. In addition most packed CEC columns require frits that add to the difficulties of manufacturing these columns. Monolithic columns can be prepared directly within a capillary or microchip, thus avoiding difficulties seen with the packing of capillaries and frit formation.

For the production of monolithic columns, a simple *in situ* polymerization process can be performed directly within the capillaries, thus avoiding packing and frit formation difficulties. Monolithic columns can also be produced with unique chromatographic properties for optimal

resolution and efficiency in protein/ peptide separations. The PPMs are covalently bonded to the capillary wall by the use of adhesion promoter such as 3-(trimethoxysilyl)propyl methacrylate. This increases the column robustness.

The chemical properties of the PPM can also be controlled by optimizing the composition of the polymerization mixture. The polymerization mixture is composed of monomers, an initiator, and a porogenic solvent. Materials used as monomers include polar materials, such as 2-cyanoethylacrylate [100], acrylamide, 2-hydroxyethylmethacrylate [101], and 2-acrylamido-2-methyl-1-propanesulfonic acid [102]. Nonpolar materials such as butylmethacrylate [102], hexylacrylate [103], lauryl methacrylate and octadecylmethacrylate [104]; and cross-liker such as ethylenedimethacrylate [105] can also be used. Initiators, such as azobisisobutyronitrile (AIBN) [106], are frequently used in monolith production. Polymerization reactions can be initiated either thermally or by UV-initiated free radical polymerization [107-108]. Different porogenic solvents with a range of polarity have been used in the preparation of PPM such as 2-propanol [109], 1-octanol [110], 1-dodecanol, and toluene [107]. The porogenic solvents have an effect on the pore size within the PPM structure. Monolithic structures with small microglobules (due to numerous nuclei that are formed within polymerization mixture) and small pores may be formed using porogenic solvents with low polarity. In contrast, the use of porogen solvent with a higher polarity can lead to the formation large size pores within the structure of the PPM capillary [111].

#### 3.4.3.1 RP CEC monolithic column

To reduce electrostatic interaction of analyte to the monolithic columns, Karanfa and El Rassi [112] developed multiple versions of a neutral, reverse phase monolithic columns for CEC

separations of proteins/peptides. One example of a column used in their work is a reverse phase hydroxylated octadecyl monolithic column (ODM-OH). This monolithic column was prepared by first pre-treating the capillary with 3-(trimethoxysilyl)propyl methacrylate, followed by the polymerization mixture of octadecyl acrylate (ODA) as the monomer and pentaerythritoltriacrylate (PETA) as the crosslinker. AIBN was used as the thermal initiator. An aqueous porogenic solvent that contained cyclohexanol and ethylene glycol was used in the fabrication of the column. The monolithic column produced a cathodal EOF over a range of pHs, despite not having a full charge. The EOF was reported to be due to the polar OH functional group on PETA lead to an increase of the surface polarity of the monolith and thus an increase in the zeta potential and resulted in an enhancement of the EOF.

The monolithic column was used for the separation of a mixture of the following proteins (pI 4.2-11): lysozyme, cytochrome c, carbonic anhydrase, β-lactoglobulin B, β-lactoglobulin A, and α-lactalbumin. The mobile phase used was 10 mM sodium phosphate (pH7) containing 50% ACN. The proteins eluted in order of pI, with lysozyme (most basic) eluting first and α-lactalbumin (most acidic) eluting last. All six proteins eluted in 11.5 min and the average number of theoretical plates was calculated to be 201,000 N/m. They also were able to use the developed ODM-OH column to separate a complex tryptic protein digest of chicken egg white lysozyme, that would have otherwise required a lengthy gradient elution method with LC.

#### 3.4.3.1 Ion-exchange CEC monolithic column

Ludewig et.al [113] reported the use of a weak-ion exchange (WCX) monolithic column for the separation of mixtures of diastereomers and α/β-isomers of α/β-D/L-Asp-L-PheOMe, L-Phe-α/β-

D/L-Asp-GlyOH and L-Phe-α/β -D/L-Asp-Gly$NH_2$. The column was produced by first pre-treatment of the capillary with 3-(trimethoxysilyl)propylmethacrylate followed by *in situ* polymerization of acrylamide, 4-acrylamidobutyric acid and methylenebisacrylamide and AIBN with decanol and DMSO as porogen solvent. The research studied the effect of the pH of the mobile phase on the mobility of the peptides and their separation. With acidic mobile phases containing ACN, the peptides are protonated and migrated mainly due to their electrophoretic mobility. At a more basic pH, the peptides have lower mobility due to deprotonation of the carboxylic acid groups and amines. However, increasing the pH of the mobile phase also caused an increase in the EOF due to an increase in the number of deprotonated carboxylic acid groups on the monolith. This also effected the elution of the peptides. The WCX monolithic columns was used to separate the diastereomers L-Phe-α/β-D/L-Asp-GlyOH with a mobile phase consisting of 20 mM phosphate buffer, pH 2.0 and 40% v/v ACN. The WCX monolithic column provided added selectivity and separation mechanisms, as the separation of all diastereomers of L-Phe- α/β -L/D-Asp-GlyOH, could not be achieved by CE nor LC.

### 3.4.4. Open tubular CEC

Open-tubular capillary electrochromatography (OT-CEC) was first reported in 1982 by Tusda et. al. [114]. He developed OT-CEC for the separation of aromatic compounds (benzene, biphenyl, naphthalene, anthracene, and 1,3,5-triphenylbenzene). Since then research on OT-CEC has focused mainly on the development of materials that can be used as stationary phases for the coating onto the inner wall of fused silica capillaries. Stationary phase materials are selected to improve selectivity based on the preferred chromatographic mechanisms. Materials with various chemical and physical properties can be used as components of the stationary phase such as long

non-polar hydrocarbon chains e.g. 1-octadecanethiol [115], high molecular weight charged polymers (e.g. polydiallyldimethylammonium chloride (pDDA) or polydopamine) and functionalized nanoparticles (e.g. β−cyclodextrin modified gold nanoparticles OT-CEC columns [116] or magnetic nanoparticle OT-CEC columns [117]). Advantages of OT-CEC over other CEC methods including ease of preparation. OT-CEC does not require particle−based packing materials or frits to keep the OT-CEC layer in place [118]. However, due to the low amount of stationary phase that is coated onto the inner surface, the phase ratios are small, which leads to low retention of the analytes. This can cause decreased selectivity for the separation of some analyte compared to packed CEC [119].

An important part of OT-CEC system is the stationary phase that coats the inner capillary wall. Two main factors affect the robustness of the stationary phase in OT-CEC. The first is the method of how the coating material is introduced, and the second is the stability of coating material under various separation conditions or after repeated electrophoresis runs. Recently, a variety of materials and coating approaches have been reported for OT-CEC column, improving both peak efficiency and resolution for the analysis proteins/ peptides. Table 3 lists examples of stationary phase materials that have been used for the analysis of various protein/ peptides.

| Analyte | OT-CEC Capillary coating | BGE composition | Detection | Remarks | Ref. |
|---|---|---|---|---|---|
| Basic peptide mixture (Trypsin, RNase A, Cyt-c, Lysozyme | AEPTS, (50 µm id, 55/30 cm $L_T/L_D$) | 10 mM phosphate (pH 3.5) | UV detection (214 nm) | 87,000 -110,000 N/m | [120] |
| Peptide mixture (bradykinin, angiotensin I, LHRH, oxytocin, and [met]-enkephalin) | Zn(II)- deuteroporphyrin, (50 µm id, 32/21 cm $L_T/L_D$) | 25 mM phosphate, (pH 4.0), 5% $^{v}/_{v}$ ACN; 10 mM hydroquinone | UV detection (214 nm) | | [121] |
| Protein mixture (lysozyme, Cyt-c, α-chymotrypsinogen A, RNase A (basic proteins) myoglobin, deoxyribonuclease I, β-lactoglobulin A, β-lactoglobulin B, α-lactalbumin, albumin (acidic proteins) | poly- ε -SUK, (50 µm id, 50/40 cm $L_T/L_D$) | 20 mM phosphate (pH 11.5) | UV detection (200 nm) | Polymer coating thickness 0.9 to 2.4 nm | [122] |
| Tryptic digest of Cyt-c | FS modified with 4-TPI/ SDEDTC/ Styrene, MAA, N-phenylacrylamide co-polymer (50 µm id, 50/41.6 cm $L_T/L_D$) | 25 mM phosphate (pH 6.8), 40% v/v ACN | UV detection (214 nm) | | [123] |
| Lysozyme, avidin, ovotransferrin, three glycoisoforms of ovalbumin proteins in egg white | GO nanosheet/ pDDA, (75 µm i.d. 60/ 50 cm $L_T/L_D$) | 5 mM phosphate buffer, pH 7.5 | UV detection (214 nm) | GO-PDDA@column shown reverse phase mechanism | [124] |
| Humman IgG and HSA | FS bonded with C5 moiety, (50 µm id, 49.5/41 cm $L_T/L_D$) | 30 mM citric acid and 25 mM β-alanine (pH 3) | UV detection (210 nm) | Higher N of C5 capillary compared to commercial etched C18 column | [125] |
| Protein mixture (RNase A, Myoglobin, Transferrin, Insulin | [Phe]-functionalized tentacle-type polymer. (50 µm id, 50.2/40 cm $L_T/L_D$) | 50 mM boric buffer (pH 8.8) | UV detection (200 nm) | Improve resolution compared to CZE | [126] |

**Table 3:** Summary of stationary phase used OT-CEC columns for the separation of protein/ peptides. Cyt-c: cytochrome c, RNase A: ribonuclease A, AEPTS: 3-[2-(2-aminoethylamino)ethyl-amino] propyl-trimethoxysilane, LHRH: luteinizing hormone releasing hormone, poly-ε-SUK: poly-ε-sodium-undecanoyl lysinate, 4-TPI: 4-(trifluoromethoxy)phenyl isocyanate, SDEDTC: sodium diethyl dithiocarbamate.

### 3.4.4.1 Covalent modification methods

Covalently bonding the stationary phase materials to the silanol groups of a fused silica capillaries inner wall has also been used to produce OT-CEC columns. Although this approach produces a stable coating with longer lifetimes in comparison to physical coating methods, it frequently requires a more complex coating procedure [127]. The stable coating provided by covalent bonds is preferred for some detection systems such as electrospray mass spectrometry (ESI−MS) where nonstable coatings, such as dynamic coating systems, may be incompatible. Ramsey's group [128] developed a microfluidic system coupled to ESI-MS, where the glass device was first coated with 3-(aminopropyl) di-isopropyl-ethoxysilane by chemical vapor deposition. This was followed by a covalent coating of the injection cross and separation channels with methyl-terminated polyethylene glycol n-hydroxy succinimide ester (NHS-$PEG_{450}$) via liquid phase PEGylation. The device was used for the separation of intact monoclonal antibodies charged variants [Figure 15].

A more complex coating method was developed by Aydoğan et.al. that uses a multistep process for the preparation of a tentacle-type polymer stationary phase attached to a polyethyleneimine (PEI) anion exchanger [129]. This column was used for the separation of three basic proteins (ribonuclease A, cytochrome c and myoglobin). The preparation procedure included initial silanization of the inner wall of a fused silica capillary. This was then followed by *in situ* graft polymerization with 3-chloro-2-hydroxypropyl methacrylate (HPMA−Cl) and PEI modification. The modified column provided a high anion exchange capacity, leading to enhancements in both retention and resolution for the separation of the three proteins. Baseline separation of all three peptides with theoretical plate numbers of 134,000 N/m was achieved by using a mobile phase of 40 mM phosphate buffer (pH 2.5) containing 25% ACN. The modified

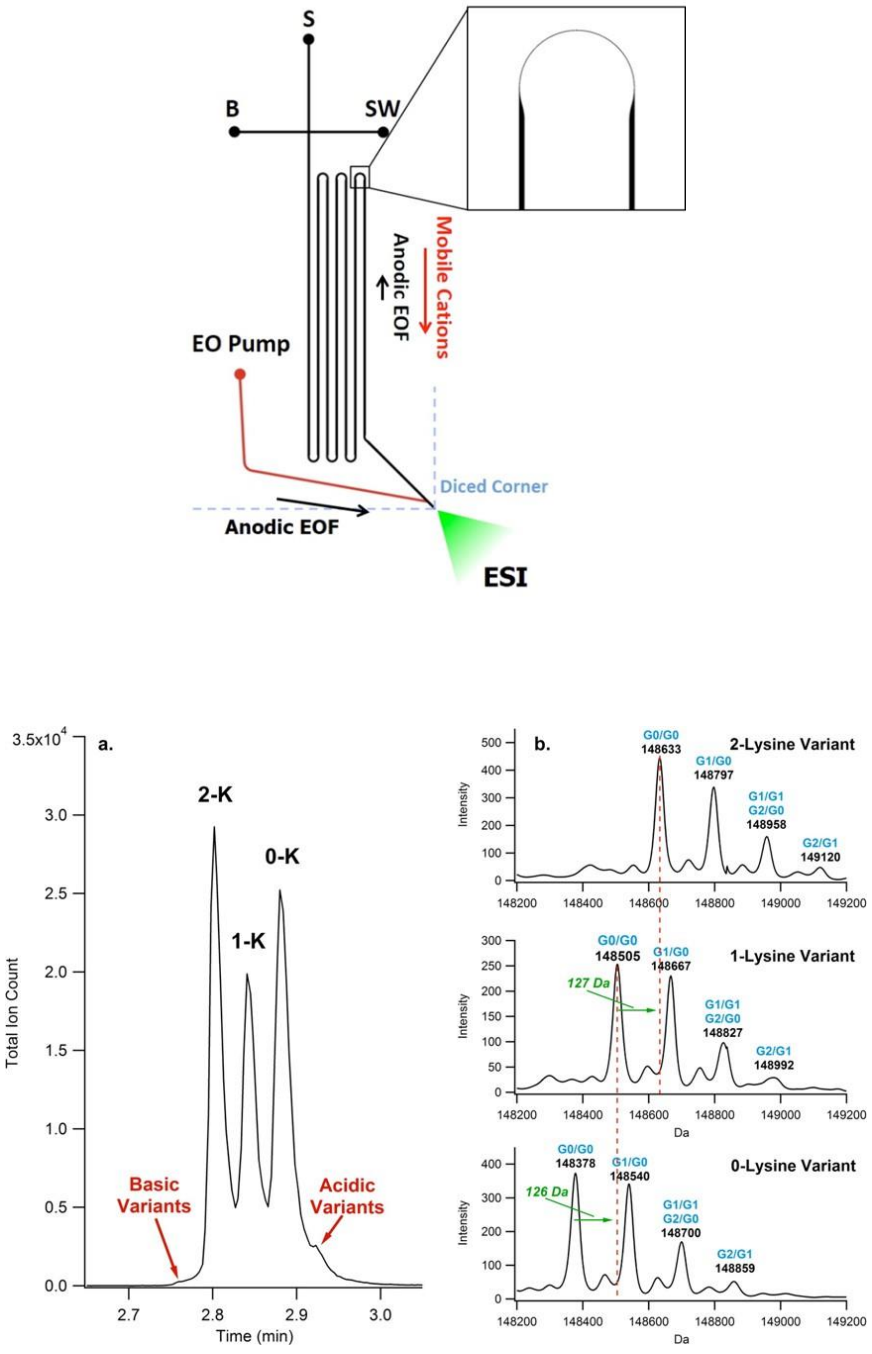


**Figure 15:** A) Schematic for CE-ESI devices with a 23-cm separation channel with an enlarged image of the asymmetric turn tapering. B) Separation of intact Infliximab charge variants using a 23-cm APS-PEG450 coated device at approximately 600 V/cm. Identified lysine variant bands are labeled as 2-K, 1-K, and 0-K[128]. *(Reprinted with permission)*

column was also shown to be stable for multiple runs with reproducible retention times for the separated proteins (SD of < 2%).

A less complicated method for preparation of OT-CEC column is to use *in situ* polymerization in the presence of porogen solvents. This forms a porous inner surface wall onto a capillary pretreated with γ-methacryloxypropyltrimethoxysilane. The porous polymeric layer stationary phase shows excellent mass transfer, due to a large number of micropores and mesopores on the porous surface, leading to enhanced resolution for protein/peptide separations. One example of the application of this method is the separation of cytochrome c and bovine serum albumin using a porous inner surface wall coated capillary made from a mixture of butyl methacrylate, ethylene glycol dimethacrylate, 2-acrylamido-2-methylpropanesulfonic acid and azobisisobutyronitrile and 1-propanol was used as the porogen solvent [130].

### 3.4.4.2 Nanoparticles coating approaches

Nanoparticles (NPs) are known to have unique physical and electrical properties. NPs have been frequently used in electrophoresis separation methods [131-132]. NPs have been used for stationary phases in OT-CEC to increase the surface area of the capillary inner wall. The large surface area to volume ratio of NPs can improve the chromatographic capacity of CEC. An advantage of the using nanoparticles in CEC is that selectivity and resolution may be improved by controlling the NPs size, shape, and capping agent. Also, NPs can easily be modified with a variety of functional groups that can include thiols, amines or carboxyl groups [133-134]. All these parameters will influence the interaction of specific analytes with the NPs.

Due to the advances in NPs synthesis methods, various methods have been found for the preparation of NPs. One of the most widely used methods for the preparation of gold nanoparticles (GNPs) is the Turkevich method, as GNPs can be prepared by chemical reduction of gold(III) chloride hydrate by sodium citrate. Miksik et. al. [135] were able to prepare a GNPs-based stationary phase that was used as an OT-CEC column. The column was prepared by rinsing a pretreated sol-gel column, with a solution of GNPs (prepared by Turkevich method). The research group evaluated the OT-CEC column by comparing them with an unmodified fused silica capillary. Both GNPs modified and the bare fused silica capillary were used for the separation of a complex tryptic digestion of bovine serum albumin (BSA). The GNP modified capillary reported better separation efficiency. The group also investigated different experimental parameters, such as BGE concentration and pH, on the separation efficiency and resolution. They reported the best separations of the tryptic peptides were found using a BGE consisting of 100 mM sodium phosphate buffer (pH 2.5), at a field strength of 175 V/cm ($L_T$ 57 cm, $L_D$ 47cm, and id 50 μm).

Another approach regarding nanoparticles for CEC involves the study of the effect of citrate stabilized gold nanoparticles coated capillary compare to bare fused capillary, for the analysis of a complex mixture of tryptic peptide fragments of human serum albumin (HSA). The immobilized GNPs OT-CEC column was prepared by rinsing a solution of GNPs to a surface modified capillary, that was pretreated with 3-aminopropyltriethoxy silane. The study has shown an improved resolution of HSA fragments by using GNP coated capillary [136]. Table 4 shows other examples of the applications of NPs in OT-CEC.

| Analyte | BGE composition | OT-CEC Capillary coating | Detection | Findings | Ref. |
|---|---|---|---|---|---|
| Synthetic analogs of an antimicrobial INWKKLGKKILGAL-$NH_2$, INSLKLGKKILGAL-$NH_2$, NWLRLGRRILGAL-$NH_2$ | 200 mM iminodiacetic acid (pH 2.3) | GNPs/ sol-gel-pretreated FS (50 µm id, 50/41.5 cm $L_T/L_D$) | UV detection (206 nm) | Use of low pH decrease basic peptides adsorption | 137 |
| ConA, BSA, α-Lac and β-Lg proteins | 40 mM phosphate buffer (pH 8.5) | $Fe_3O_4$-COOH MNPs/ pDDA, (50 µm i.d. 63/ 37 cm $L_T/L_D$) | UV detection (214 nm) | Two variants of β-Lg, three variants of BSA and nine glycolisoforms of OVA were separated. | 138 |
| Tryptic digest of native and glycated BSA and HTF | 100 mM phosphate buffer (pH 2.5) | GNPs/ sol-gel-pretreated FS | UV detection (214nm) | OT-CEC separation of complex peptide mixtures | 135 |
| Green fluorescent protein and GFP N212Y | 300 mM tricine, (pH7.5), containing 2% (w/w) anionic lipid-based NPs | Anionic lipid-based liquid crystalline NPs. (50 µm i.d. 24/ 6.7 cm $L_T/L_D$) | LIF detection, ($\lambda_{Ex}/\lambda_{Em}$ 488 nm/ 520 nm) | Separation of equally charged proteins | 139 |
| Glycine-ABEI in human saliva sample | 5 mM phosphate buffer (pH 8.5), containing 0.75 mM $H_2O_2$ | Thiolated β-cyclodextrin modified GNPs/ MPTMS pretreated FS (75µm i.d. 60/ 55.5 cm $L_T/L_D$) | chemiluminescence detection | Thiolated β-cyclodextrin modified capillary proved improve selectivity | 140 |
| GFP samples from E. coli | 100 mM tricine, (pH 7.5), containing 2% (w/w) cationic NPs | Cationic lipid-based liquid crystalline NPs (50 µm i.d. 24/ 6.7 cm $L_T/L_D$) | LIF detection, ($\lambda_{EX}/\lambda_{Em}$ 488 nm /520 nm | High efficiency (800,000 N/m) | 139 |
| Bradykinin, Angiotensin I, LHRH, Oxytocin, and Methionine-enkephalin | 20 mM potassium phosphate (pH 6.5) | GNPs / APTES pretreated FS (75 µm i.d. 41/ 31 cm $L_T/L_D$) | UV detection (214 nm) | Stability column | 136 |

**Table 4**: Summary of nanoparticles-based stationary phase of OT-CEC columns for the separation of protein/ peptides. MNPs: Magnetic nanoparticles, pDDA: polydiallydimethylammonium chloride, MPTMS: 3-mercaptopropyltrimethoxysilane, ABEI: N-(4-Aminobutyl)-N-ethylisoluminol, ConA: Conalbumin, OVA: Ovalbumin, α-Lac: α-Lactalbumin, β-Lg: β-lactoglobulin, GO: Graphene oxide, BSA: Bovine serum albumin, HTF: Human transferrin, APTES: 3-Amino propyl triethoxy silane, LHRH: Luteinizing hormone-releasing hormone.

### 3.4.4.3 Noncovalent coating method

Unlike other capillary coating methods used in OT−CEC, noncovalent coating has the advantage of being relatively easier to produce than covalent coatings, with a minimum amount of time spent for the preparation of the OT-CEC column. Based on the stationary phase materials used, noncovalent coating can incorporate and mixture of electrostatic or hydrophilic interactions.

#### 3.4.4.3.1 Static coating

This approach of coating involves a strong physical adsorption of the coating materials onto the inner wall of fused silica capillary. Although, the coating material is not required to be within the background electrolyte, the coated stationary phase should be stable for a number of runs and regeneration of the coating surface may be required after repeated runs. The removal of the coating material from the capillary may require a complex rinsing method. Materials that are most commonly used for static coating are long chain polymers. The advantage of static coating over covalent coating is the ease of the coating method, the minimal surface chemistry adaptation required for the coating process, and the possibility of the coating regeneration of capillaries. The adsorbed materials used for capillary coating can be neutral or positive molecules, as well as multilayers of alternating negatively and positively charged polymers [Figure 16].

There has been continuous research regarding the development of coating materials for static coating in OT-CEC. For example, Ullsten et.al. [141] synthesized a novel quaternary ammonium substituted agarose polymer (Q-agarose) [Figure 16]. The synthesized cationic polymer was coated onto the inner surface of a negatively charged fused silica capillary via multi-site electrostatic interaction. The coated capillary produced an intermediate anodal EOF over the

pH range of 2-11and was reported to be stable and exhibit reproducible analyte migration times (RSD 4%). The capillary coating repelled moderately basic proteins/peptides, giving separation efficiencies of up to 300,000 N/m.

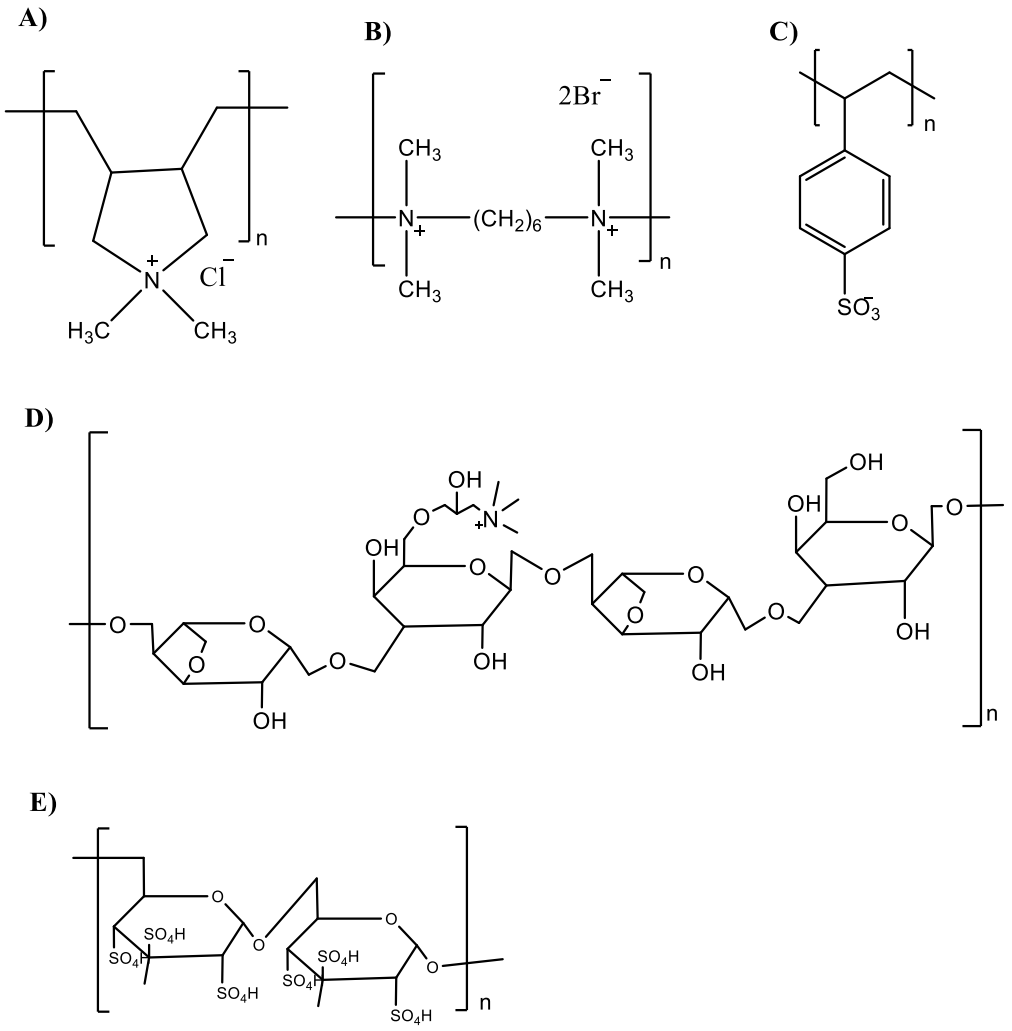


**Figure 16:** Chemical structure of various polymers used in OT-CEC: A) polydiallyldimethylammonium chloride (pDDA), B) polybrene (PB), C) polystyrene sulfonate, D) Q-agarose, E) dextran sulfate.

Multilayer coating methods are also popular for protein/peptide analysis using OT-CEC. The layers are held together mainly by electrostatic interactions. The desired thickness, charge, and function of the modified wall is a function of the number of coating cycles used to form the OT−CEC. Successive multiple ionic-polymer layer (SMIL) coating has the advantage not only of high stability after repeated use, but also many columns are stable in both strongly basic (1 M NaOH) and strongly acidic (1M HCl) solutions. A polybrene (PB)-modified capillary has been demonstrated to improve the separation of model proteins in comparison to that obtained with a bare fused silica capillary. Production of the PB capillary was achieved by a 15-min rinse with 10% PB solution to form the first layer (cationic), this was followed by 15 min rinse of an anionic polymer such as dextran sulfate or hyaluronic acid, to form the second layer. Finally, the capillary was once again rinsed with 10% PB solution over 15 min to form the third and final layer. The (PB)−modified capillary was used for the successful analysis of four basic proteins (α-chymotripsinogen A, ribonuclease A, lysozyme, and cytochrome c), wherein the case of the uncoated capillary, the proteins did not elute due to irreversible adsorption to the capillary wall [142].

### 3.5 Conclusion

Capillary electrochromatography methods have shown to be an ideal analytical technique for the analysis of proteins/ peptides. Compared to CE and ME, the added stationary phases can improve both separation efficiency, selectivity, and resolution for certain analytes. This is due to the reduction of the nonspecific analyte-wall adsorption and increase in analyte partition between CEC stationary phase and mobile phase respectively. However, there are some disadvantages associated with CEC. Most forms of CEC are a time-consuming and labor-intensive method for the production of the CEC column. The packaging or covalently bonding of the stationary phase

of CEC capillary columns often involves multiple steps. Also, under some conditions, packed CEC columns can exhibit difficulties with obtaining a stable current due to the formation of air bubbles at the packing materials and the frits. Other disadvantages of CEC stationary phase materials are that many are pH sensitive, with a narrow pH range that CEC column can be used for protein and peptide analysis.

The use of OT-CEC eliminated problems related to packed CEC. With recent developments in OT-CEC columns, different materials such as long chain charged polymers or nanoparticles that are functionalized with various chemical groups could be used to improve CEC analysis of therapeutic proteins or proteins/ peptides that can be used as disease markers such as elevated levels of the dynorphin A.

Chapter 4 presents the use of CEC column coated with gold nanoparticles for the separation of fragments of the basic peptide dynorphin A(1-17).

## 3.6 References


1. Xu, Y., Tutorial: capillary electrophoresis. *The Chemical Educator* **1996,** *1* (2), 1-14.

2. Evenhuis, C. J.; Haddad, P. R., Joule heating effects and the experimental determination of temperature during CE. *Electrophoresis* **2009,** *30* (5), 897-909.

3. Dolník, V.; Liu, S.; Jovanovich, S., Capillary electrophoresis on microchip. *Electrophoresis* **2000,** *21* (1), 41-54.

4. Štěpánová, S.; Kašička, V., Analysis of proteins and peptides by electromigration methods in microchips. *J. Sep. Sci.*, n/a-n/a.

5. Nordman, N.; Barrios-Lopez, B.; Laurén, S.; Suvanto, P.; Kotiaho, T.; Franssila, S.; Kostiainen, R.; Sikanen, T., Shape-anchored porous polymer monoliths for integrated online solid-phase extraction-microchip electrophoresis-electrospray ionization mass spectrometry. *Electrophoresis* **2015,** *36* (3), 428-432.

6. Nge, P. N.; Yang, W.; Pagaduan, J. V.; Woolley, A. T., Ion-permeable membrane for on-chip preconcentration and separation of cancer marker proteins. *Electrophoresis* **2011,** *32* (10), 1133-1140.

7. Kumar, S.; Sahore, V.; Rogers, C. I.; Woolley, A. T., Development of an integrated microfluidic solid-phase extraction and electrophoresis device. *Analyst* **2016,** *141* (5), 1660-1668.

8. Mitra, I.; Alley, W. R.; Goetz, J. A.; Vasseur, J. A.; Novotny, M. V.; Jacobson, S. C., Comparative Profiling of N-Glycans Isolated from Serum Samples of Ovarian Cancer Patients and Analyzed by Microchip Electrophoresis. *J. Proteome Res.* **2013,** *12* (10), 4490-4496.

9. Yagi, Y.; Kakehi, K.; Hayakawa, T.; Suzuki, S., Application of Microchip Electrophoresis Sodium Dodecyl Sulfate for the Evaluation of Change of Degradation Species of Therapeutic Antibodies in Stability Testing. *Anal. Sci.* **2014,** *30* (4), 483-488.

10. Cong, H.; Xu, X.; Yu, B.; Liu, H.; Yuan, H., Fabrication of universal serial bus flash disk type microfluidic chip electrophoresis and application for protein analysis under ultra low voltage. *Biomicrofluidics* **2016,** *10* (2), 024107.

11. Abad-Villar, E. M.; Tanyanyiwa, J.; Fernandez-Abedul, M. T.; Costa-Garcia, A.; Hauser, P. C., Detection of human immunoglobulin in microchip and conventional capillary electrophoresis with contactless conductivity measurements. *Anal. Chem.* **2004,** *76* (5), 1282-8.

12. Sikanen, T.; Aura, S.; Franssila, S.; Kotiaho, T.; Kostiainen, R., Microchip capillary electrophoresis–electrospray ionization–mass spectrometry of intact proteins using uncoated Ormocomp microchips. *Anal. Chim. Acta* **2012,** *711*, 69-76.

13. Mikkonen, S.; Rokhas, M. K.; Jacksén, J.; Emmer, Å., Sample preconcentration in open microchannels combined with MALDI-MS. *Electrophoresis* **2012,** *33* (22), 3343-3350.

14. Jacobson, S. C.; Moore, A. W.; Ramsey, J. M., Fused Quartz Substrates for Microchip Electrophoresis. *Anal. Chem.* **1995,** *67* (13), 2059-2063.

15. Lacher, N. A.; Lunte, S. M.; Martin, R. S., Development of a Microfabricated Palladium Decoupler/Electrochemical Detector for Microchip Capillary Electrophoresis Using a Hybrid Glass/Poly(dimethylsiloxane) Device. *Anal. Chem.* **2004,** *76* (9), 2482-2491.

16. Vandaveer, W. R.; Pasas-Farmer, S. A.; Fischer, D. J.; Frankenfeld, C. N.; Lunte, S. M., Recent developments in electrochemical detection for microchip capillary electrophoresis. *Electrophoresis* **2004,** *25* (21-22), 3528-3549.

17. Swickrath, M. J.; Shenoy, S.; Mann, J. A.; Belcher, J.; Kovar, R.; Wnek, G. E., The design and fabrication of autonomous polymer-based surface tension-confined microfluidic platforms. *Microfluid. Nanofluid.* **2008,** *4* (6), 601-611.

18. Roy, S.; Das, T.; Yue, C. Y., High Performance of Cyclic Olefin Copolymer-Based Capillary Electrophoretic Chips. *ACS Applied Materials & Interfaces* **2013,** *5* (12), 5683-5689.

19. Jena, R. K.; Yue, C. Y., Cyclic olefin copolymer based microfluidic devices for biochip applications: Ultraviolet surface grafting using 2-methacryloyloxyethyl phosphorylcholine. *Biomicrofluidics* **2012,** *6* (1), 012822.

20. Kim, J. H.; Kang, C. J.; Kim, Y. S., Development of a microfabricated disposable microchip with a capillary electrophoresis and integrated three-electrode electrochemical detection. *Biosens. Bioelectron.* **2005,** *20* (11), 2314-7.

21. Legendre, L.; Landers, J.; Ferrance, J., Microfluidic Devices for Electrophoretic Separations. In *Handbook of Capillary and Microchip Electrophoresis and Associated Microtechniques, Third Edition*, CRC Press: 2007; pp 335-358.

22. Kim, M.-S.; Cho, S. I.; Lee, K.-N.; Kim, Y.-K., Fabrication of microchip electrophoresis devices and effects of channel surface properties on separation efficiency. *Sensors Actuators B: Chem.* **2005,** *107* (2), 818-824.

23. Williams, K. R.; Muller, R. S., Etch rates for micromachining processing. *Journal of Microelectromechanical systems* **1996,** *5* (4), 256-269.

24. Temiz, Y.; Lovchik, R. D.; Kaigala, G. V.; Delamarche, E., Lab-on-a-chip devices: How to close and plug the lab? *Microelectron. Eng.* **2015,** *132*, 156-175.

25. Huynh, B. H.; Fogarty, B. A.; Nandi, P.; Lunte, S. M., A microchip electrophoresis device with on-line microdialysis sampling and on-chip sample derivatization by naphthalene 2,3-dicarboxaldehyde/2-mercaptoethanol for amino acid and peptide analysis. *J. Pharm. Biomed. Anal.* **2006,** *42* (5), 529-534.

26. Nakanishi, H.; Abe, H.; Nishimoto, T.; Arai, A., Micro-fabrication and analytical performances of quartz and glass microchips for electrophoresis. *Bunseki kagaku* **1998,** *47* (6), 361-368.

27. Iliescu, C.; Taylor, H.; Avram, M.; Miao, J.; Franssila, S., A practical guide for the fabrication of microfluidic devices using glass and silicon. *Biomicrofluidics* **2012,** *6* (1), 016505-016505-16.

28. Berthold, A.; Nicola, L.; Sarro, P. M.; Vellekoop, M. J., Glass-to-glass anodic bonding with standard IC technology thin films as intermediate layers. *Sensors and Actuators A: Physical* **2000,** *82* (1–3), 224-228.

29. Huang, Z.; Sanders, J. C.; Dunsmor, C.; Ahmadzadeh, H.; Landers, J. P., A method for UV-bonding in the fabrication of glass electrophoretic microchips. *Electrophoresis* **2001,** *22* (18), 3924-3929.

30. Moreira Gabriel, E. F.; Tomazelli Coltro, W. K.; Garcia, C. D., Fast and versatile fabrication of PMMA microchip electrophoretic devices by laser engraving. *Electrophoresis* **2014,** *35* (16), 2325-32.

31. Fogarty, B. A.; Heppert, K. E.; Cory, T. J.; Hulbutta, K. R.; Martin, R. S.; Lunte, S. M., Rapid fabrication of poly(dimethylsiloxane)-based microchip capillary electrophoresis devices using CO2 laser ablation. *Analyst* **2005,** *130* (6), 924-930.

32. McCormick, R. M.; Nelson, R. J.; Alonso-Amigo, M. G.; Benvegnu, D. J.; Hooper, H. H., Microchannel Electrophoretic Separations of DNA in Injection-Molded Plastic Substrates. *Anal. Chem.* **1997,** *69* (14), 2626-2630.

33. Saylor, R. A.; Reid, E. A.; Lunte, S. M., Microchip electrophoresis with electrochemical detection for the determination of analytes in the dopamine metabolic pathway. *Electrophoresis* **2015,** *36* (16), 1912-1919.

34. Lacher, N. A.; de Rooij, N. F.; Verpoorte, E.; Lunte, S. M., Comparison of the performance characteristics of poly(dimethylsiloxane) and Pyrex microchip electrophoresis devices for peptide separations. *J. Chromatogr.* **2003,** *1004* (1–2), 225-235.

35. Lacher, N. A.; Garrison, K. E.; Martin, R. S.; Lunte, S. M., Microchip capillary electrophoresis/electrochemistry. *Electrophoresis* **2001,** *22* (12), 2526-36.

36. Martin, R. S.; Gawron, A. J.; Lunte, S. M.; Henry, C. S., Dual-Electrode Electrochemical Detection for Poly(dimethylsiloxane)-Fabricated Capillary Electrophoresis Microchips. *Anal. Chem.* **2000,** *72* (14), 3196-3202.

37. Wang, J.; Tian, B.; Sahlin, E., Integrated Electrophoresis Chips/Amperometric Detection with Sputtered Gold Working Electrodes. *Anal. Chem.* **1999,** *71* (17), 3901-3904.

38. Slentz, B. E.; Penner, N. A.; Regnier, F., Sampling BIAS at Channel Junctions in Gated Flow Injection on Chips. *Anal. Chem.* **2002,** *74* (18), 4835-4840.

39. Wu, Y.; Xie, J.; Wang, F.; Chen, Z., Electrokinetic separation of peptides and proteins using a polyvinylamine-coated capillary with UV and ESI-MS detection. *J. Sep. Sci.* **2008,** *31* (5), 814-823.

40. Freitag, R.; Hilbrig, F., Theory and practical understanding of the migration behavior of proteins and peptides in CE and related techniques. *Electrophoresis* **2007,** *28* (13), 2125-2144.

41. Andrade, J. D.; Hlady, V.; Wei, A. P.; Ho, C. H.; Lea, A. S.; Jeon, S. I.; Lin, Y. S.; Stroup, E., Proteins at interfaces: Principles, multivariate aspects, protein resistant surfaces, and direct imaging and manipulation of adsorbed proteins. *Clin. Mater.* **1992,** *11* (1), 67-84.

42. Guzman, N. A.; Moschera, J.; Iqbal, K.; Waseem Malick, A., Effect of buffer constituents on the determination of therapeutic proteins by capillary electrophoresis. *J. Chromatogr.* **1992,** *608* (1), 197-204.

43. Bohlin, M. E.; Johannesson, I.; Carlsson, G.; Heegaard, N. H. H.; Blomberg, L. G., Estimation of the amount of β2-glycoprotein I adsorbed at the inner surface of fused silica capillaries after acidic, neutral and alkaline pretreatment. *Electrophoresis* **2012,** *33* (12), 1695-1702.

44. Andrade, J. D.; Hlady, V., Protein adsorption and materials biocompatibility: A tutorial review and suggested hypotheses. In *Biopolymers/Non-Exclusion HPLC*, Springer Berlin Heidelberg: Berlin, Heidelberg, 1986; pp 1-63.

45. Lucy, C. A.; MacDonald, A. M.; Gulcev, M. D., Non-covalent capillary coatings for protein separations in capillary electrophoresis. *J. Chromatogr. A* **2008,** *1184* (1-2), 81-105.

46. Stutz, H., Protein attachment onto silica surfaces – a survey of molecular fundamentals, resulting effects and novel preventive strategies in CE. *Electrophoresis* **2009,** *30* (12), 2032-2061.

47. Graf, M.; García, R. G.; Wätzig, H., Protein adsorption in fused-silica and polyacrylamide-coated capillaries. *Electrophoresis* **2005,** *26* (12), 2409-2417.

48. Zhu, M.; Rodriguez, R.; Hansen, D.; Wehr, T., Capillary electrophoresis of proteins under alkaline conditions. *J. Chromatogr.* **1990,** *516* (1), 123-131.

49. Elhamili, A.; Wetterhall, M.; Puerta, A.; Westerlund, D.; Bergquist, J., The effect of sample salt additives on capillary electrophoresis analysis of intact proteins using surface modified capillaries. *J. Chromatogr.* **2009,** *1216* (17), 3613-3620.

50. Bekri, S.; Leclercq, L.; Cottet, H., Influence of the ionic strength of acidic background electrolytes on the separation of proteins by capillary electrophoresis. *J. Chromatogr.* **2016,** *1432*, 145-151.

51. Breadmore, M. C.; Shallan, A. I.; Rabanes, H. R.; Gstoettenmayr, D.; Abdul Keyon, A. S.; Gaspar, A.; Dawod, M.; Quirino, J. P., Recent advances in enhancing the sensitivity of electrophoresis and electrochromatography in capillaries and microchips (2010–2012). *Electrophoresis* **2013,** *34* (1), 29-54.

52. Yang, Y.; Boysen, R. I.; Hearn, M. T., Optimization of field-amplified sample injection for analysis of peptides by capillary electrophoresis-mass spectrometry. *Anal. Chem.* **2006,** *78* (14), 4752-8.

53. Lauer, H. H.; McManigill, D., Capillary zone electrophoresis of proteins in untreated fused silica tubing. *Anal. Chem.* **1986,** *58* (1), 166-170.

54. Kostel, K. L., Chapter 9 Capillary electrophoresis of proteins and peptides. *Progress in Pharmaceutical and Biomedical Analysis* **1996,** *2*, 345-386.

55. Whatley, H., Basic Principles and Modes of Capillary Electrophoresis. In Clinical and Forensic Applications of Capillary Electrophoresis, Petersen, J. R.; Mohammad, A. A., Eds. Humana Press: Totowa, NJ, 2001; pp 21-58.

56. Rodriguez, I.; Li, S. F. Y., Surface deactivation in protein and peptide analysis by capillary electrophoresis. *Anal. Chim. Acta* **1999,** *383* (1–2), 1-26.

57. McCormick, R. M., Capillary zone electrophoretic separation of peptides and proteins using low pH buffers in modified silica capillaries. *Anal. Chem.* **1988,** *60* (21), 2322-2328.

58. Znaleziona, J.; Drahoňovský, D.; Drahoš, B.; Ševčík, J.; Maier, V., Novel cationic coating agent for protein separation by capillary electrophoresis†. *J. Sep. Sci.* **2016**.

59. Tang, S.; Liu, S.; Guo, Y.; Liu, X.; Jiang, S., Recent advances of ionic liquids and polymeric ionic liquids in capillary electrophoresis and capillary electrochromatography. *J. Chromatogr.* **2014,** *1357*, 147-157.

60. Melanson, J. E.; Baryla, N. E.; Lucy, C. A., Double-Chained Surfactants for Semipermanent Wall Coatings in Capillary Electrophoresis. *Anal. Chem.* **2000,** *72* (17), 4110-4114.

61. Baryla, N. E.; Melanson, J. E.; McDermott, M. T.; Lucy, C. A., Characterization of Surfactant Coatings in Capillary Electrophoresis by Atomic Force Microscopy. *Anal. Chem.* **2001,** *73* (19), 4558-4565.

62. Mohabbati, S.; Westerlund, D., Improved properties of the non-covalent coating with N,N-didodecyl-N, N-dimethylammonium bromide for the separation of basic proteins by

capillary electrophoresis with acidic buffers in 25 μm capillaries. *J. Chromatogr.* **2006,** *1121* (1), 32-39.

63. Guo, X.-F.; Chen, H.-Y.; Zhou, X.-H.; Wang, H.; Zhang, H.-S., N-methyl-2-pyrrolidonium methyl sulfonate acidic ionic liquid as a new dynamic coating for separation of basic proteins by capillary electrophoresis. *Electrophoresis* **2013,** *34* (24), 3287-3292.

64. Zhu, Z.; Lu, J. J.; Liu, S., Protein Separation by Capillary Gel Electrophoresis: A Review. *Anal. Chim. Acta* **2012,** *709*, 21-31.

65. Guttman, A.; Horvath, J.; Cooke, N., Influence of temperature on the sieving effect of different polymer matrixes in capillary SDS gel electrophoresis of proteins. *Anal. Chem.* **1993,** *65* (3), 199-203.

66. Na, D. H.; Park, E. J.; Youn, Y. S.; Moon, B. W.; Jo, Y. W.; Lee, S. H.; Kim, W.-B.; Sohn, Y.; Lee, K. C., Sodium dodecyl sulfate-capillary gel electrophoresis of polyethylene glycolylated interferon alpha. *Electrophoresis* **2004,** *25* (3), 476-479.

67. Hsieh, J. F.; Chen, S. T., Comparative studies on the analysis of glycoproteins and lipopolysaccharides by the gel-based microchip and SDS-PAGE. *Biomicrofluidics* **2007,** *1* (1), 14102.

68. Yao, S.; Anex, D. S.; Caldwell, W. B.; Arnold, D. W.; Smith, K. B.; Schultz, P. G., SDS capillary gel electrophoresis of proteins in microfabricated channels. *Proc. Natl. Acad. Sci. U. S. A.* **1999,** *96* (10), 5372-5377.

69. Seyfried, B. K.; Marchetti-Deschmann, M.; Siekmann, J.; Bossard, M. J.; Scheiflinger, F.; Turecek, P. L.; Allmaier, G., Microchip capillary gel electrophoresis of multiply PEGylated high-molecular-mass glycoproteins. *Biotechnol J* **2012,** *7* (5), 635-41.

70. Strain, H. H., On the Combination of Electrophoretic and Chromatographic Adsorption Methods. *J. Am. Chem. Soc.* **1939,** *61* (5), 1292-1293.

71. Berraz, G., *An. Asoc. Quim. Argent.* **1943,** *31*, 96-97.

72. Svec, F., Capillary electrochromatography: a rapidly emerging separation method. *Adv. Biochem. Eng. Biotechnol.* **2002,** *76*, 1-47.

73. Colón, L. A.; Reynolds, K. J.; Alicea-Maldonado, R.; Fermier, A. M., Advances in capillary electrochromatography. *Electrophoresis* **1997,** *18* (12-13), 2162-2174.

74. Cooper, P. A.; Jessop, K. M.; Moffatt, F., Capillary electrochromatography for pesticide analysis: effects of environmental matrices. *Electrophoresis* **2000,** *21* (8), 1574-9.

75. Adu, J. K.; Euerby, M. R.; Tettey, J. N. A.; Skellern, G. G., Capillary electrochromatography of pharmaceuticals. In *Sep. Sci. Technol.*, Satinder, A.; Jimidar, M. I., Eds. Academic Press: 2008; Vol. Volume 9, pp 439-476.

76. Lion, N.; Rohner, T. C.; Dayon, L.; Arnaud, I. L.; Damoc, E.; Youhnovski, N.; Wu, Z. Y.; Roussel, C.; Josserand, J.; Jensen, H.; Rossier, J. S.; Przybylski, M.; Girault, H. H., Microfluidic systems in proteomics. *Electrophoresis* **2003,** *24* (21), 3533-3562.

77. Patrick, J. S.; Lagu, A. L., Review applications of capillary electrophoresis to the analysis of biotechnology-derived therapeutic proteins. *Electrophoresis* **2001,** *22* (19), 4179-4196.

78. Mistry, K.; Krull, I.; Grinberg, N., Capillary electrochromatography: An alternative to HPLC and CE. *J. Sep. Sci.* **2002,** *25* (15-17), 935-958.

79. Gonzalez, C.; Remcho, V.; Koesdjojo, M., Principles and Practice of Capillary Electrochromatography. In *Handbook of Capillary and Microchip Electrophoresis and Associated Microtechniques, Third Edition*, CRC Press: 2007; pp 183-226.

80. Li, Y.; Xiang, R.; Wilkins, J. A.; Horváth, C., Capillary electrochromatography of peptides and proteins. *Electrophoresis* **2004,** *25* (14), 2242-2256.

81. De Smet, S.; Lynen, F., Kinetic performance evaluation and perspectives of contemporary packed column capillary electrochromatography. *J. Chromatogr.* **2014,** *1355*, 261-268.

82. Jorgenson, J. W.; Lukacs, K. D., High-resolution separations based on electrophoresis and electroosmosis. *J. Chromatogr.* **1981,** *218*, 209-216.

83. Colón, L. A.; Maloney, T. D.; Fermier, A. M., Packing columns for capillary electrochromatography. *J. Chromatogr.* **2000,** *887* (1–2), 43-53.

84. J. Reynolds, K.; A. Colon, L., Capillary electrochromatography in columns packed by gravity.Preliminary study. *Analyst* **1998,** *123* (7), 1493-1495.

85. Yang, Y.; Boysen, R. I.; Matyska, M. T.; Pesek, J. J.; Hearn, M. T. W., Open-Tubular Capillary Electrochromatography Coupled with Electrospray Ionization Mass Spectrometry for Peptide Analysis. *Anal. Chem.* **2007,** *79* (13), 4942-4949.

86. Wang, G.; Lowry, M.; Zhong, Z.; Geng, L., Direct observation of frits and dynamic air bubble formation in capillary electrochromatography using confocal fluorescence microscopy. *J. Chromatogr.* **2005,** *1062* (2), 275-283.

87. Carney, R. A.; Robson, M. M.; Bartle, K. D.; Myers, P., Investigation into the Formation of Bubbles in Capillary Electrochromatography. *J. High. Resolut. Chromatogr.* **1999,** *22* (1), 29-32.

88. Bandilla, D.; Skinner, C. D., Capillary electrochromatography of peptides and proteins. *J. Chromatogr.* **2004,** *1044* (1–2), 113-129.

89. Schmeer, K.; Behnke, B.; Bayer, E., Capillary Electrochromatography-Electrospray Mass Spectrometry: A Microanalysis Technique. *Anal. Chem.* **1995,** *67* (20), 3656-3658.

90. Liu, Q.; Wang, L.; Zhou, Z.; Wang, Q.; Yan, L.; Zhang, B., Toward rapid preparation of capillary columns for electrochromatography use. *Electrophoresis* **2014,** *35* (6), 836-839.

91. Fanali, C.; D'Orazio, G.; Fanali, S., Nano-liquid chromatography and capillary electrochromatography hyphenated with mass spectrometry for tryptic digest protein analysis: A comparison. *Electrophoresis* **2012,** *33* (16), 2553-2560.

92. Walhagen, K.; Unger, K. K.; Keah, H. H.; Hearn, M. T., Application of CEC procedures for the analysis of synthetic peptides: characterization of linear immunogenic peptides that mimic a HIV-1 gp120 epitope. *J. Pept. Res.* **2002,** *59* (4), 159-73.

93. Rocco, A.; Aturki, Z.; D'Orazio, G.; Fanali, S.; Šolínová, V.; Hlaváček, J.; Kašička, V., CEC separation of insect oostatic peptides using a strong-cation-exchange stationary phase. *Electrophoresis* **2007,** *28* (11), 1689-1695.

94. Park, J.; Lee, D.; Kim, W.; Horiike, S.; Nishimoto, T.; Lee, S. H.; Ahn, C. H., Fully Packed Capillary Electrochromatographic Microchip with Self-Assembly Colloidal Silica Beads. *Anal. Chem.* **2007,** *79* (8), 3214-3219.

95. Jemere, A. B.; Martinez, D.; Finot, M.; Harrison, D. J., Capillary electrochromatography with packed bead beds in microfluidic devices. *Electrophoresis* **2009,** *30* (24), 4237-4244.

96. He, B.; Ji, J.; Regnier, F. E., Capillary electrochromatography of peptides in a microfabricated system. *J. Chromatogr.* **1999,** *853* (1–2), 257-262.

97. Jemere, A. B.; Oleschuk, R. D.; Harrison, D. J., Microchip-based capillary electrochromatography using packed beds. *Electrophoresis* **2003,** *24* (17), 3018-3025.

98. Pittler, E.; Grawatsch, N.; Paul, D.; Gübitz, G.; Schmid, M. G., Enantioseparation of amino acids, α-hydroxy acids, and dipeptides by ligand-exchange CEC using silica-based chiral stationary phases. *Electrophoresis* **2009,** *30* (16), 2897-2904.

99. Liao, T.; Guo, Z.; Li, J.; Liu, M.; Chen, Y., One-step packing of anti-voltage photonic crystals into microfluidic channels for ultra-fast separation of amino acids and peptides. *Lab on a Chip* **2013,** *13* (4), 706-713.

100. Tegeler, T. J.; Mechref, Y.; Boraas, K.; Reilly, J. P.; Novotny, M. V., Microdeposition Device Interfacing Capillary Electrochromatography and Microcolumn Liquid Chromatography with Matrix-Assisted Laser Desorption/Ionization Mass Spectrometry. *Anal. Chem.* **2004,** *76* (22), 6698-6706.

101. Peterson, D. S.; Rohr, T.; Svec, F.; Fréchet, J. M. J., Enzymatic Microreactor-on-a-Chip: Protein Mapping Using Trypsin Immobilized on Porous Polymer Monoliths Molded in Channels of Microfluidic Devices. *Anal. Chem.* **2002,** *74* (16), 4081-4088.

102. Yu, C.; Svec, F.; Fréchet, J. M. J., Towards stationary phases for chromatography on a microchip: Molded porous polymer monoliths prepared in capillaries by photoinitiated in

situ polymerization as separation media for electrochromatography. *Electrophoresis* **2000,** *21* (1), 120-127.

103. Augustin, V.; Proczek, G.; Dugay, J.; Descroix, S.; Hennion, M.-C., Online preconcentration using monoliths in electrochromatography capillary format and microchips. *J. Sep. Sci.* **2007,** *30* (17), 2858-2865.

104. Yang, R.; Pagaduan, J. V.; Yu, M.; Woolley, A. T., On chip preconcentration and fluorescence labeling of model proteins using monolithic columns: device fabrication, optimization, and automation. *Anal. Bioanal. Chem.* **2015,** *407* (3), 737-747.

105. Lu, M.; Feng, Q.; Lu, Q.; Cai, Z.; Zhang, L.; Chen, G., Preparation and evaluation of the highly cross-linked poly(1-hexadecane-co-trimethylolpropane trimethacrylate) monolithic column for capillary electrochromatography. *Electrophoresis* **2009,** *30* (20), 3540-3547.

106. Waguespack, B. L.; Hodges, S. A.; Bush, M. E.; Sondergeld, L. J.; Bushey, M. M., Capillary electrochromatography column behavior of butyl and lauryl acrylate porous polymer monoliths. *J. Chromatogr.* **2005,** *1078* (1–2), 171-180.

107. Moore, R. E.; Licklider, L.; Schumann, D.; Lee, T. D., A Microscale Electrospray Interface Incorporating a Monolithic, Poly(styrene−divinylbenzene) Support for On-Line Liquid Chromatography/Tandem Mass Spectrometry Analysis of Peptides and Proteins. *Anal. Chem.* **1998,** *70* (23), 4879-4884.

108. Lämmerhofer, M.; Svec, F.; Fréchet, J. M. J.; Lindner, W., Capillary electrochromatography in anion-exchange and normal-phase mode using monolithic stationary phases. *J. Chromatogr.* **2001,** *925* (1–2), 265-277.

109. Mayr, B.; Hölzl, G.; Eder, K.; Buchmeiser, M. R.; Huber, C. G., Hydrophobic, Pellicular, Monolithic Capillary Columns Based on Cross-Linked Polynorbornene for Biopolymer Separations. *Anal. Chem.* **2002,** *74* (23), 6080-6087.

110. Ivanov, A. R.; Zang, L.; Karger, B. L., Low-Attomole Electrospray Ionization MS and MS/MS Analysis of Protein Tryptic Digests Using 20-μm-i.d. Polystyrene−Divinylbenzene Monolithic Capillary Columns. *Anal. Chem.* **2003,** *75* (20), 5306-5316.

111. Eeltink, S.; Svec, F., Recent advances in the control of morphology and surface chemistry of porous polymer-based monolithic stationary phases and their application in CEC. *Electrophoresis* **2007,** *28* (1-2), 137-47.

112. Karenga, S.; El Rassi, Z., A novel, neutral hydroxylated octadecyl acrylate monolith with fast electroosmotic flow velocity and its application to the separation of various solutes including peptides and proteins in the absence of electrostatic interactions. *Electrophoresis* **2010,** *31* (19), 3192-3199.

113. Ludewig, R.; Nietzsche, S.; Scriba, G. K. E., A weak cation-exchange monolith as stationary phase for the separation of peptide diastereomers by CEC. *J. Sep. Sci.* **2011,** *34* (1), 64-69.

114. Tsuda, T.; Nomura, K.; Nakagawa, G., Open-tubular microcapillary liquid chromatography with electro-osmosis flow using a UV detector. *J. Chromatogr.* **1982,** *248* (2), 241-247.

115. Chen, X.; Wei, Y.; Lu, J.-Y.; Zhang, A.-Z.; Ye, F.-G.; Zhao, S.-L., Preparation and Evaluation of C18 Modified Capillary Open-Tubular Column Based on Thiol-ene Click Chemistry for Capillary Electrochromatography. *Chinese Journal of Analytical Chemistry* **2012,** *40* (10), 1584-1588.

116. Fang, L.; Yu, J.; Jiang, Z.; Guo, X., Preparation of a β-Cyclodextrin-Based Open-Tubular Capillary Electrochromatography Column and Application for Enantioseparations of Ten Basic Drugs. *PLoS One* **2016,** *11* (1), e0146292.

117. Zhu, Y.; Zhou, C.; Qin, S.; Ren, Z.; Zhang, L.; Fu, H.; Zhang, W., A novel open-tubular capillary electrochromatography with magnetic nanoparticle coating as stationary phase. *Electrophoresis* **2012,** *33* (2), 340-347.

118. Freitag, R.; Constantin, S., Investigation of factors influencing the performance of open-tubular stationary phases in capillary electrochromatography. *J. Sep. Sci.* **2003,** *26* (9-10), 835-843.

119. Zhu, X.; Kamande, M. W.; Thiam, S.; Kapnissi, C. P.; Mwongela, S. M.; Warner, I. M., Open-tubular capillary electrochromatography/electrospray ionization-mass spectrometry using polymeric surfactant as a stationary phase coating. *Electrophoresis* **2004,** *25* (4-5), 562-8.

120. Zhang, X.; Lin, X.; Chen, Z.; Wang, X.; Wu, X.; Xie, Z., Triamine-bonded stationary phase for open tubular capillary electrochromatography. *J. Sep. Sci.* **2010,** *33* (20), 3184-3193.

121. Yone, A.; Carballo, R. R.; Grela, D. A.; Rezzano, I. N.; Vizioli, N. M., Study of peptide–ligand interactions in open-tubular capillary columns covalently modified with porphyrins. *Electrophoresis* **2011,** *32* (20), 2840-2847.

122. Moore, L.; LeJeune, Z. M.; Luces, C. A.; Gates, A. T.; Li, M.; El-Zahab, B.; Garno, J. C.; Warner, I. M., Lysine-Based Zwitterionic Molecular Micelle for Simultaneous Separation of Acidic and Basic Proteins Using Open Tubular Capillary Electrochromatography. *Anal. Chem.* **2010,** *82* (10), 3997-4005.

123. Ali, F.; Cheong, W. J., Open tubular capillary column for the separation of cytochrome C tryptic digest in capillary electrochromatography. *J. Sep. Sci.* **2015,** *38* (20), 3645-54.

124. Qu, Q.; Gu, C.; Gu, Z.; Shen, Y.; Wang, C.; Hu, X., Layer-by-layer assembly of polyelectrolyte and graphene oxide for open-tubular capillary electrochromatography. *J. Chromatogr.* **2013,** *1282,* 95-101.

125. Pesek, J. J.; Matyska, M. T.; Salgotra, V., Retention of Proteins and Metalloproteins in Open Tubular Capillary Electrochromatography with Etched Chemically Modified Columns. *Electrophoresis* **2008,** *29* (18), 3842-3849.

126. Xu, L.; Sun, Y., Protein separation by open tubular capillary electrochromatography employing a capillary coated with phenylalanine functionalized tentacle-type polymer under both cathodic and anodic electroosmotic flows. *J. Chromatogr.* **2008,** *1183* (1–2), 129-134.

127. Kapnissi-Christodoulou, C. P.; Zhu, X.; Warner, I. M., Analytical separations in open-tubular capillary electrochromatography. *Electrophoresis* **2003,** *24* (22-23), 3917-3934.

128. Redman, E. A.; Batz, N. G.; Mellors, J. S.; Ramsey, J. M., Integrated Microfluidic Capillary Electrophoresis-Electrospray Ionization Devices with Online MS Detection for the Separation and Characterization of Intact Monoclonal Antibody Variants. *Anal. Chem.* **2015,** *87* (4), 2264-2272.

129. Aydogan, C.; Cetin, K.; Denizli, A., Novel tentacle-type polymer stationary phase grafted with anion exchange polymer chains for open tubular CEC of nucleosides and proteins. *Analyst* **2014,** *139* (15), 3790-3795.

130. Liu, H.; Li, X.; Huang, L.; Zhang, L.; Zhang, W., An open tubular capillary electrochromatography column with porous inner surface for protein separation. *Anal. Biochem.* **2013,** *442* (2), 186-188.

131. Huang, M.-F.; Huang, C.-C.; Chang, H.-T., Improved separation of double-stranded DNA fragments by capillary electrophoresis using poly(ethylene oxide) solution containing colloids. *Electrophoresis* **2003,** *24* (17), 2896-2902.

132. Palmer, C. P.; Hilder, E. F.; Quirino, J. P.; Haddad, P. R., Electrokinetic Chromatography and Mass Spectrometric Detection Using Latex Nanoparticles as a Pseudostationary Phase. *Anal. Chem.* **2010,** *82* (10), 4046-4054.

133. Shen, C.-C.; Tseng, W.-L.; Hsieh, M.-M., Selective extraction of thiol-containing peptides in seawater using Tween 20-capped gold nanoparticles followed by capillary electrophoresis with laser-induced fluorescence. *J. Chromatogr. A* **2012,** *1220*, 162-168.

134. Ban, E.; Yoo, Y. S.; Song, E. J., Analysis and applications of nanoparticles in capillary electrophoresis. *Talanta* **2015,** *141* (0), 15-20.

135. Miksik, I.; Lacinova, K.; Zmatlikova, Z.; Sedlakova, P.; Kral, V.; Sykora, D.; Rezanka, P.; Kasicka, V., Open-tubular capillary electrochromatography with bare gold nanoparticles-based stationary phase applied to separation of trypsin digested native and glycated proteins. *J. Sep. Sci.* **2012,** *35* (8), 994-1002.

136. Hamer, M.; Yone, A.; Rezzano, I., Gold nanoparticle-coated capillaries for protein and peptide analysis on open-tubular capillary electrochromatography. *Electrophoresis* **2012,** *33* (2), 334-339.

137. Řezanka, P.; Ehala, S.; Koktan, J.; Sýkora, D.; Žvátora, P.; Vosmanská, M.; Král, V.; Mikšík, I.; Čeřovský, V.; Kašička, V., Application of bare gold nanoparticles in open-tubular CEC separations of polyaromatic hydrocarbons and peptides. *J. Sep. Sci.* **2012,** *35* (1), 73-78.

138. Wang, W.; Xiao, X.; Chen, J.; Jia, L., Carboxyl modified magnetic nanoparticles coated open tubular column for capillary electrochromatographic separation of biomolecules. *J. Chromatogr.* **2015,** *1411*, 92-100.

139. Nilsson, C.; Harwigsson, I.; Birnbaum, S.; Nilsson, S., Cationic and anionic lipid-based nanoparticles in CEC for protein separation. *Electrophoresis* **2010,** *31* (11), 1773-1779.

140. Xie, H.; Wang, Z.; Kong, W.; Wang, L.; Fu, Z., A novel enzyme-immobilized flow cell used as end-column chemiluminescent detection interface in open-tubular capillary electrochromatography. *Analyst* **2013,** *138* (4), 1107-1113.

141. Ullsten, S.; Soderberg, L.; Folestad, S.; Markides, K. E., Quaternary ammonium substituted agarose as surface coating for capillary electrophoresis. *Analyst* **2004,** *129* (5), 410-415.

142. Katayama, H.; Ishihama, Y.; Asakawa, N., Stable Cationic Capillary Coating with Successive Multiple Ionic Polymer Layers for Capillary Electrophoresis. *Anal. Chem.* **1998,** *70* (24), 5272-5277.

# Chapter 4

## Separation of Dynorphin Peptides by Capillary Electrochromatography using a Polydiallyldimethylammonium Chloride Gold Nanoparticles-modified Capillary

Published as:

Al-Hossaini AM, Suntornsuk L, Lunte SM; Separation of dynorphin peptides by capillary electrochromatography using a polydiallyldimethylammonium chloride gold nanoparticles-modified capillary; *Electrophoresis*, 37, (Sep 2016), pp 2297-2304.

## 4.1 Introduction

Dynorphin A (Dyn A) is an endogenous opioid peptide that is derived from the precursor peptide preprodynorphin[1-2]. This peptide has high affinity for the κ opioid receptor[3]. Dyn A has been found to exhibit both antinociceptive and analgesic effects within the central nervous system[4] and is also involved in the body's immune response as well as cardiovascular and temperature regulation[5]. However, upregulation of Dyn A due to pathophysiological states (neurotrauma, neurodegeneration, or drug abuse) has been shown to cause nonopioid activity such as hyperalgesia, allodynia, and excitotoxicity[6]. These activities are mainly glutamatergic, and are mediated through the N-methyl-D-aspartate receptor[7-9]. Dyn A's toxic effects have been linked to neurotoxicity and cell death[7, 10].

Capillary electrophoresis (CE) can provide high separation efficiencies and short analysis times. It also requires low sample volumes and small amounts of run buffer[11]. However, one limitation for the analysis of proteins and peptides with high pI values is the adsorption of these species onto the inner surface of fused-silica capillaries, due to their interaction with ionized silanol groups[12]. This adsorption can lead to a loss of separation efficiency, irreproducibility of migration times, and peak tailing[13-15]. Coating of the inner surface can decrease the amount of adsorption of analytes onto fused-silica capillaries[16]. The capillary coating can be either produced by covalent or physical bonding. Although the use of a permanent covalent coating does provide a more stable and reproducible EOF, preparation of these capillaries can be tedious and time-consuming[16]. Physical coating using polycharged polymers, for example polydiallyldimethylammonium chloride (pDDA), can produce a stable surface, although the bonding strength is weaker than that of covalent bonding[17]. These large polycharged molecules offer several bonding sites to the capillary wall, ensuring a stable coating[16-17]. Unfortunately, improving the separation through the

modified surface is limited to a uniform (flat) surface and the chemical stability of the coating material[18]. Gold nanoparticles (GNP), due to their unique chemical and physical properties, are another material that has been used to coat capillaries for peptide and protein CE separations[19-22]. An advantage of using nanoparticles in CE is that selectivity can be improved by controlling the size, shape, and type of coating used on the gold particle. All these parameters will influence the interaction of specific analytes with the GNP. The GNP also provide a greater surface area for these interactions compared to modified silica capillaries. Capillaries coated with citrate[23], didodecyldimethylammonium bromide[24], and octadecylamine[25] capped GNP have been reported previously for CEC. Recently, Zhang et al.[26] reported a separation of heroin and basic impurities using GNP that were stabilized using a cationic polymer of a quaternary ammonium salt pDDA (pDDA-GNP).

The aim of this work was to evaluate GNP for the separation of the opioid peptide Dyn A(1–17) and its metabolites [Table 1] using a CEC capillary coated with pDDA-GNP. It was shown that the pDDA-GNP were able to reduce the electrostatic undesirable adsorption of these positively charged peptides onto the surface of fused silica capillaries, leading to a highly efficient separation.

| **Peptide** | **Structure** | **M.W. (g/mol)** | **pI** |
|---|---|---|---|
| Dynorphin A 1-17 | YGGFLRRIRPKLKWDNQ | 2147.52 | 11.41 |
| Dynorphin A 2-17 | GGFLRRIRPKLKWDNQ | 1984.34 | 12.13 |
| Dynorphin A 1-13 | YGGFLRRIRPKLK | 1603.98 | 12.13 |
| Dynorphin A 1-11 | YGGFLRRIRPK | 1362.65 | 12.12 |
| Dynorphin A 1-8 | YGGFLRRI | 981.17 | 11.13 |
| Dynorphin A 1-7 | YGGFLRR | 868.01 | 11.13 |
| Dynorphin A 1-6 | YGGFLR | 711.82 | 9.84 |
| Leu-enkephalin | YGGFL | 555.63 | 5.93 |

**Table 1:** Structure and pI of all eight opioid peptides used in this study.

## 4.2 Materials and methods

### 4.2.1 Reagents and chemicals

Dyn A(1–17), Dyn A(2–17), Dyn A(1–13), Dyn A(1–8), and Dyn A(1–7) were purchased from Biomatik (Cambridge, ON, Canada). Dyn A(1–6) and Dyn A(1–11) were purchased from Shanghai MoCell Biotech (Shanghai, China). Leu-enkephalin (Leu-ENK) was received from Alfa Aesar (Ward Hill, MA, USA). Gold (III) chloride hydrate, 20% polydiallyldimethylammonium chloride (M.W. 200,000–350,000 Da) solution, sodium acetate trihydrate, sodium phosphate monobasic, sodium phosphate dibasic, and β-cyclodextrin (β-CD) were received from Sigma–Aldrich (St. Louis, MO, USA). Acetic acid, hydrochloric acid, methanol, and sodium hydroxide (molecular biology grade >98%) were purchased from Fisher Scientific (Fair Lawn, NJ, USA). Sequencing grade-modified trypsin was purchased from Promega (Madison, WI, USA). All water used was Milli-Q grade (resistivity of 18 MΩ). Aqueous filter membranes (0.45 μm) were purchased from Fisher Scientific. Polyimide-coated fused-silica capillaries 75 μm id, 375 μm od were received from Polymicro Technologies (Phoenix, AZ, USA).

### 4.2.2 Equipment

Analyses were performed on a Beckman Coulter P/ACE MDQ (Brea, CA, USA) CE system with a UV detector operating at 214 nm. Polyimide-coated fused-silica capillaries 75 μm id, 375 μm od (Polymicro Technologies) were employed in the study. The total length of the capillaries (unless stated otherwise) was 49 cm, the effective length (from injection to detector) was 39 cm. A 0.5 cm detection window was made by burning off the outer polyimide capillary coating with Window Maker® (Eatontown, NJ, USA). Samples were introduced using

hydrodynamic injection by applying 0.5 psi head pressure for 5 s. Electrophoretic separations were performed at applied voltage of (±) 10–20 kV. Following each run, the fused silica capillaries were rinsed with 0.1 M NaOH, water, and BGE for 3 min each. Modified capillaries were rinsed with BGE for 3 min before each sample injection. Data were recorded using the 32 Karat software (Beckman Coulter).

### 4.2.3 Synthesis of pDDA-stabilized GNP

PDDA-stabilized GNP were synthesized based on the method described by Chen et al.[27]. A solution of 250 μL of the polymer (4% pDDA solution), 200 μL of 0.5 M NaOH, and 100 μL $AuHCl_4$(10 mg/mL) in 40 mL of Milli-Q water was brought to boiling under vigorous stirring. The solution gradually turned from a colorless solution to a wine-red color [Figure 1]. When no more color change was observed, the heat was removed and the solution was left to stir at room temperature for an additional 15 min. The size and shape of the GNP were confirmed using transmission electron microscopy [Figure 2].

### 4.2.4 Preparation of buffer and standard solutions

A stock solution of 100 mM sodium acetate buffer (pH 5) was prepared using sodium acetate trihydrate and acetic acid. The pH was adjusted using 1 M sodium hydroxide or 1 M hydrochloric acid. The BGE used for CE was achieved by further dilution of the stock solution and was filtered through a 0.45 μm membrane filter before use. For the GNP-modified capillary, 5% v/v pDDA-GNP was added to the BGE. A tryptic digest of Dyn A(1–17) was prepared as follows: trypsin was added to a solution of Dyn A(1–17) in 5 mM phosphate buffer (pH 7) at an

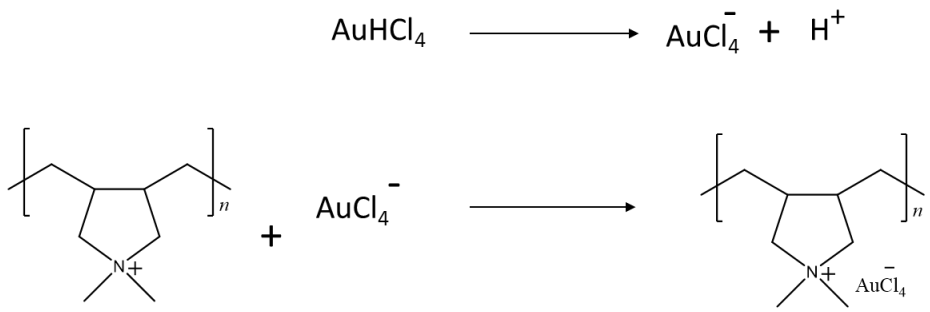


**Figure 1**: The proposed electrostatic interaction of $AuCl_4^-$ with pDDA molecule.

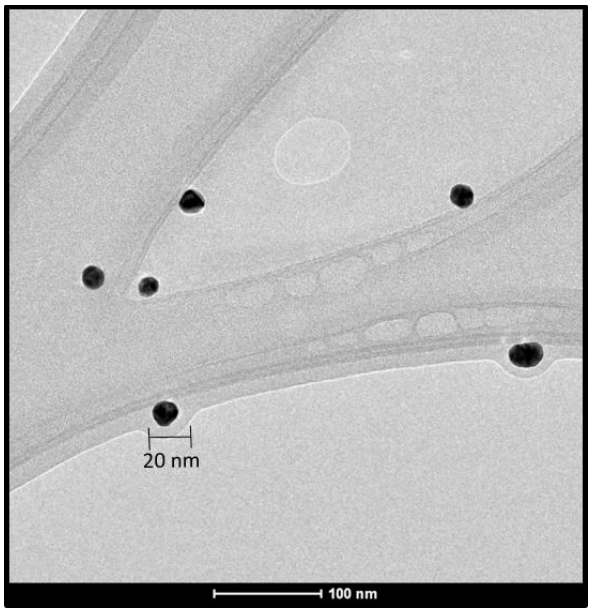


**Figure 2:** Transmission Electron Microscope (TEM) image showing size and shape of pDDA-gold nanoparticles (FEI Tecnai F20 XT Field Emission Transmission Electron Microscope).

enzyme:substrate ratio of 1:150 (mass/mass). The sample was then incubated at 37°C for up to 9 h. Small aliquots of the studied solution were collected hourly and then further diluted in the BGE.

### 4.2.5 Capillary column coating procedure

All solutions used for the modification of the capillary were freshly prepared. New fused-silica capillaries were preconditioned by rinsing for 5 min each with 0.1 M HCl, water, methanol, water, 0.1 N NaOH, water, followed by a 10-min rinse with the BGE. The pDDA coating was done by rinsing the capillary with 0.1 N NaOH for 5 min followed by $H_2O$ for 5 min; this was followed by rinsing the capillary 0.2% pDDA solution for 30 min and then rinsing the capillary with 0.02% pDDA in BGE for 10 min. A −12 kV potential was applied across the capillary for 10 min following the conditioning for equilibration of the BGE within the pDDA-coated capillary.

The pDDA-GNP coating procedure was as follows. The process was started by rinsing the capillary with 0.1 N NaOH for 20 min followed by $H_2O$ for 15 min to ionize the silanol groups on the capillary surface. The capillary is then rinsed with (1:1) pDDA-GNP solution for 15 min, and the solution was held within the capillary for an additional 15 min (total 30 min). Next, the capillary was washed with $H_2O$ to remove any excess unadsorbed GNP on the capillary surface. Finally, the modified capillary was rinsed with BGE for 15 min. A −12 kV potential was applied across the capillary for 10 min following the conditioning for equilibration of the buffer within the modified capillary [Figure 3]. Before each electrophoresis run, the modified capillary was rinsed with BGE for 3 min. The GNP-coated capillary was conditioned each day by rinsing with BGE for 10 min. Whenever changes of BGE components were required, the capillary was reconditioned

with the new BGE for 10 min. For overnight storage, the modified capillary was rinsed with Milli-Q water for 10 min and then stored in water.

### 4.2.6 Electrophoresis procedure

Stock solutions of the peptides Leu-ENK, Dyn A(1–17), and the Dyn A(1–17) fragments Dyn A(1–6), Dyn A(1–7), Dyn A(1–8), Dyn A(1–11), Dyn A(1–13), and Dyn A(2–17) were prepared in Milli-Q water at a concentration of 1 mg/mL and stored at −20°C in polypropylene microcentrifuge tubes. The peptides were then diluted to the required concentrations using the same BGE for each run. Samples were injected by applying 0.5 psi head pressure for 5 s. The separation voltage was between 12–20 kV in either normal or reverse polarity depending on capillary charge surface. To evaluate different electrophoresis conditions, five representative peptides—Leu-ENK, Dyn A(1–6), Dyn A(1–7), Dyn A(1–8), and Dyn A(1–11)—were chosen. These peptides mainly differ structurally in the number of cationic residues and size. Leu-ENK is neutral at pH5 and was used for the measurement of the EOF. In addition, a mixture of Dyn A(1–17) and seven other peptide fragments (Leu-ENK, Dyn A(1–6), Dyn A(1–7), Dyn A(1–8), Dyn A(1–11), Dyn A(1–13), and Dyn A(2–17)) was separated using pDDA-GNP-coated capillaries.

## 4.3 Results and discussion:

### 4.3.1 Separation of opioid peptides using unmodified fused silica

The separation of the mixture of the five opioid peptides was first attempted using an unmodified fused-silica capillary and a BGE of 20 mM sodium acetate buffer (pH 5). The

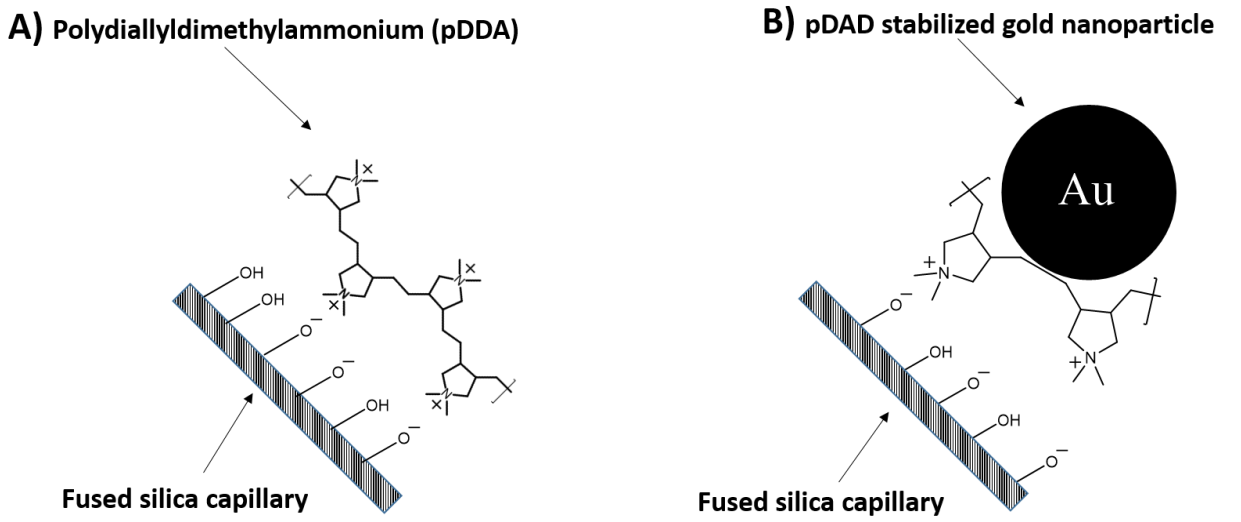


**Figure 3:** Illustration showing the interaction of capillary wall with A) a monolayer of polydiallyldimethylammonium chloride (pDDA); B) pDDA-stabilized gold nanoparticles.

separation voltage was +12 kV using a capillary having a total length of 39 cm. Under these conditions, no peaks were observed in the electropherogram, most likely due to the irreversible adsorption of the peptides onto the surface of the fused-silica capillary.

### 4.3.2 Separation of opioid peptides using a pDDA-coated capillary

The peptide mixture was then injected into a capillary coated with the cationic polymer (pDDA). This positively charged polymer adsorbed onto the negatively charged capillary wall, creating a positive surface. The excess positive charges from the polymer generated a significant EOF toward the anode (EOF = $-5.2 \times 10^{-4}$ $cm^2/Vs$). The surface also repelled the positively charged peptides and blocked the ionized silanol groups, thereby inhibiting adsorption of these peptides to the capillary wall.

Figure 4A shows the electropherogram obtained for the separation of five opioid peptides, Leu-ENK, Dyn A(1–6), Dyn A(1–7), Dyn A(1–8), and Dyn A(1–11). A BGE consisting of 20 mM sodium acetate buffer (pH 5) containing 0.02% v/v pDDA and a separation voltage of 15 kV (reverse polarity) was used. The separation of all five peptides was accomplished in <9 min with detection at the anode. The order of migration was Leu-ENK, Dyn A(1–6), Dyn A(1–8), Dyn A( 1–7), and finally, Dyn A(1–11). The resolution between each peak and its neighboring peak was calculated. For the peptides Leu-ENK, Dyn A(1–6), Dyn A(1–8), Dyn A(1–7), and Dyn A(1–11), R values were calculated to be 9.4, 6.93, 1.93, and 11.4, respectively. The migration order was predicted as follows: Leu-ENK is neutral at pH 5 and, therefore, migrated first. The remaining four dynorphin peptides all have one or more arginine groups in their chemical structures. Dyn A(1–11) also has an additional lysine group. Although Dyn A(1–8) and Dyn A(1–7) have an equal

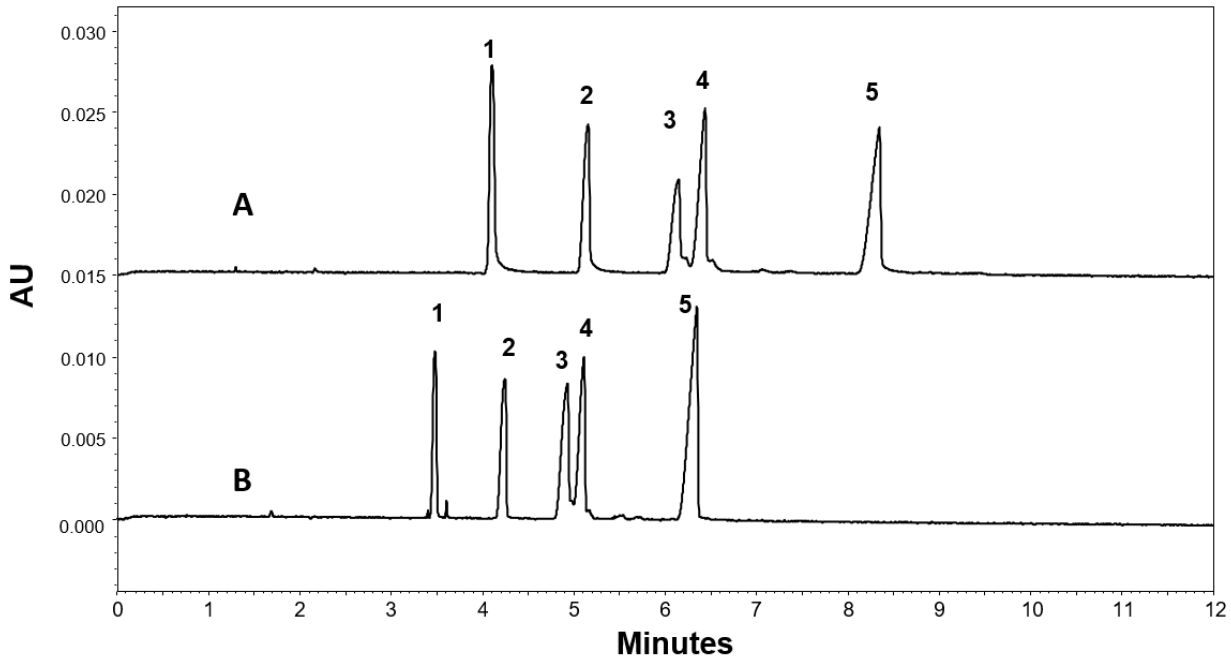


**Figure 4**: Separation of (1) Leu-ENK, (2) Dyn A(1–6), (3) Dyn A(1–8), (4) Dyn A(1–7), (5) Dyn A(1–11). A) pDDA-modified capillary [BGE: 20 mM sodium acetate containing 0.02% pDDA (pH 5)]; B) pDDA-GNP-modified capillary [BGE: 20 mM sodium acetate containing 5% pDDA-GNP (pH 5)]. HV: –15 kV, $L_T$ = 49 cm, $L_D$ = 39 cm, id = 75 μm. UV detection λ= 214 nm.

number of arginine groups in their structures, the extra isoleucine group of Dyn A(1–8) led to an overall lower charge-to-size ratio and faster migration than for Dyn A(1–7).

### 4.3.3 Separation of opioid peptides using pDDA-GNP-coated capillary

Figure 4B shows an electropherogram for the separation of the same five peptides using the pDDA-GNP-coated capillary. In this case, the BGE consisted of 20 mM sodium acetate buffer (pH 5) containing 5% pDDA-GNP. The GNP-coated capillary exhibited a very fast anodal EOF separation (EOF = −6.3 × 10−4 cm2/Vs), which is 20% greater than with a pDDA-coated capillary. We believe the pDDA-GNP adsorbed onto the capillary wall increased the surface area of the modified capillary surface, generating a larger net positive charge. The high EOF provided shorter analysis time and improved peak symmetry, with no change in the separation order from the previous method. The resolutions between each peak and its neighboring peak were Leu-ENK and Dyn A(1–6) (R = 7.83), Dyn A(1–6) and Dyn A(1–8) (R = 5.31), Dyn A(1–8) and Dyn A(1–7) (R = 1.4), and finally, the resolution between Dyn A(1–7) and Dyn A(1–11) was calculated to be R = 8.71. The EOF measured for pDDA-GNP-coated capillaries exhibited a notable same-day reproducibility (%RSD) of 0.76% and a between-day reproducibility of 1.68%. The pDDA-GNP capillaries were stable for several days, and the same capillary could be reused for up to 72 runs. We never had to discard a capillary due to instability.

### 4.3.4 Effect of BGE concentration

Different concentrations of sodium acetate—10, 20, 30, 40, and 50 mM (pH 5) containing a constant amount of GNP—were studied with the goal of improving resolution between each of

the five peptides Leu-ENK, Dyn A(1–6), Dyn A(1–7), Dyn(1–8), and Dyn(1–11) [Figure 5]. The increase in salt concentration lowers the double-layer thickness and zeta potential, leading to slower EOF. Higher concentrations of sodium acetate in the BGE produced an improvement in the separation of all five peptides, but at the expense of longer run times.

### 4.3.5 Effect of capillary length

The effect of capillary length on the separation was evaluated in an attempt to improve the resolution of Dyn A(1–7) and Dyn A(1–8). Using a constant field strength of –306 V/cm, two capillary lengths were evaluated one with a total length of 39 cm and an effective length of 29 cm and a second with a total length of 49 cm and an effective length of 39 cm. The increase in capillary length led to an improvement in resolution, with an increase in the overall migration times of all five opioid peptides [Figure 6].

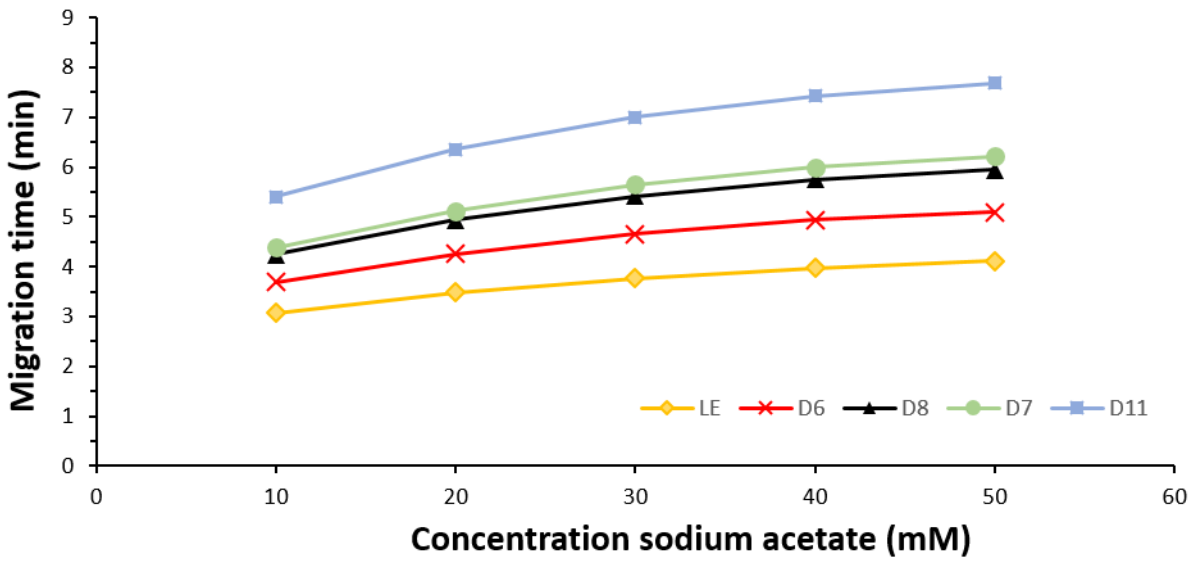


**Figure 5:** The effect of BGE concentration [sodium acetate 10–50 mM, each containing 5% GNP (pH5)] on separation of Leu-ENK, Dyn A(1–6), Dyn A(1–8), Dyn A(1–7), and Dyn A(1–11). GNP-modified capillary; HV: –15 KV, $L_T$ = 49 cm, $L_D$ = 39 cm, id= 75 µm. UV detection λ= 214 nm.

A)

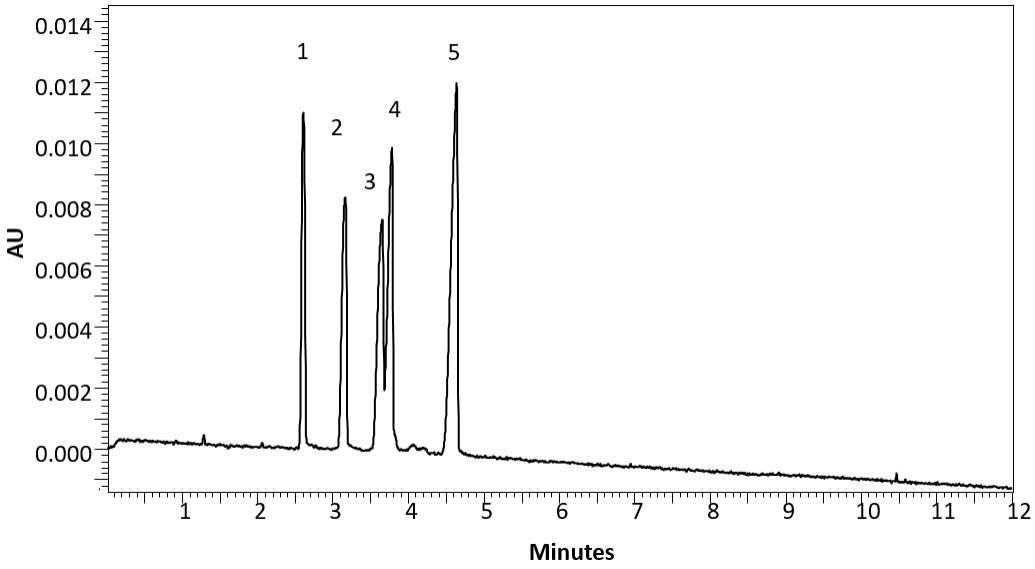


B)

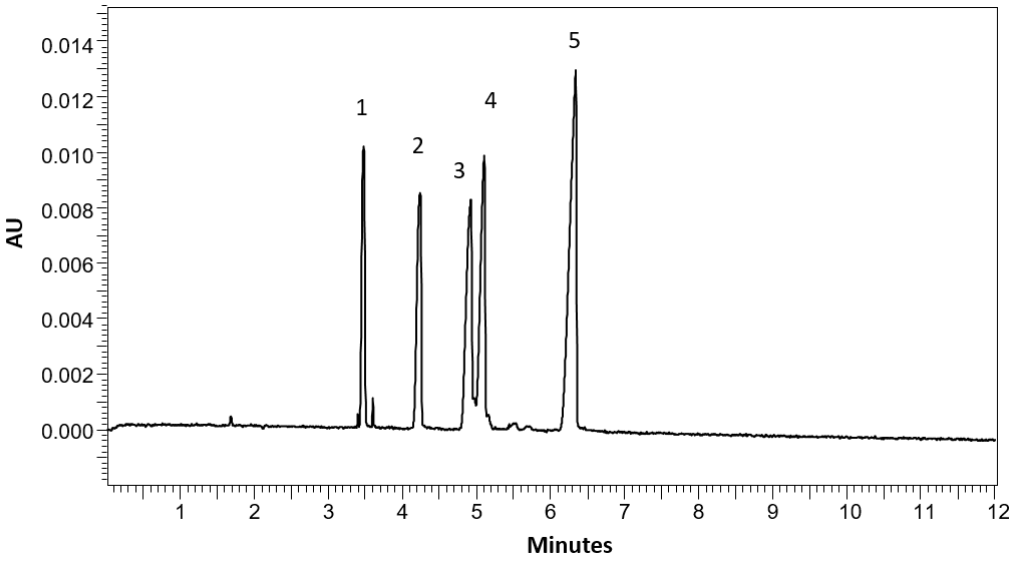


**Figure 6:** Effect of capillary length of GNP-modified capillary on separation of (1) Leu-ENK, (2) Dyn A(1–6), (3) Dyn A(1–8), (4) Dyn A(1–7), (5) Dyn A(1–11). Field strength –306 V/cm. A) $L_T$ = 39 cm, $L_D$ = 29 cm, id = 75 µm, B) $L_T$ = 49 cm, $L_D$ = 39 cm, id = 75 µm.

### 4.3.6 Effect of organic solvent and BGE additives

Methanol was then evaluated as an organic modifier in an attempt to improve the resolution of Dyn A(1–8) and Dyn A(1–7). Organic modifiers can reduce EOF due to their low dielectric constants[28]. Methanol was added to the BGE at a final concentration of 10% v/v. The effect of methanol on the separation is shown in figure 7. The two peptides exhibited longer migration times, and there was some improvement in resolution (R = 2.15) compared to BGE without methanol (R = 1.89). In a previous report, Zhang et al. [26] studied the influence of adding methanol as buffer additive. They found that concentrations <10% in the BGE caused instability of the separation current. Higher concentrations of methanol were avoided in these studies since too much methanol may adversely affect the stability of pDDA nanoparticle capillary coating.

A structurally unmodified β-CD was also investigated as a BGE modifier in an effort to improve resolution of Dyn A(1–8) and Dyn A(1–7). The concentration of β-CD in the BGE was 1.5 mM. Peptides with aromatic residues (tyrosine or tryptophan) are known to form inclusion complexes with CD[29]. It was hoped that differences in the overall secondary structure of the two peptides could contribute to small differences in the affinities to the β-CD cavity and, thus, improve resolution[30-32]. Unfortunately, there was no substantial improvement in the resolution of Dyn A(1–8) and Dyn A(1–7) with or without β-CD in the BGE (40 mM sodium acetate containing 5% GNP) R = 1.72 and 1.7, respectively [Figure 8]. However, an increase in resolution was seen with a BGE having an equal amount of β-CD at a higher sodium acetate concentration (BGE = 50 mM sodium acetate, R = 1.78) compared to the lower BGE concentration (20 mM sodium acetate, R = 1.39) containing equal concentrations of β-CD.

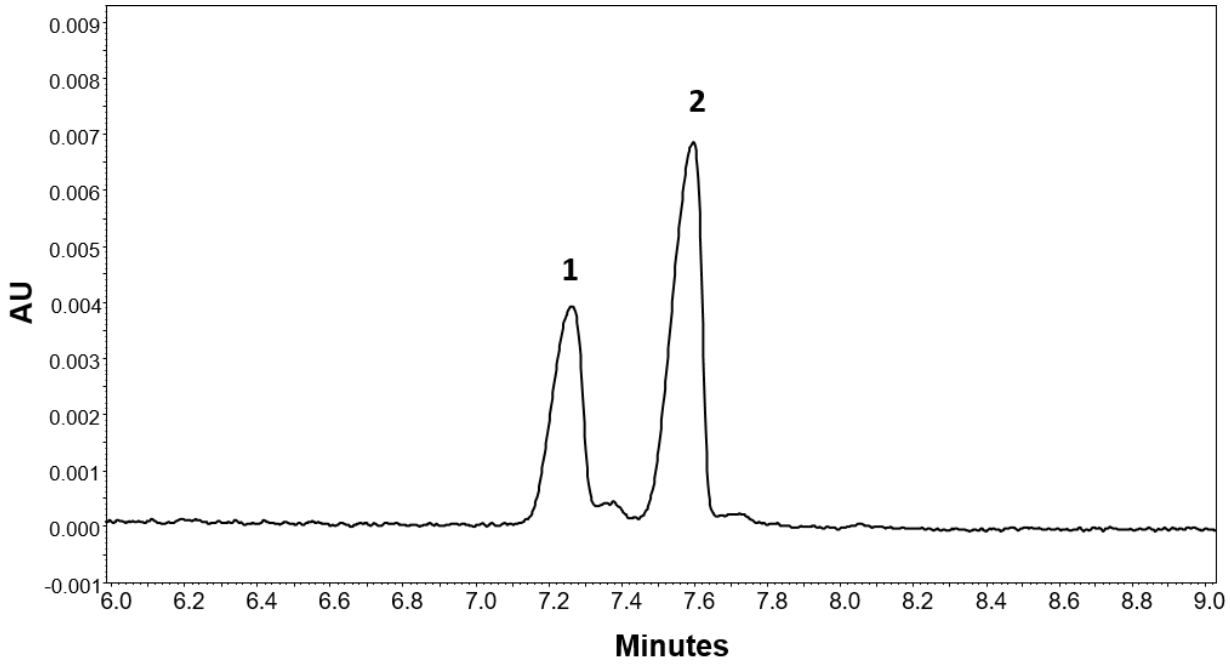


**Figure 7:** The effect of 10% (v/v) methanol on the resolution of (1) Dyn A(1–8), (2) Dyn A(1–7). GNP-modified capillary; HV: –15 kV, $L_T$ = 49 cm, $L_D$ = 39 cm, id = 75 µm. BGE: 50 mM sodium acetate containing 5% GNP and 10% $CH_3OH$ (pH 5). UV detection λ = 214 nm.

A)

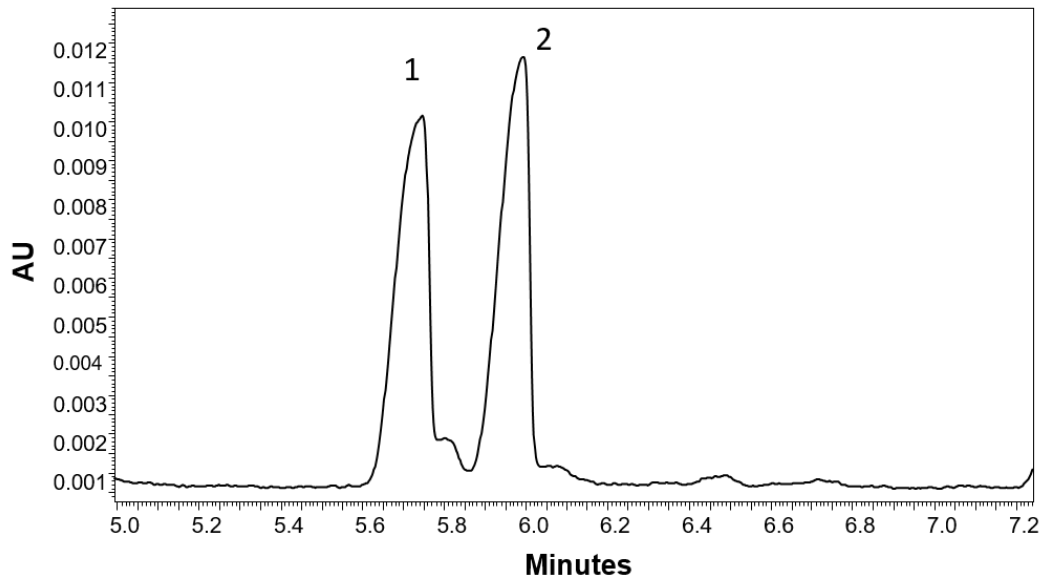


B)

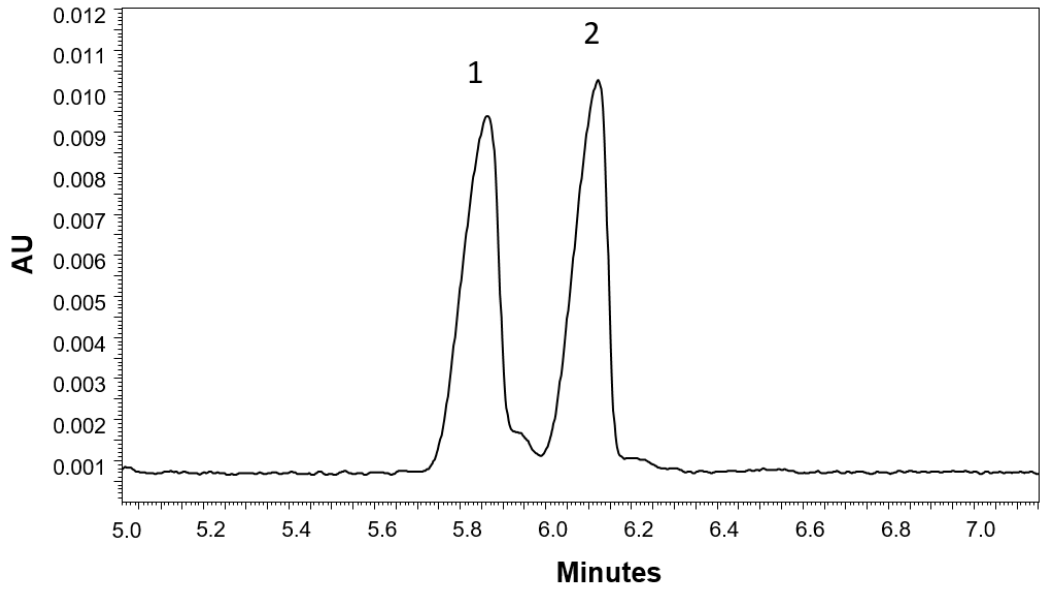


**Figure 8:** Effect of β-CD as BGE additive on the resolution of (1) Dyn A(1-8) and (2) Dyn A(1-7). A) BGE without β-CD. B) BGE containing 1.5 mM β-CD. R = 1.7 and 1.72, respectively.

### 4.3.7 Separation of metabolites of Dyn A(1–17)

*In vivo* enzymatic degradation of Dyn A(1–17) produces fragments of the peptides with different pharmacological activity. An attempt to separate a standard mixture of Dyn A(1–17) and seven fragments of the opioid peptide (Dyn A(1–6), Dyn A(1–7), Dyn A(1–8), Dyn A(1–11), Dyn A(1–13), Dyn A(2–17), and leu-ENK) was studied at concentrations of 20, 40, 60, and 80 mM sodium acetate, each containing 5% v/v GNP [Figure 9]. The order of migration of the eight peptides was as follows: Leu-ENK, Dyn A(1–6), Dyn A(1–8), Dyn A(1–7), Dyn A(1–17), Dyn A(2–17), Dyn A(1–11), and Dyn A(1–13). The optimal BGE was determined to be 40 mM sodium acetate [Figure 10]. The calculated resolutions were 9.72, 6.28, 1.69, 1.15, 1.71, 5.8, and 2.55. At lower concentrations of BGE, there was a decrease in resolution between Dyn A(1–8) and Dyn A(1–7) of 0.86 (peaks 3 and 4) and between Dyn A(1–17) and Dyn A(2–17) a decrease of 0.94 (peaks 5 and 6). Concentrations higher than 40 mM also showed good separations for both Dyn A(1–8) and Dyn A(1–7), but Dyn A(1–7) and Dyn A(1–17) (peaks 4 and 5) comigrated. The increase in concentration of the BGE decreased the double-layer thickness, affecting the zeta potential and leading to slower EOF. This caused an increase in the migration time of all eight Dyn A fragments.

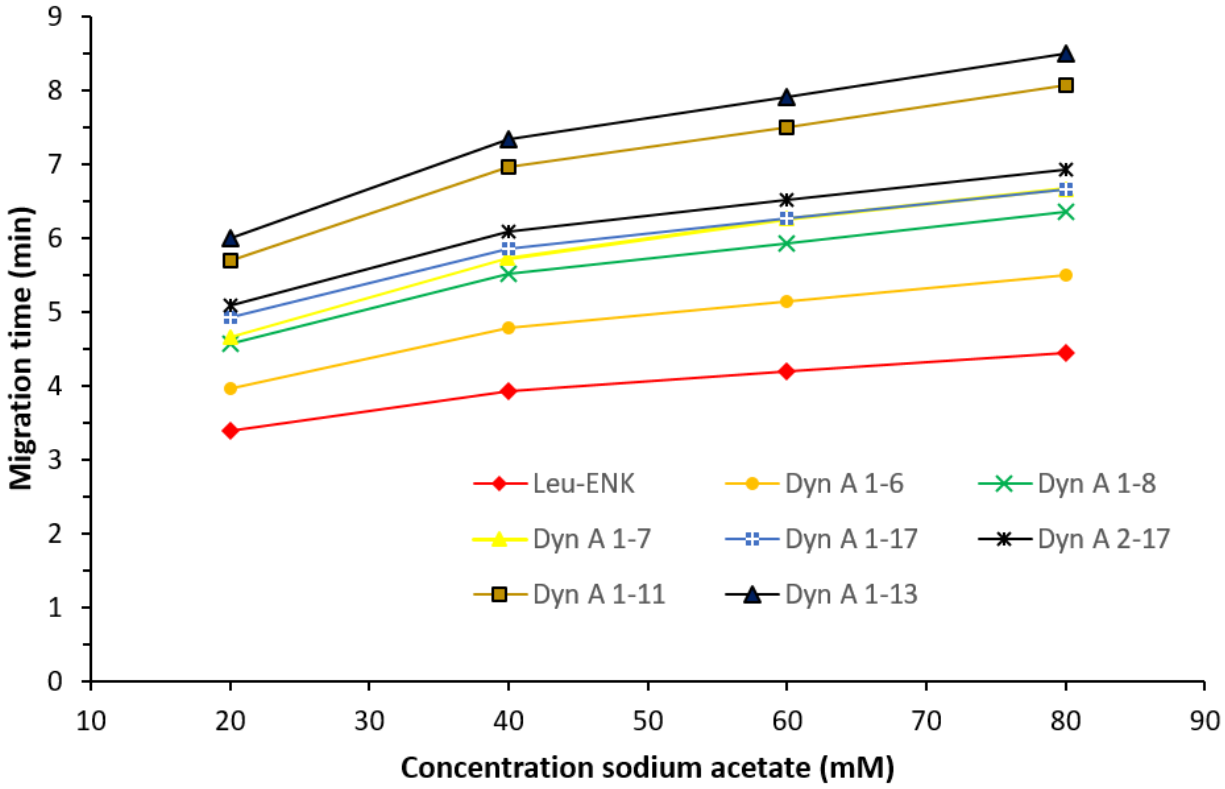


**Figure 9:** The effect of BGE concentration on separation of pDDA-GNP-modified capillary; BGE: 20–80 mM sodium acetate containing 5% GNP (pH 5).

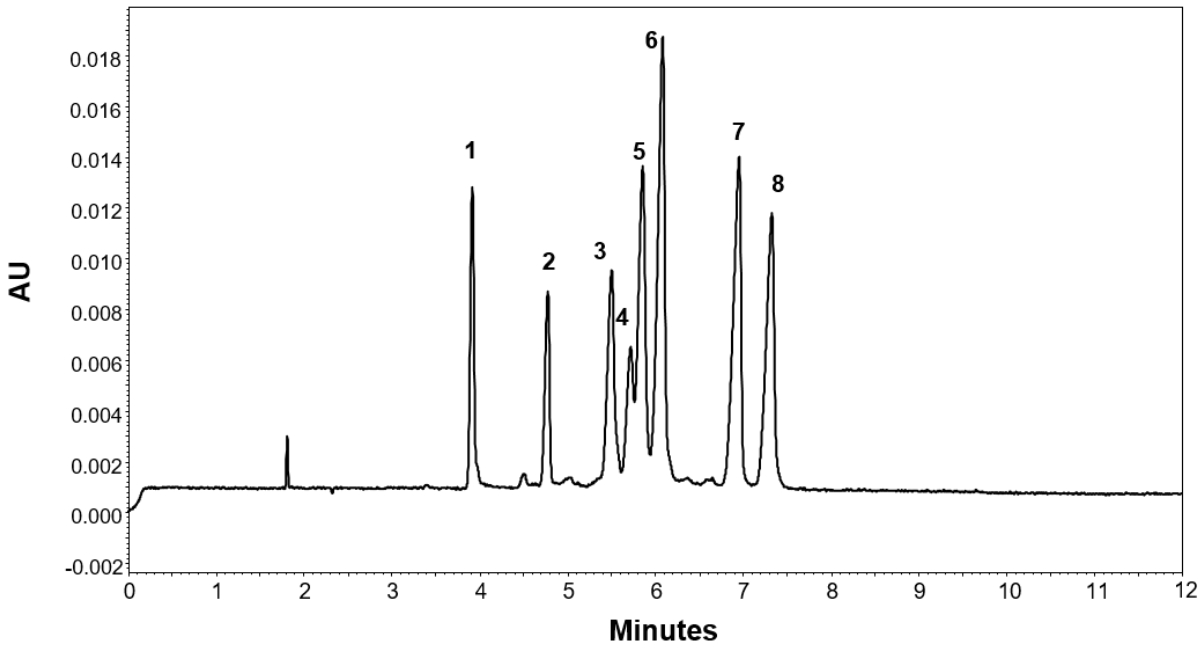


**Figure 10:** Electropherogram showing separation of (1) Leu-ENK, (2) Dyn A(1–6), (3) Dyn A(1–8), (4) Dyn A(1–7), (5) Dyn A(1–17), (6) Dyn A(2–17), (7) Dyn A(1–11), and (8) Dyn A(1–13). BGE 40 mM sodium acetate containing 5% pDDA-GNP (pH 5). UV detection $\lambda$ = 214 nm. HV = –15 kV, $L_T$ = 49 cm, $L_D$ = 39 cm, id = 75 µm;

### 4.3.8 Separation of tryptic digest of Dyn A(1–17)

To demonstrate the separation, tryptic peptide fragments of Dyn A(1–17) were analyzed using the GNP-coated capillaries. Figure 11 shows an electropherogram of the tryptic digest of Dyn A(1–17) at different time points. Peptide fragments were identified based on the migration times of the available standards of Dyn A(1–17) fragments. The electropherogram shows a decrease in the parent peptide Dyn A(1–17) (peak 4) and the appearance of its tryptic digest products Dyn A 1–7 (peak 3) and Dyn A(1–11) (peak 5), which are the N-terminus fragments of Dyn A(1–17). Two unknown peaks were also observed at approximately 3.8 and 5.2 min (asterisk). We believe the unknown peaks correspond to C-terminus fragments Dyn A(12–17) and Dyn A(8–17), respectively. This is based on data reported in the literature concerning the identification of a tryptic digest of Dyn A(1–17) by LC-MS [33]. However, we were unable to confirm this conclusively due to the unavailability of the peptide standard. Using a GNP-coated capillary, we were able to follow the progress of the digestion of Dyn A(1–17) by trypsin over time [Figure 11 and Figure 12]. The GNP-coated capillary was shown to be stable, and can be adapted for the analysis of complex biological samples.

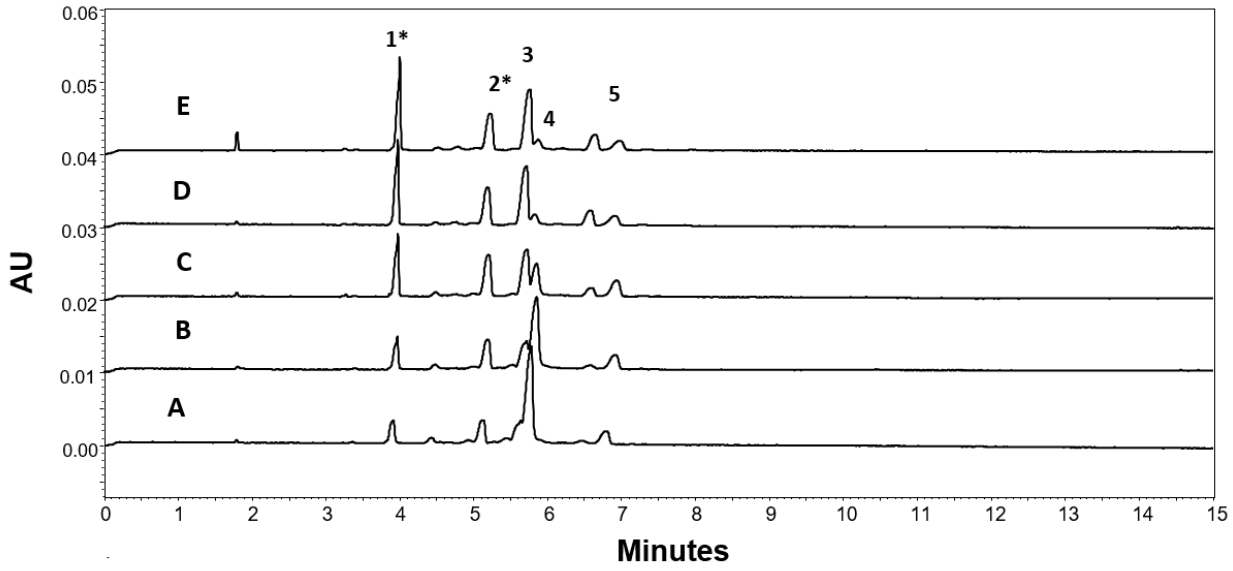


**Figure 11:** Separation of peptides generated by a tryptic digest of dynorphin A(1-17). (A) 0 min, (B) 1 h, (C) 3 h, (D) 6 h, (E) 9 h. (1) Dyn A(12-17), (2) Dyn A(8-17), (3) Dyn A(1–7), (4) Dyn A(1–17), (5) Dyn A(1–11), based on migration time of standards. (*) Peak identity was predicted based on charge and size and migration time. GNP-modified capillary; HV = –15 kV, $L_T$ = 49 cm, $L_D$ = 39 cm, id = 75 µm; BGE: 40 mM sodium acetate containing 5% GNP (pH 5). UV detection λ = 214 nm.

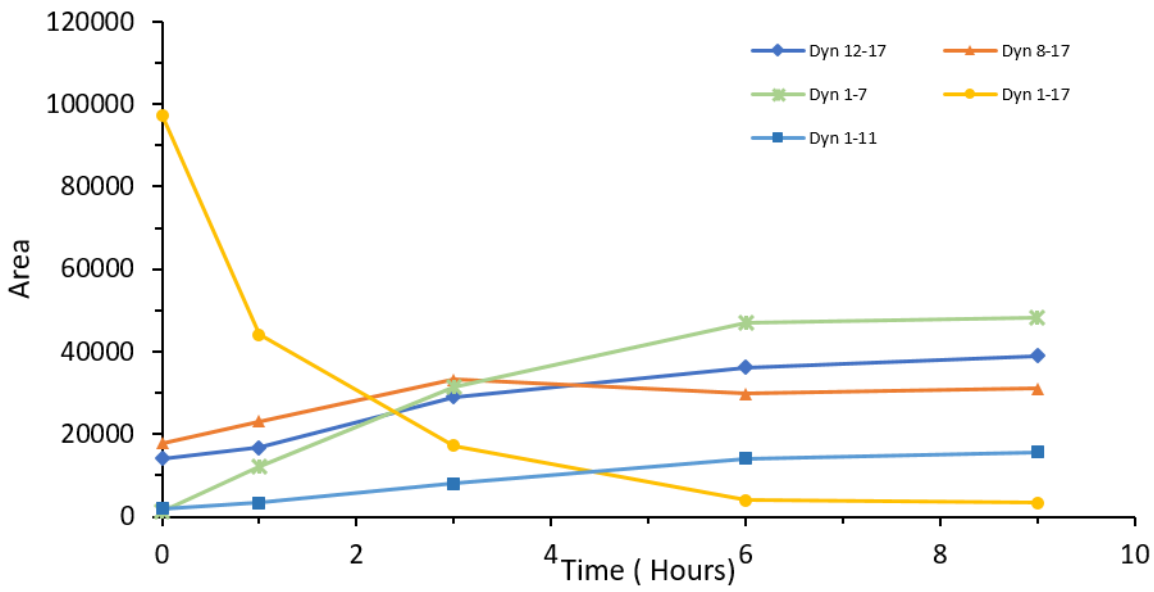


**Figure 12:** Graph showing the tryptic digest of Dyn A(1-17) over time.

## 4.4 Conclusion

CE separations of peptides having a high pI are challenging. This is due to the electrostatic adsorption of cationic peptides onto ionized silanol groups in the capillary wall. Here, we have developed a method based on the use of pDDA-stabilized GNP as a static coating for the separation of Dyn A(1–17) and its biologically active metabolites. The GNP coating acts as a physical barrier between the analytes and the capillary wall. In addition, the charge-to-charge repulsion between the pDDA-stabilized GNP and cationic groups of the peptide minimizes adsorption of the analyte to the capillary wall. Different BGE parameters and additives were evaluated to improve the separation of dynorphin and its metabolites. Finally, the approach was demonstrated for a tryptic digest of Dyn A(1–17), which was analyzed using pDDA-stabilized GNP-coated capillaries.

In the future, coupling of pDDA-stabilized GNP-coated capillaries to more sensitive detection methods—for example fluorescence or mass spectrometry—to achieve lower levels for the detection of pathophysiological levels of Dyn A(1–17) and its metabolites will be undertaken.

## 4.5 References


1. Brugos, B.; Hochhaus, G., Metabolism of dynorphin A(1-13). *Pharmazie* **2004,** *59* (5), 339-43.

2. Ruda, M. A.; Iadarola, M. J.; Cohen, L. V.; Young, W. S., In situ hybridization histochemistry and immunocytochemistry reveal an increase in spinal dynorphin biosynthesis in a rat model of peripheral inflammation and hyperalgesia. *Proceedings of the National Academy of Sciences* **1988,** *85* (2), 622-626.

3. Sloan, C. D. K.; Audus, K. L.; Aldrich, J. V.; Lunte, S. M., The permeation of dynorphin A 1–6 across the blood brain barrier and its effect on bovine brain microvessel endothelial cell monolayer permeability. *Peptides* **2012,** *38* (2), 414-417.

4. Lai, J.; Ossipov, M. H.; Vanderah, T. W.; Malan, T. P., Jr.; Porreca, F., Neuropathic pain: the paradox of dynorphin. *Mol. Interv.* **2001,** *1* (3), 160-7.

5. Smith, A. P.; Lee, N. M., Pharmacology of dynorphin. *Annu. Rev. Pharmacol. Toxicol.* **1988,** *28*, 123-40.

6. Hauser, K. F.; Foldes, J. K.; Turbek, C. S., Dynorphin A (1–13) Neurotoxicity in Vitro: Opioid and Non-Opioid Mechanisms in Mouse Spinal Cord Neurons. *Exp. Neurol.* **1999,** *160* (2), 361-375.

7. Singh, I. N.; Goody, R. J.; Goebel, S. M.; Martin, K. M.; Knapp, P. E.; Marinova, Z.; Hirschberg, D.; Yakovleva, T.; Bergman, T.; Bakalkin, G.; Hauser, K. F., Dynorphin A (1–17) induces apoptosis in striatal neurons in vitro through α-amino-3-hydroxy-5-methylisoxazole-4-propionate/kainate receptor-mediated cytochrome C release and caspase-3 activation. *Neuroscience* **2003,** *122* (4), 1013-1023.

8. Shippenberg, T. S.; Zapata, A.; Chefer, V. I., Dynorphin and the pathophysiology of drug addiction. *Pharmacol. Ther.* **2007,** *116* (2), 306-321.

9. Kurt, F. H.; Pamela, E. K.; Tatiana, Y.; Dineke, S. V.; Georgy, B., Dynorphins in Central Nervous System Pathology. In *Neuropeptides in Neuroprotection and Neuroregeneration*, CRC Press: 2012.

10. Tan-No, K.; Cebers, G.; Yakovleva, T.; Hoon Goh, B.; Gileva, I.; Reznikov, K.; Aguilar-Santelises, M.; Hauser, K. F.; Terenius, L.; Bakalkin, G., Cytotoxic Effects of Dynorphins through Nonopioid Intracellular Mechanisms. *Exp. Cell Res.* **2001,** *269* (1), 54-63.

11. Latosinska, A.; Frantzi, M.; Vlahou, A.; Mischak, H., Clinical applications of capillary electrophoresis coupled to mass spectrometry in biomarker discovery: Focus on bladder cancer. *PROTEOMICS – Clinical Applications* **2013,** *7* (11-12), 779-793.

12. Lucy, C. A.; MacDonald, A. M.; Gulcev, M. D., Non-covalent capillary coatings for protein separations in capillary electrophoresis. *J. Chromatogr. A* **2008,** *1184* (1-2), 81-105.

13. Kapnissi-Christodoulou, C. P.; Zhu, X.; Warner, I. M., Analytical separations in open-tubular capillary electrochromatography. *Electrophoresis* **2003,** *24* (22-23), 3917-3934.

14. MacDonald, A. M.; Bahnasy, M. F.; Lucy, C. A., A modified supported bilayer/diblock polymer – Working towards a tunable coating for capillary electrophoresis. *J. Chromatogr.* **2011,** *1218* (1), 178-184.

15. Neiman, B.; Grushka, E.; Lev, O., Use of gold nanoparticles to enhance capillary electrophoresis. *Anal. Chem.* **2001,** *73* (21), 5220-5227.

16. Kamande, M. W.; Kapnissi, C. P.; Zhu, X.; Akbay, C.; Warner, I. M., Open-tubular capillary electrochromatography using a polymeric surfactant coating. *Electrophoresis* **2003,** *24* (6), 945-951.

17. Córdova, E.; Gao, J.; Whitesides, G. M., Noncovalent Polycationic Coatings for Capillaries in Capillary Electrophoresis of Proteins. *Anal. Chem.* **1997,** *69* (7), 1370-1379.

18. Pei, L.; Lucy, C. A., Insight into the stability of poly(diallydimethylammoniumchloride) and polybrene poly cationic coatings in capillary electrophoresis. *J. Chromatogr.* **2014,** *1365*, 226-233.

19. Miksik, I.; Lacinova, K.; Zmatlikova, Z.; Sedlakova, P.; Kral, V.; Sykora, D.; Rezanka, P.; Kasicka, V., Open-tubular capillary electrochromatography with bare gold nanoparticles-based stationary phase applied to separation of trypsin digested native and glycated proteins. *J. Sep. Sci.* **2012,** *35* (8), 994-1002.

20. Kleindienst, G.; Huber, C. G.; Gjerde, D. T.; Yengoyan, L.; Bonn, G. K., Capillary electrophoresis of peptides and proteins in fused-silica capillaries coated with derivatized polystyrene nanoparticles. *Electrophoresis* **1998,** *19* (2), 262-269.

21. Zhao, T.; Zhou, G.; Wu, Y.; Liu, X.; Wang, F., Gold nanomaterials based pseudostationary phases in capillary electrophoresis: A brand-new attempt at chondroitin sulfate isomers separation. *Electrophoresis* **2015,** *36* (4), 588-595.

22. Sýkora, D.; Kašička, V.; Mikšík, I.; Řezanka, P.; Záruba, K.; Matějka, P.; Král, V., Application of gold nanoparticles in separation sciences. *J. Sep. Sci.* **2010,** *33* (3), 372-387.

23. Rezanka, P.; Ehala, S.; Koktan, J.; Sykora, D.; Zvatora, P.; Vosmanska, M.; Kral, V.; Miksik, I.; Cerovsky, V.; Kasicka, V., Application of bare gold nanoparticles in open-tubular CEC separations of polyaromatic hydrocarbons and peptides. *J. Sep. Sci.* **2012,** *35* (1), 73-78.

24. Yu, C.-J.; Su, C.-L.; Tseng, W.-L., Separation of Acidic and Basic Proteins by Nanoparticle-Filled Capillary Electrophoresis. *Anal. Chem.* **2006,** *78* (23), 8004-8010.

25. Qu, Q.; Zhang, X.; Shen, M.; Liu, Y.; Hu, X.; Yang, G.; Wang, C.; Zhang, Y.; Yan, C., Open-tubular capillary electrochromatography using a capillary coated with octadecylamine-capped gold nanoparticles. *Electrophoresis* **2008,** *29* (4), 901-909.

26. Zhang, Z.; Yan, B.; Liu, K.; Liao, Y.; Liu, H., CE-MS analysis of heroin and its basic impurities using a charged polymer-protected gold nanoparticle-coated capillary. *Electrophoresis* **2009,** *30* (2), 379-87.

27. Chen, H. J.; Wang, Y. L.; Wang, Y. Z.; Dong, S. J.; Wang, E. K., One-step preparation and characterization of PDDA-protected gold nanoparticles. *Polymer* **2006,** *47* (2), 763-766.

28. Sarmini, K.; Kenndler, E., Capillary zone electrophoresis in mixed aqueous–organic media: effect of organic solvents on actual ionic mobilities, acidity constants and separation selectivity of substituted aromatic acids.: I. Methanol. *J. Chromatogr.* **1998,** *806* (2), 325-335.

29. Irie, T.; Uekama, K., Cyclodextrins in peptide and protein delivery. *Adv Drug Deliv Rev* **1999,** *36* (1), 101-123.

30. Scriba, G. K., Recent advances in enantioseparations of peptides by capillary electrophoresis. *Electrophoresis* **2003,** *24* (22-23), 4063-77.

31. Scriba, G. K., Recent developments in peptide stereoisomer separations by capillary electromigration techniques. *Electrophoresis* **2009,** *30 Suppl 1*, S222-8.

32. Suss, F.; Poppitz, W.; Sanger-van de Griend, C. E.; Scriba, G. K., Influence of the amino acid sequence and nature of the cyclodextrin on the separation of small peptide enantiomers by capillary electrophoresis using randomly substituted and single isomer sulfated and sulfonated cyclodextrins. *Electrophoresis* **2001,** *22* (12), 2416-23.

# Chapter 5

# Capillary Electrochromatography and Microchip electrophoresis with Laser Induced Fluorescence Detection for the Separation and Detection of Opioid Peptides

## 5.1 Introduction

Capillary electrophoresis (CE) is a separation technique that has shown to be extremely useful for the separation of biomolecules. The use of small inner-diameter (i.d.) capillaries in CE makes it possible to analyze (submicroliter) small volume samples. However, due to the short path length for on capillary detection in CE widely used detection methods, such as UV absorption, do not work well for the detection of low concentrations of biologically active peptides. Detection limits are generally in the micromolar to submicromolar range[1].

Endogenous concentrations of dynorphins in CNS and blood are in the nanomolar to picomolar range. Thus, the detection of these neuropeptides at endogenous levels require more sensitive detection methods than UV, such as fluorescence detection. Laser induced fluorescence (LIF) detection has been used extensively with CE and microchip electrophoresis (ME) [2-4]. However, very few peptides exhibit native fluorescence. Therefore, it is necessary to label the peptides with a fluorophore to improve the limits of detection (LOD)[5] for the analytes. The amine groups on peptides can either react either with a dye that is highly fluorescent or with a fluorogenic reagent that will then produce a fluorescent product. The fluorogenic labels can also change electrophoretic mobility of the analyte, and assist (or make worse) the CE and ME separation. Some of the properties of an ideal fluorescence derivatization reagent include a fast reaction rate and the formation of a stable fluorescence product that can produce a strong fluorescent signal[6]. Fluorescence derivatization of peptides is frequently accomplished by the reaction of a fluorogenic label with amine groups of the peptides, mainly its N-terminus or amine containing residues such as lysine or arginine[7-8].

One of the drawbacks of fluorescence derivatization is that many peptides with more than one derivatization site, such as peptides with more than one lysine residue, can form multiple

products with different degrees of fluorescence labeling[9-10] or cause a decrease in fluorescence intensity due to intramolecular quenching[11]. In addition, another downside of fluorescence derivatization is that, in some cases, the derivatization reaction rate is slow and may require a high peptide concentration for the peptide to be derivatized, where the fluorescent derivatized peptide is then diluted to lower concentration for CE-LIF and ME-LIF analysis[5]. Various functional groups within a peptide structure can also alter the reactivity of the primary amine group through inductive and steric effects[7].

Naphthalene-2,3-dicarboxaldehyde (NDA) is a fluorogenic reagent that can react rapidly with primary amines on amino acids, peptides and proteins in the presence of cyanide ions (CN) as the nucleophile, to produce a 1-cyanobenz[f]isoindole (CBI) products [Figure 1A][12-14]. Favorable properties of NDA include that the probe is not fluorescent, the reaction is reported to be rapid, a stable fluorogenic CBI derivative is produced and there is a minimal effect of pH on the fluorescent signal intensity[12, 15]. The CBI fluorescent product has two excitation wavelengths in the visible region: ($\lambda_{ex}$) of 420, and 440 nm and an emission wavelength of ($\lambda_{em}$) ~ 490 nm[16].

Another widely used reagent for the derivatization of peptides is fluorescein isothiocyanate (FITC). FITC is a highly fluorescent reagent. It is known to form FITC fluorescent derivatives by reacting with primary amines to produce a fluorescent product. In this case, the excitation wavelength is 488 nm and the emission wavelength ~ 520 nm[17-18] [Figure 1B]. However, products of the FITC reaction can undergo extensive photobleaching, and the fluorescence intensity is pH sensitive[19]. Another disadvantage of FITC labeling is that the reagent itself produces a strong fluorescent signal that can interfere with the analytical separation by co-migrating with the analytes of interest.

A)

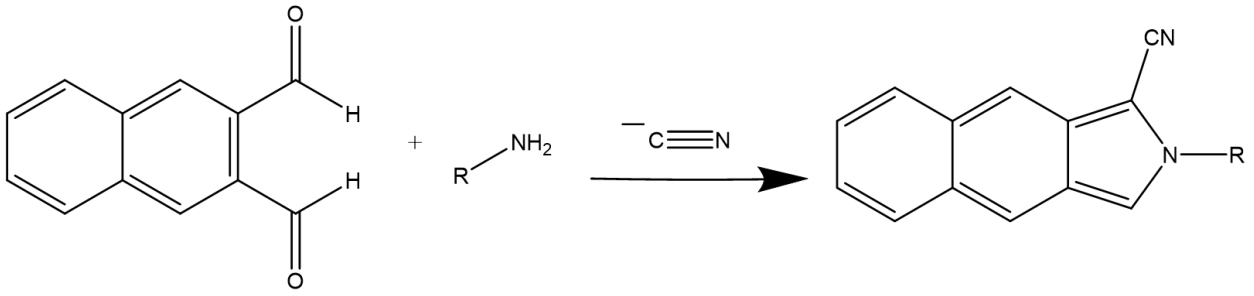


Naphthalene-2,3-dicarboxaldehyde Primary amine 1-cyanobenz[f]isoindole(CBI) products

B)

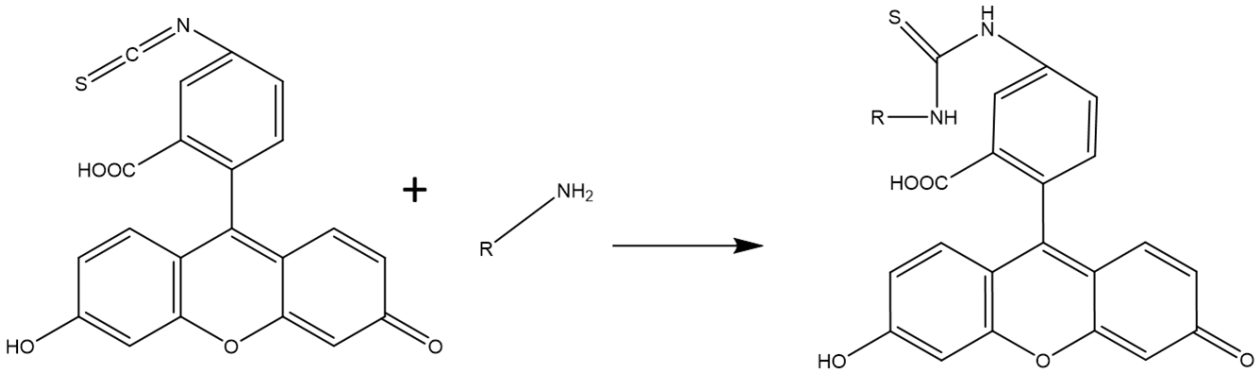


Fluorescein isothiocyanate (FITC) Primary amine FITC derivative

**Figure 1:** A) The formation of fluorescent CBI derivative by the reaction of NDA with a primary amine in the presence of CN. B) The reaction of the fluorescent dye of fluorescein isothiocyanate (FITC) with a primary amine producing an FITC derivative.

The ability to couple microdialysis (MD) sampling to CE-LIF and ME-LIF offers a method to perform online continuous sampling of dynorphins in the brain and spinal cord with high temporal and spatial resolution. The use of a slow flow rate (0.1-2 µL/min) in MD sampling is preferred for obtaining higher analyte recovery[20], which is ideal for the analysis of low concertation of bioactive peptides such as dynorphins in the brain. The coupling MD-ME can be further developed to undergo on chip fluorescent derivatization and detection using LIF[20-21]. The ultimate goal of this project is to develop and on-line system for continuous monitoring of these peptides in awake freely moving animals to better understand neurodegenerative disease. This chapter describes the first steps towards an on-line separation system. Experimental results obtained for the development of a separation and detection of derivatized dynorphins by capillary and microchip electrophoresis with LIF detection are described.

## 5.2 Materials and methods

### 5.2.1 Reagents and chemicals

Dyn A (1–17), Dyn A (1–13), Dyn A (1–8), and Dyn A (1–7) were purchased from Biomatik (Cambridge, ON, Canada). Dyn A (1–6) was purchased from Shanghai MoCell Biotech (Shanghai, China). Leu-enkephalin (Leu-ENK) was received from Alfa Aesar (Ward Hill, MA). Polydiallyldimethylammonium chloride (pDDA) 20% solution with an average molecular weight of 200–350 kDa, sodium phosphate monobasic, sodium phosphate dibasic, boric acid sodium dodecyl sulfate (SDS) and Brij® 35 were received from Sigma–Aldrich (St. Louis, MO). Hydrochloric acid and sodium hydroxide (molecular biology grade >98%), HPLC grade methanol, acetonitrile, and dimethyl sulfoxide (DMSO) were purchased from Fisher Scientific (Fair Lawn,

NJ). All water used was Milli-Q grade (resistivity of 18 MΩ). Aqueous filter membranes (0.2 μm) were purchased from Fisher Scientific. Polyimide-coated fused-silica capillaries were received from Polymicro Technologies (Phoenix, AZ).

### 5.2.2 Equipment

#### 5.2.2.1 CEC-LIF

Analyses were performed on a Beckman Coulter P/ACE MDQ (Brea, CA) CE system. Polyimide-coated fused-silica capillaries 50 μm id, 375 μm od (Polymicro Technologies) were employed in the study. The total length of the capillary was 75 cm, the effective length (from injection to detector) was 60 cm. A 0.5 cm detection window was made by burning off the outer polyimide capillary coating with Window Maker® (Eatontown, NJ). Samples were introduced using hydrodynamic injection by applying 0.5 psi head pressure for 5 s. Electrophoretic separations were performed at an applied voltage of −20 kV. Following each run, the pDDA modified capillaries were rinsed with BGE for 3 min before the next sample injection. Data were recorded using the 32 Karat software (Beckman Coulter).

LIF detection was accomplished using a 442-nm CL-2000 diode laser (Crysta Laser; Reno, NV), and monitoring emission data were collected with an external fluorescence detector (Picometrics; Ramonville, France). The LIF detector was controlled with 32 Karat software (Beckman).

#### 5.2.2.2 Preparation of buffer and standard solutions

A stock solution of 200 mM sodium phosphate buffer (pH 6.8) was prepared using sodium phosphate monobasic and sodium phosphate dibasic. The pH was adjusted using 1 M sodium hydroxide or 1 M hydrochloric acid to the required pH. The BGE used for electrophoresis separation was prepared by further dilution of the stock solution to the required concentration. A stock solution of NDA was prepared in equal volumes of acetonitrile and water to a final concentration of 5 mM. A 20-mM solution of NaCN was prepared in water. Both NDA and NaCN solutions were protected from light and stored at 4ºC for a maximum of one week. All BGE solutions used were filtered with a 0.2 µm membrane filter before use. Standard solutions of opioid peptides used were prepared in $H_2O$ to 1 mg/ml, and then further diluted to the required working concentration.

Derivatization of the peptide to produce a CBI-product was accomplished by mixing 15 µL of 500 µM of the peptide in phosphate buffer (pH6.8) with 25 µL NDA and 10 µL NaCN to (approximately ratio of 1: 16: 26 peptide: NDA: CN), and then allowing it to react for 15 mins. The solution was then brought to a final volume of 150 µL with phosphate buffer (pH 6.8) and injected into the CE.

The FITC-peptide derivatization was accomplished by slowly adding the florescent FITC dye to a solution of 100 µM of the peptide in 100 mM phosphate buffer solution (pH7) at a ratio of 2:1. The solution mixture was then protected from light and left to react overnight at room temperature.

#### 5.2.2.3 Capillary column coating procedure

All solutions used for the modification of the fused silica capillaries were freshly prepared daily. The capillary coating procedure is similar to the method described previously in chapter 4. Briefly, a new fused-silica capillary was preconditioned with 0.1 M HCl, followed by water, methanol, water, 0.1 N NaOH, finally water for 5 mins each. This was followed by rinsing the capillary with 0.1 N NaOH for 5 min followed by $H_2O$ for 5 min; this was followed by rinsing the capillary 0.2% pDDA solution for 30 min and then rinsing the capillary with 0.02% pDDA in BGE for 10 min. A −20 kV potential was applied across the capillary for 10 min following the conditioning for equilibration of the BGE within the pDDA-coated capillary.

#### 5.2.2.4 Fabrication of silicon master and PDMS/ glass microchip electrophoresis

The fabrication procedure for the creation of the silicon master with a simple-t design has been described elsewhere[22]. Briefly, a 4-inch silicon wafer was spin coated with SU-8 negative photoresist (thickness 15 μm) using Brewer Science Cee 200CBX spin coater (Rolla, MO). This was followed by a soft bake at 65℃ for 2 min then a 5 min bake at 95°C. After the wafer is cooled to room temperature, a photomask with the design of the microfluidic channels is placed over the negative photoresist coated wafer, and then exposed to UV light using a UV flood source. The master is then post-baked at 65°C for 1 min, then 95°C for 2 min and placed in an SU-8 developer for 30 seconds to remove the uncrosslinked photoresist. Next, it is rinsed with 2-propanol and dried with nitrogen. Finally, a hard bake is performed at 200°C for two hours. The height (15 μm) and width (40 μm) of the raised structure on the surface of the fabricated silicon master was measured using an Alpha Step-200 surface profiler. A mixture of PDMS/curing agent (10:1) is poured over

the silicon master and then cured at a temperature of 70°C for 4 hours. The PDMS channels are then peeled from the silicon master, and reservoir holes were punched into the PDMS by using a biopsy punch (Harris Uni-Core, Ted Pella, Inc., Redding, CA). Finally, the PDMS layer was placed over a glass plate. This silicon master can be used to produce a large number of PDMS chips.

**5.2.2.5 Fabrication of glass microchip electrophoresis:**

The fabrication of glass microchips was accomplished using standard photolithography and wet chemical etching methods. Our group[20, 23] previously described the fabrication method of glass/glass microchip. Briefly, a photomask with the microchip design was placed over a 1.8 µm thick positive photoresist (AZ1518), chrome coated 4″ × 4″ borosilicate substrate (Telic Company, Valencia, CA). The substrate was then exposed to UV light using a UV flood source (ABM Inc., Scotts Valley, CA) for 4 seconds. The UV exposed photoresist was then removed by placing the glass substrate into AZ300® MIF developer (Capitol Scientific, Inc., Austin, TX) for 20 seconds. The glass plate was washed with $H_2O$, dried with nitrogen gas and placed on a programmable hotplate (Thermo Scientific, Waltham, MA) and baked at 100 °C for 10 min. The Cr layer was then removed using a Cr etchant solution, CR-7S (OM Group. Fremont, Ca) to reveal the underlying glass. The exposed glass was etched using a glass etchant solution composed of $HF/HNO_3/H_2O$ (20:40:40) to a depth of approximately 15 µm (note: extreme caution must be taken when handling solutions containing HF). Once the desired depth of the trench was reached, the plate was washed with a $CaCO_3$ suspension and then water.

The depth of the trench was measured using Alpha-step 200 profilometer (KLA-Tencor, Milpitas, CA). Reservoir holes (0.5 cm diameter) were drilled into the glass plate using a

MicroLux® Drill Presse (Berkeley Heights, NJ). A glass coverplate and the newly etched glass plate were both rinsed with a calcium assisted bonding solution containing (0.5% Alconox® and 0.5% calcium acetate)[24] and then sealed together under running D.I $H_2O$. The two plates were held together using binder clips, and placed into a low-temperature oven at 70 ℃ for 2 hours. At that time, the chip was inspected for the absence of Newton rings, and then the temperature was increased to 115 °C for 3 hours. The binder clips were then removed, and the glass microchip is placed in Isotemp® programmable furnace (Fisher Scientific, Fair Lawn, NJ), and weights were placed over the sealed glass plates. The following temperature program was used to thermally bond the glass plates: the temperature program began by an initial temperature of 25 °C then the temperature was ramped up to 590 °C a rate of 3 °C/min, then to 630°C at a rate of 3.5 °C/min and held at 630°C for 10 hours. The temperature was then lowered to 590 °C at a rate of 2.5 °C/min, followed by 565 °C at a rate of 1.5 °C/min and held at 565 °C for 30 minutes, this was followed by the lowering of the furnace temperature to 505 °C at a rate of 0.5 °C/min, and finally the temperature was ramped down to 25 °C at a rate of 5 °C/min.

#### 5.2.2.6 Equipment and microchip operation

Fluorescence detection was accomplished using a Nikon Eclipse Ti-U inverted microscope (Nikon, Melville, NY) coupled with either a 445-nm laser PhoxX diode laser (Market Tech, Scotts Valley, CA) or 488-nm diode laser (Spectra-Physics, Irvine, CA) for excitation and a photomultiplier (Hammatsu Corporation, Bridgewater, NJ) as the excitation source. The signal was amplified using a SR570 low noise current preamplifier at 2 μA/V (Stanford Research Systems, Sunnyvale, CA).

The applied high voltage was supplied to buffer (B) and sample reservoirs (S) by a 15-kV high voltage power supply (Ultravolt, Ronkonkoma, NY), with the sample waste (SW) and buffer waste (BW) reservoirs kept at ground. The samples were injected by the gated injected method, that was described in previously in chapter 3. An in-house written LabVIEW program was used for both control of the high voltage power supply and data acquisition [Figure 2].

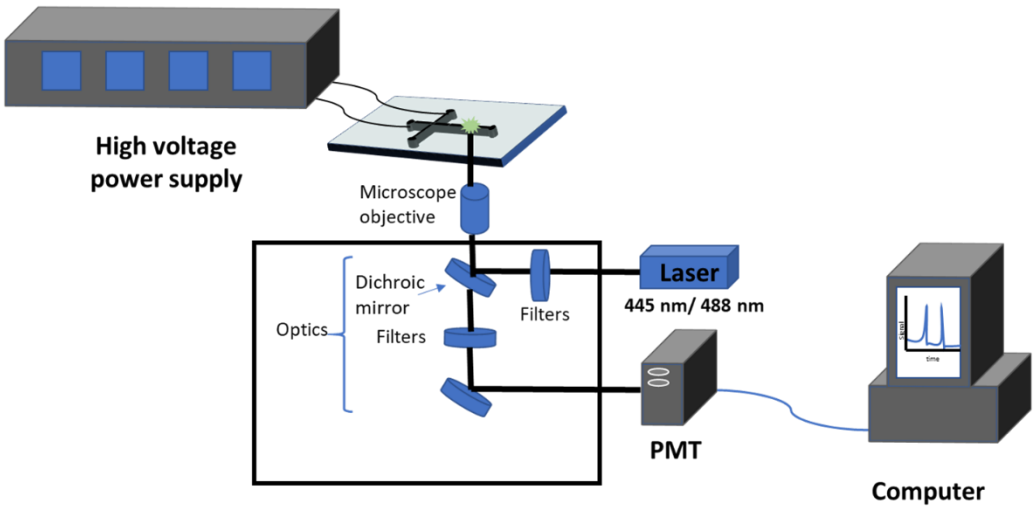


**Figure 2:** Diagram of the capillary microchip LIF system.

## 5.3 Results and discussion

### 5.3.1 Separation of CBI-dynorphin fragments using a pDDA-coated capillary coupled to LIF

Peptide mixtures of NDA-derivatized Leu-ENK, Dyn A (1-6), Dyn A (1-7) and Dyn A (1-8) were injected into the modified pDDA coated capillary via pressure injection and the separation voltage was applied. In the case of this modified capillary, the positively charged polymer adsorbs onto the wall of the negatively charged fused silica capillary. This causes electrostatic repulsion

between the adsorbed polymer and the cationic peptides. The order of migration was Leu-ENK, followed by Dyn A (1–6), Dyn A (1–8), and finally Dyn A (1–7). The BGE consisted of 20–80 mM phosphate buffer (pH 6.8) containing 0.02% v/v pDDA. The separation voltage was –20 kV (reverse polarity). The effect of phosphate buffer concentration on the resolution of the four peaks is shown in figure 3.

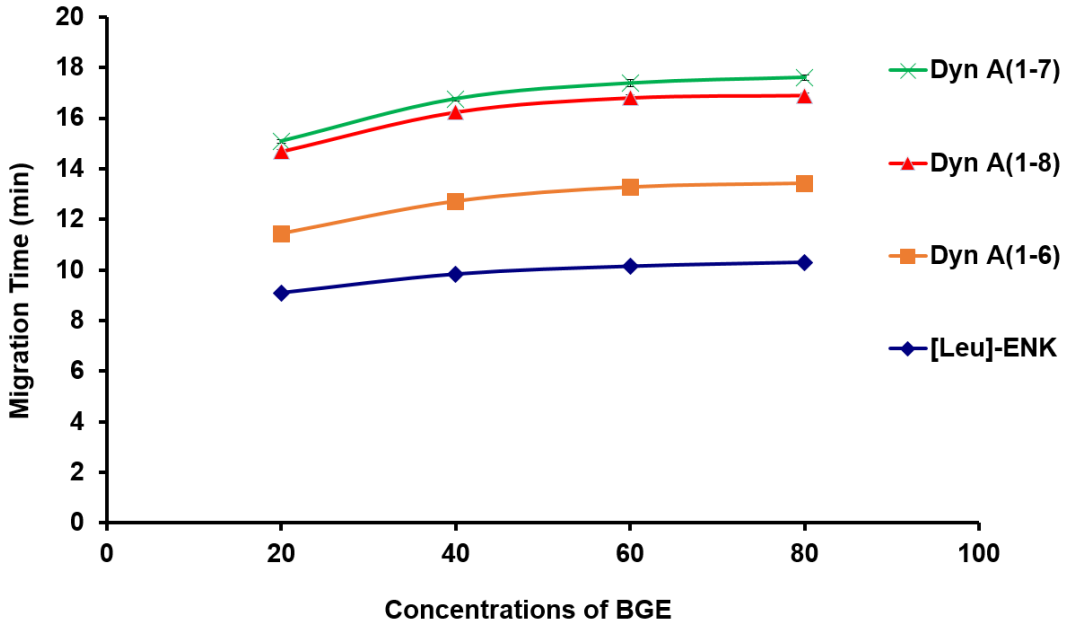


**Figure 3:** Migration times of the four peptides at BGE concentrations 20, 40 60 and 80 mM phosphate buffer containing 0.02% pDDA. pDDA-modified capillary. HV= –266 V/cm, $L_T$= 75 cm, $L_D$ = 60 cm i.d.= 50 µm.

The separation efficiencies for the dynorphin peaks were calculated for different concentrations of phosphate [Figure 4]. The number of theoretical plates (N) was calculated by the following equation:

$$N = 5.54 \, (t / W_{0.5})^2$$

where (t) is the time in seconds and ($W_{0.5}$) is width at half the peak height. The increase in BGE phosphate concentration from 20 mM to 60 mM increased the number of theoretical plates from approximately 110,000 to 140,000 and 195,000 to 20,000 N for CBI-Dyn A (1-8) and CBI-Dyn A(1-7) respectively. However, at 80 mM phosphate, a noticeable decrease in peak efficiency for both Dyn A (1-8) and Dyn A (1-7) was observed. That is most likely due to the effect of Joule heating at higher BGE concentrations, causing band broadening and thus higher $W_{0.5}$ value[25].

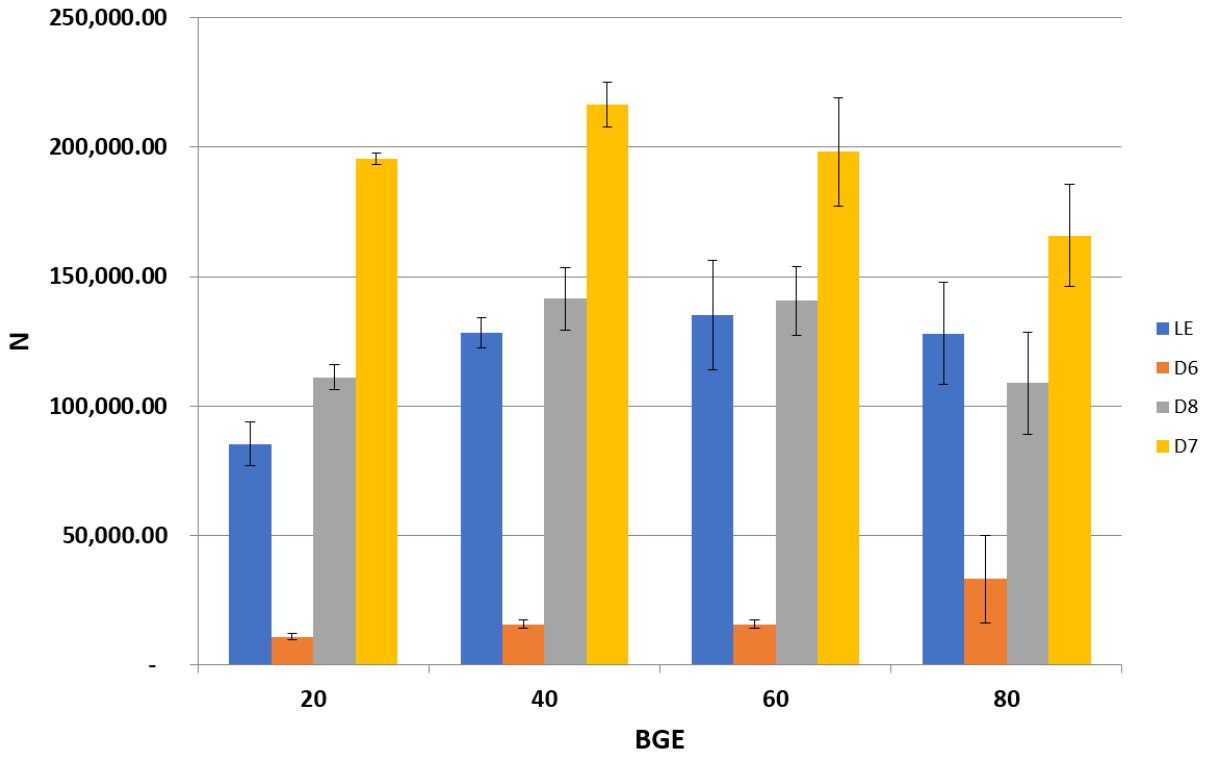


**Figure 4:** Number of theoretical plates (N) the four CBI-peptides at BGE concentrations 20, 40 60 and 80 mM phosphate buffer containing 0.02% pDDA using pDDA-modified capillary. HV= –266 V/cm, $L_T$= 75 cm, $L_D$ = 60 cm, i.d.= 50 µm.

The optimum BGE was found to be composed of a phosphate buffer at a concentration of 40 mM containing 0.02% pDDA. . The electropherogram obtained for the separation of the four opioid peptides, Leu-ENK, Dyn A (1–6), Dyn A (1–7), Dyn A (1–8) is shown in figure 5.

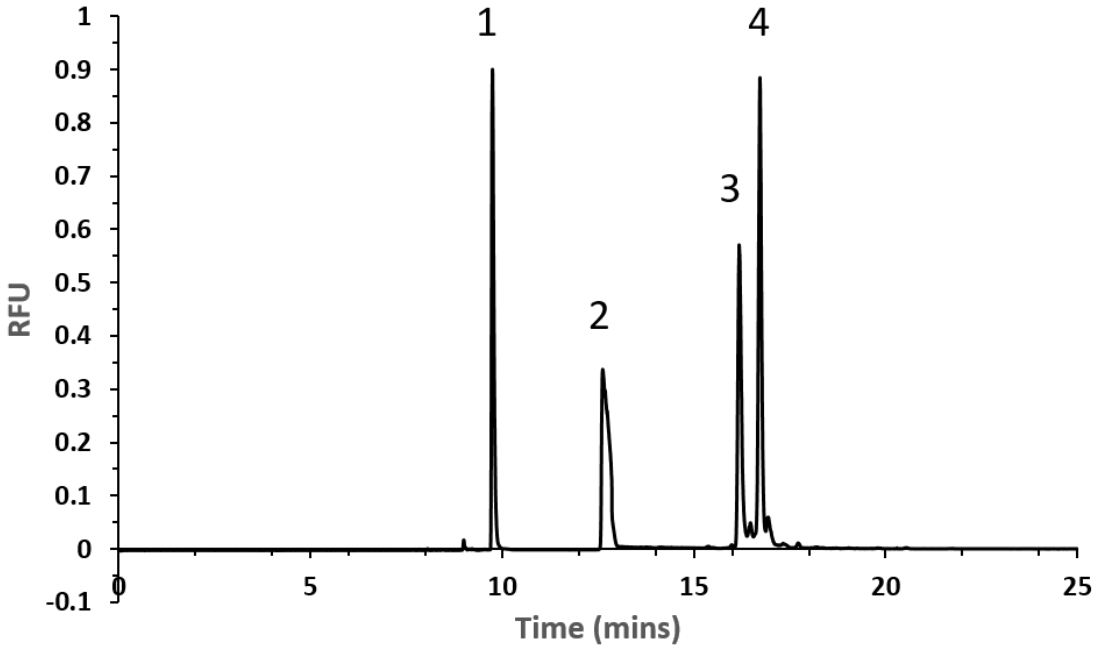


**Figure 5:** Separation of (1) CBI-Leu-ENK, (2) CBI-Dyn A (1–6), (3) CBI-Dyn A (1–8), (4) CBI-Dyn A (1–7). pDDA-modified capillary. HV= –20 kV, $L_T$= 75 cm, $L_D$ = 60 cm i.d.= 50 µm; BGE: 40 mM phosphate buffer solution (pH 6.8) containing 0.02% pDDA.

A major goal of this project was to develop a microchip electrophoresis system that can detect dynorphin and its metabolites at endogenous concentrations by using a sensitive detection method, such as LIF. This method could then be further developed to be used as an on-line derivatization and analysis system for detection of dynorphin in brain microdialysis samples. Therefore the next step was to tranfer the capillary method to a microchip format

### 5.3.2 Development of a microchip electrophoresis system for the separation of dynorphins

As was previously mentioned, ME is a fast separation technique, which has the abilities to for performing multiple sequential injections. ME also has the potential to incorporate continuous sampling by coupling to MD with on chip derivatization. Thus, the development of ME system that can offer continuous sampling, with on-chip derivatization, separation and LIF detection of abnormal levels of dynorphins would be useful for monitoring and the study the effect of these opioid peptides has on neurological disorders.

#### 5.3.2.1 PDMS/ glass hybrid microchip electrophoresis of FITC derivatized dynorphins

FITC was initially was chosen as the derivatizing agent for the ME-LIF analysis of the dynorphins fragments due to its excellent fluorescence quantum yield ( > 0.85) and its compatibility with the 488 nm Argon ion laser. In order to perform an electrophoretic separation on a microchip, a stable electroosmotic flow (EOF) is required for both sample injection and to move all analytes to the detector. Materials such as PDMS do not have a strong surface charge. Thus surfactants, such as SDS, are frequently used to provide a charge to the channel walls. The addition of SDS provides a negatively charged layer by hydrophobic interaction of the surfactant hydrophobic tail to the wall of the PDMS[26] microchip. ME analysis of FITC derivatized Dyn A (1-8), Dyn A(1-13), Dyn A(1-17) was first performed [Figure 6A, 6B and Figure 7 respectively] using a BGE comprising of 15 mM sodium phosphate (pH 7), 2 mM SDS and 5% DMSO. The applied voltages to the buffer and sample reservoir was 2,400 V and 2,200 V respectively. The peptide samples were injected using a 1 s gated injection method.

Molecules derivatized with FITC typically produce derivatives with strong fluorescent intensity. However, the disadvantages of the use of FITC for dynorphins derivatization included the long reaction time that was required. In addition, the reagent also produced a high-intensity fluorescent signal, that hindered the separation of dynorphin peptides derivatized with FITC [Figure 8].

**A)**

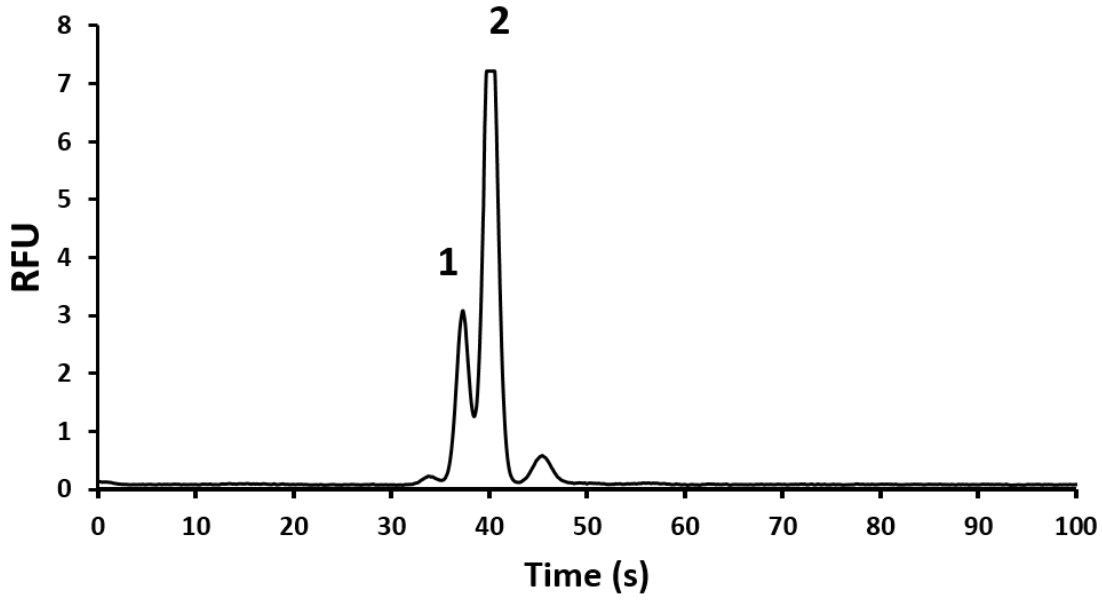


**B)**

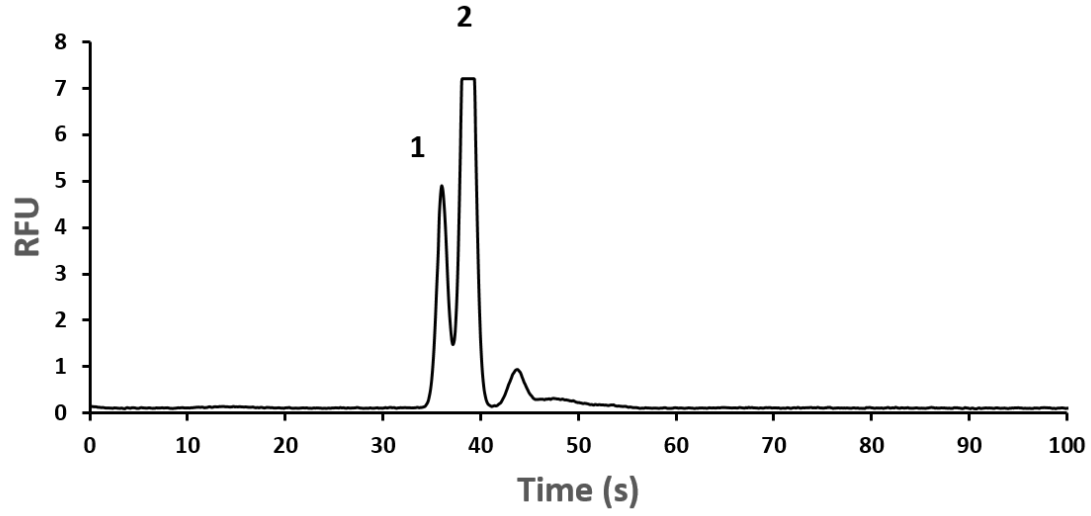


**Figure 6:** PDMS/glass ME of FITC labeled dynorphins. A: 20 µM FITC-Dyn A 1-8 (1), FITC (2). B: electropherogram of 20 µM FITC-Dyn A1-13 (1), FITC (2). Separation channel length 5 cm. HV (B/S): 2400/ 2200 V. BGE: 15 mM sodium phosphate (pH7) with 2mM SDS and 5% DMSO.

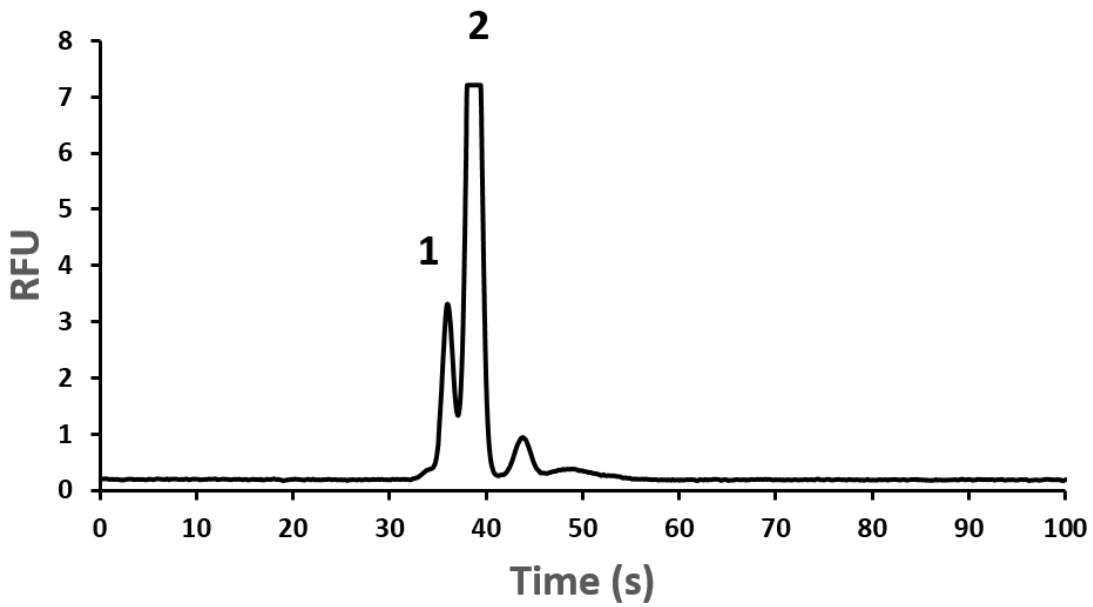


**Figure 7:** Electropherogram of 20 µM FITC-Dyn A 1-17 (1), FITC (2). The PDMS/ glass microchip used with a 5-cm separation channel, HV: 2,400 V (B), 2,200 V (S), 1-sec gated injection. BGE: 15 mM sodium phosphate (pH7) with 2mM SDS and 5% DMSO.

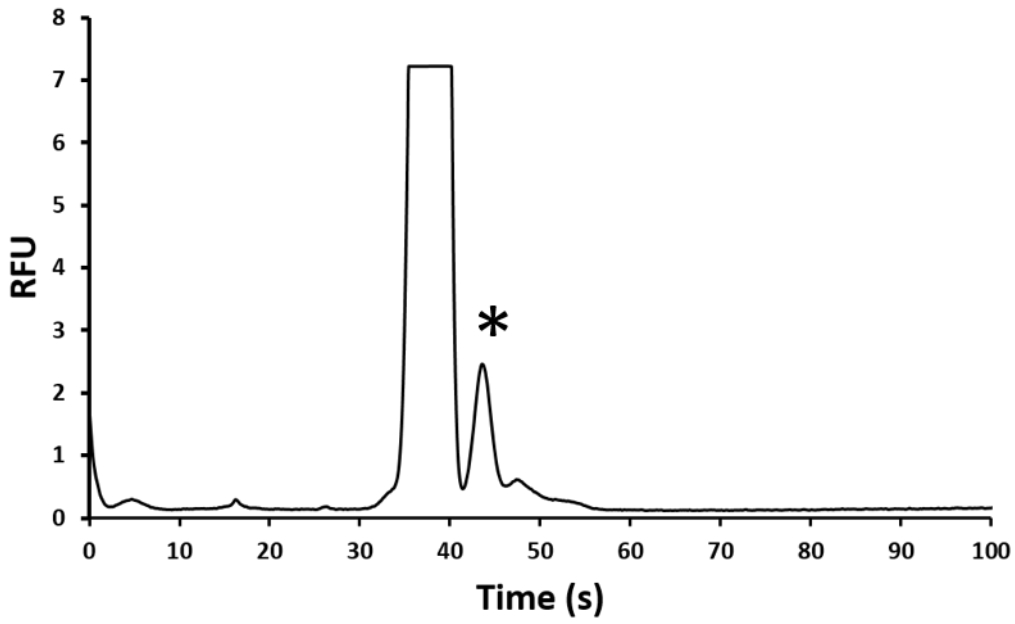


**Figure 8:** Electropherogram of a mixture of FITC labeled Dyn A (1-8), FITC-Dyn A (1-13) and FITC-Dyn A (1-17). PDMS/ glass microchip used with a 5-cm separation channel, HV: 2,400 V (B), 2,200 V (S), 1-sec gated injection. BGE: 15 mM sodium phosphate (pH7) with 2mM SDS and 5% DMSO. Excess FITC comigrated with all three labeled peptides. *Shows degradation product of FITC peak.

### 5.3.2.2 Glass/ glass microchip electrophoresis of NDA/CN derivatized dynorphins

The composition of the BGE is known affect the migration time, resolution of analytes, and the amount of current within the ME channels. The initial separation of the two NDA/CN derivatized peptides Leu-ENK and Dyn A (1-8) was performed by using a 15 cm long serpentine glass/glass microchip with an applied voltage of 8,500 V (B) and 7,500 V (S) that corresponds to a field strength of ~ 430 V/cm (calculated using Kirchoff's Laws). A 1 s gated injection was used. The BGE constituted of 15 mM boric acid (pH 10) containing 10% methanol. The electrolyte

within BGE and reaction mixture was changed from sodium phosphate to boric acid because boric acid is less conductive and thus produced lower current than BGE containing sodium phosphate. Attempts to use phosphate as BGE was found to cause excessively high currents.

Figure 9 shows the electropherogram of a mixture of the two peptides CBI-Dyn A (1-8) and CBI-Leu-ENK. The peak of CBI-Dyn A (1-8) exhibited some tailing and a lower peak height than was expected (LOD ≈ 5 µM). An attempt was then performed to improve peak height and reduce peak tailing of CBI-Dyn A (1-8) by the addition of Brij-35 as an additive to the BGE (0.02 and 0.06 mM). Brij®-35 is a nonionic surfactant (critical micelle concentration 0.09 mM) that has been shown to decrease absorption of cationic peptides to microchip glass channels. Unfortunately, the addition of Brij®-35 did not improve either the peak shape nor peak height [Figures 10A and 10B].

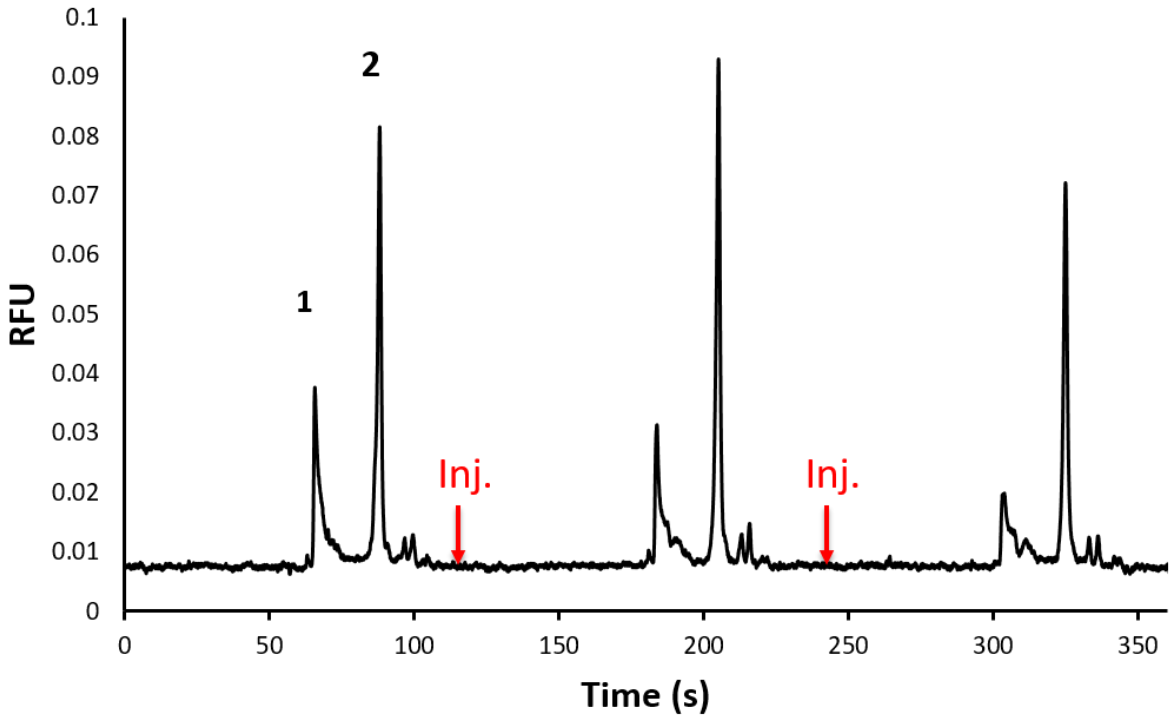


**Figure 9:** Electropherogram of ME injection of a mixture of (1) 25 µM Dyn A (1-8) and (2) 25 µM Leu-ENK on a 15 cm serpentine glass/glass microchip. BGE: 15 mM boric acid (pH 10) with 10 % methanol.

**A)**

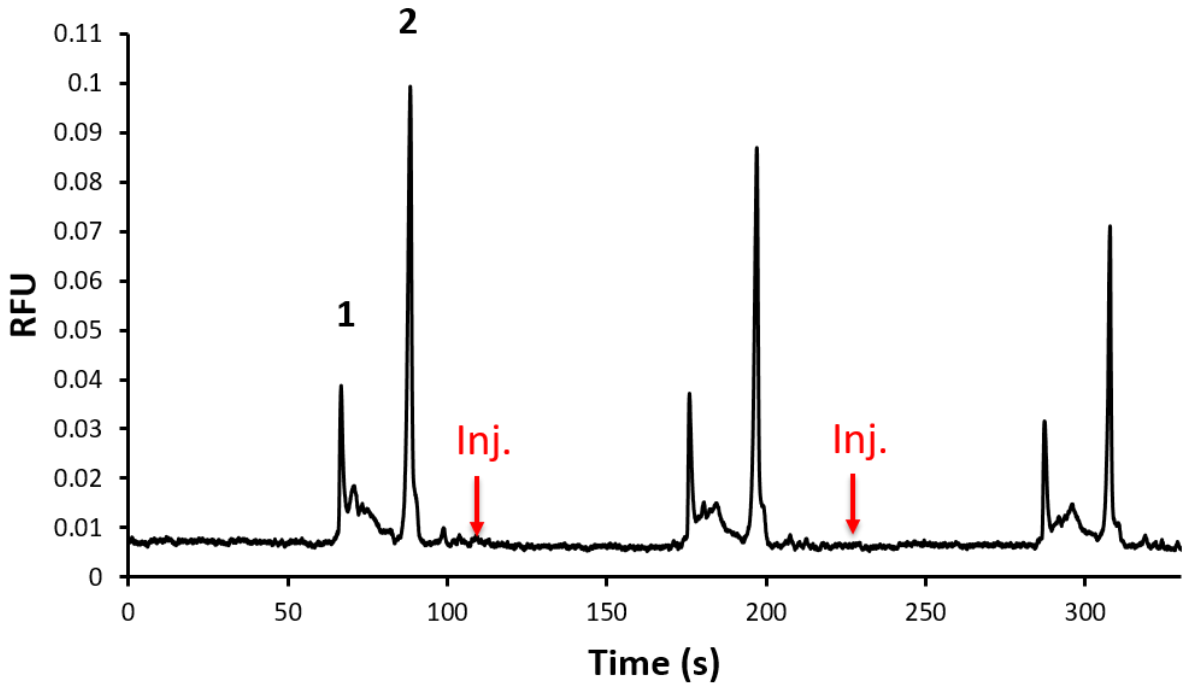


**B)**

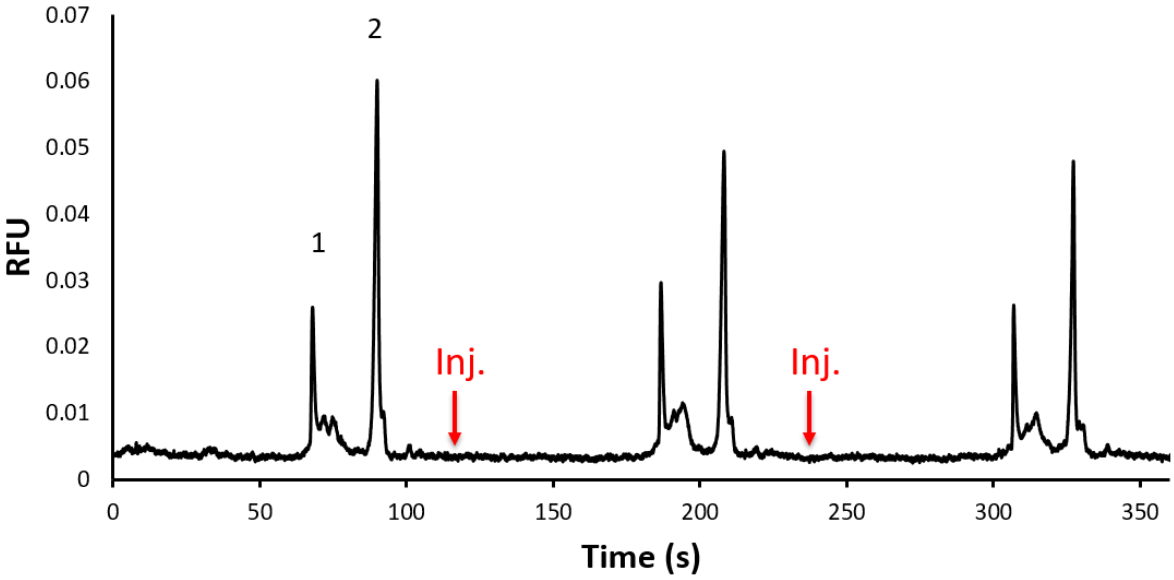


**Figure 10:** The ME electropherogram of a mixture of (1) 25 µM Dyn A (1-8) and (2) 25 µM Leu-ENK on a 15-cm serpentine glass/glass microchip. BGE: 15 mM boric acid (pH 10) containing 10 % methanol and A) 0.02 mM and B) 0.06 mM.

For the analysis of the fluorescent derivatized peptide CBI-Dyn A (1-17), both the sample reaction mixture and BGE composition and pH were adjusted to contain a higher concentration of an organic solvent. In addition, the pH was increased to pH 10. The addition of DMSO was found to improve the solubility of CBI-Dyn A(1-17), where the absence of DMSO in the BGE lead to the disappearance of the peak. Increasing the pH of the reaction mixture to pH 10 increased the rate of the reaction of the amine on Lys (approximately 4 mins) compared to that of the N-terminal of Dyn A (1-17). The selective derivatization of peptides with more than one primary amine has been previously described by our group and others for ϵ-amino group of the Lys residue for opioid peptide substance P (1-11) and some of its fragments with NDA/CN. Figure 11 shows a microchip electropherogram if an injection of 25 μM of CBI-Dyn A (1-17) on a 15-cm glass microchip, with BGE composed of 5 mM boric acid

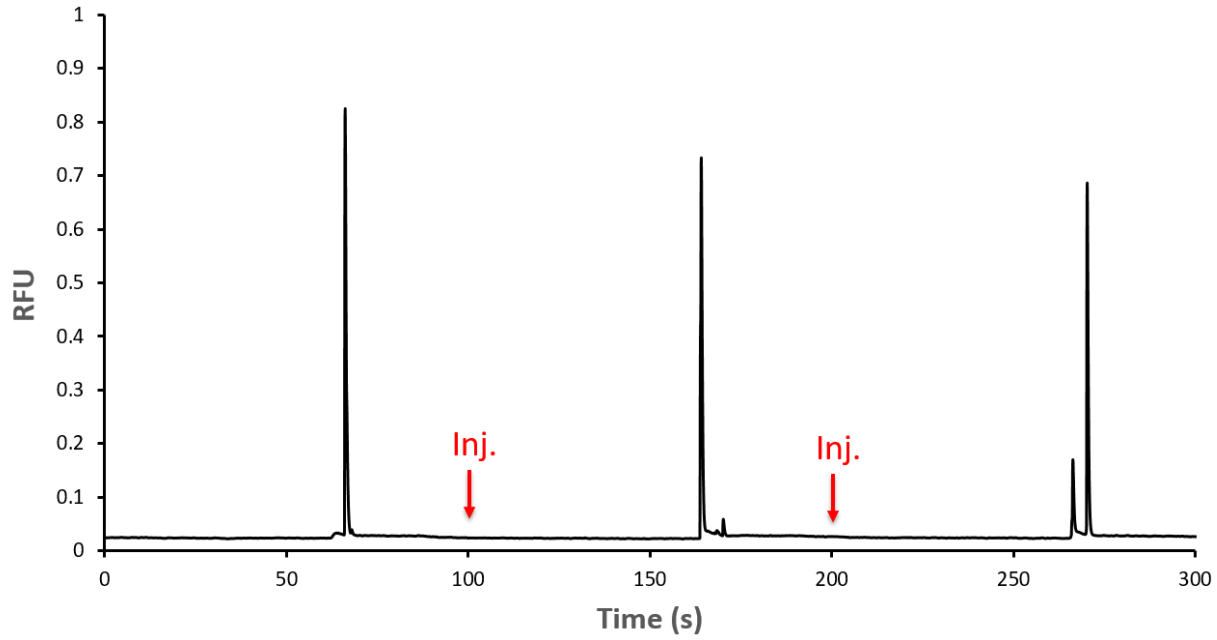


**Figure 11:** Microchip electropherograms of a gated injection of 25 µM Dyn A (1-17) derivatized with NDA/CN. HV: 8,500 V (B), 7,500 V (S), 1-second gated injection. BGE: 5 mM boric acid (pH 10) containing 15% DMSO.

### 5.4 Conclusions and Future Directions

For the development of a microchip system with continuous sampling and analysis of dynorphins, the selection of fluorescent derivatization method is vital. The use of the fluorogenic agent NDA/CN for the fluorescent derivatization of dynorphin was found to be a preferred derivatizing method compared to FITC. The use of FITC as a derivatizing agent for microchip electrophoresis of dynorphin will require additional steps of sample preparation to remove excess FITC dye from the sample prior to analysis. This can be accomplished using as solid-phase extraction (SPE) or size exclusion chromatography before the introduction of the peptide sample into the microchip. For MD samples this would mean that the sample would need to be derivatized

pre-column over several hours, and then an additional step of removing any excess FITC would be needed since excess FITC has shown to interfere with ME analysis of these peptides. Thus the use of NDA/CN is a more favorable fluorescent derivatizing method for the application. However, the difference in reaction rates between various fragments of dynorphin and the fluorogenic agent may require future adaptation in the microchip design, for example, valves to split the sample to react at different reaction conditions, or the incorporation of mixing channels to increase the reaction rates.

## 5.5 Reference


1. Na, D. H.; Lee, K. C., Capillary Separation Techniques. In *Handbook of Pharmaceutical Biotechnology*, John Wiley & Sons, Inc.: 2006; pp 469-510.

2. Laing, T. D.; Marenco, A. J.; Moore, D. M.; Moore, G. J.; Mah, D. C. W.; Lee, W. E., Capillary electrophoresis laser-induced fluorescence for screening combinatorial peptide libraries in assays of botulinum neurotoxin A. *J. Chromatogr. B* **2006,** *843* (2), 240-246.

3. Verpillot, R.; Esselmann, H.; Mohamadi, M. R.; Klafki, H.; Poirier, F.; Lehnert, S.; Otto, M.; Wiltfang, J.; Jean-Louis, V.; Taverna, M., Analysis of amyloid-beta peptides in cerebrospinal fluid samples by capillary electrophoresis coupled with LIF detection. *Anal. Chem.* **2011,** *83* (5), 1696-703.

4. Ban, E.; Song, E. J., Recent developments and applications of capillary electrophoresis with laser-induced fluorescence detection in biological samples. *J. Chromatogr. B Analyt. Technol. Biomed. Life Sci.* **2013,** *929*, 180-6.

5. Banks, P. R., Fluorescent derivatization for low concentration protein analysis by capillary electrophoresis. *TrAC, Trends Anal. Chem.* **1998,** *17* (10), 612-622.

6. De Antonis, K. M.; Brown, P. R., Analysis of derivatized peptides using high-performance liquid chromatography and capillary electrophoresis. *Adv. Chromatogr.* **1997,** *37*, 425-52.

7. García-Campaña, A. M.; Taverna, M.; Fabre, H., LIF detection of peptides and proteins in CE. *Electrophoresis* **2007,** *28* (1-2), 208-232.

8. Kostel, K. L.; Lunte, S. M., Evaluation of capillary electrophoresis with post-column derivatization and laser-induced fluorescence detection for the determination of substance P and its metabolites. *Journal of Chromatography B: Biomedical Sciences and Applications* **1997,** *695* (1), 27-38.

9. Banks, P. R.; Paquette, D. M., Monitoring of a conjugation reaction between fluorescein isothiocyanate and myoglobin by capillary zone electrophoresis. *J. Chromatogr.* **1995,** *693* (1), 145-154.

10. Craig, D. B.; Dovichi, N. J., Multiple Labeling of Proteins. *Anal. Chem.* **1998,** *70* (13), 2493-2494.

11. Soper, S. A.; Chamberlin, S.; Johnson, C. K.; Kuwana, T., The Intramolecular Loss of Fluorescence by Lysine Derivatized with Naphthalenedialdehyde. *Appl. Spectrosc.* **1990,** *44* (5), 858-863.

12. Zotou, A.; Notou, M., Study of the naphthalene-2,3-dicarboxaldehyde pre-column derivatization of biogenic mono- and diamines in mixture and fluorescence-HPLC determination. *Anal. Bioanal. Chem.* **2012,** *403* (4), 1039-48.

13. De Montigny, P.; Riley, C. M.; Sternson, L. A.; Stobaugh, J. F., Fluorogenic derivatization of peptides with naphthalene-2,3-dicarboxaldehyde/cyanide: Optimization of yield and application in the determination of leucine-enkephalin spiked human plasma samples. *J. Pharm. Biomed. Anal.* **1990,** *8* (5), 419-429.

14. Lunte, S. M.; Mohabbat, T.; Wong, O. S.; Kuwana, T., Determination of desmosine, isodesmosine, and other amino acids by liquid chromatography with electrochemical detection following precolumn derivatization with naphthalenedialdehyde/cyanide. *Anal. Biochem.* **1989,** *178* (1), 202-7.

15. De Montigny, P.; Stobaugh, J. F.; Givens, R. S.; Carlson, R. G.; Srinivasachar, K.; Sternson, L. A.; Higuchi, T., Naphthalene-2,3-dicarboxyaldehyde/cyanide ion: a rationally designed fluorogenic reagent for primary amines. *Anal. Chem.* **1987,** *59* (8), 1096-1101.

16. Lacroix, M.; Garrigues, J.-C.; Couderc, F., Reaction of Naphthalene-2,3-Dicarboxaldehyde with Enkephalins for LC-Fluorescence and LC-MS Analysis: Conformational Studies by Molecular Modeling and H/D Exchange Mass Spectrometry. *J. Am. Soc. Mass Spectrom.* **2007,** *18* (9), 1706-1713.

17. Little, M. J.; Paquette, D. M.; Harvey, M. D.; Banks, P. R., Single-label fluorescent derivatization of peptides. *Anal. Chim. Acta* **1997,** *339* (3), 279-288.

18. Yang, W.-c.; Yeung, E. S.; Schmerr, M. J., Detection of prion protein using a capillary electrophoresis-based competitive immunoassay with laser-induced fluorescence detection and cyclodextrin-aided separation. *Electrophoresis* **2005,** *26* (9), 1751-1759.

19. Mahmoudian, J.; Hadavi, R.; Jeddi-Tehrani, M.; Mahmoudi, A. R.; Bayat, A. A.; Shaban, E.; Vafakhah, M.; Darzi, M.; Tarahomi, M.; Ghods, R., Comparison of the Photobleaching and Photostability Traits of Alexa Fluor 568- and Fluorescein Isothiocyanate- conjugated Antibody. *Cell Journal (Yakhteh)* **2011,** *13* (3), 169-172.

20. Huynh, B. H.; Fogarty, B. A.; Martin, R. S.; Lunte, S. M., On-Line Coupling of Microdialysis Sampling with Microchip-Based Capillary Electrophoresis. *Anal. Chem.* **2004,** *76* (21), 6440-6447.

21. Huynh, B. H.; Fogarty, B. A.; Nandi, P.; Lunte, S. M., A microchip electrophoresis device with on-line microdialysis sampling and on-chip sample derivatization by naphthalene 2,3-dicarboxaldehyde/2-mercaptoethanol for amino acid and peptide analysis. *J. Pharm. Biomed. Anal.* **2006,** *42* (5), 529-534.

22. Meneses, D.; Gunasekara, D. B.; Pichetsurnthorn, P.; da Silva, J. A. F.; de Abreu, F. C.; Lunte, S. M., Evaluation of in-channel amperometric detection using a dual-channel microchip electrophoresis device and a two-electrode potentiostat for reverse polarity separations. *Electrophoresis* **2015,** *36* (3), 441-448.

23. Oborny, N. J.; Costa, E. E. M.; Suntornsuk, L.; Abreu, F. C.; Lunte, S. M., Evaluation of a Portable Microchip Electrophoresis Fluorescence Detection System for the Analysis of Amino Acid Neurotransmitters in Brain Dialysis Samples. *Analytical sciences : the international journal of the Japan Society for Analytical Chemistry* **2016,** *32* (1), 35-40.

24. Allen, P. B.; Chiu, D. T., Calcium-Assisted Glass-to-Glass Bonding for Fabrication of Glass Microfluidic Devices. *Anal. Chem.* **2008,** *80* (18), 7153-7157.

25. Tang, G. Y.; Yang, C.; Gong, H. Q.; Chai, J. C.; Lam, Y. C., Numerical simulation of Joule heating effect on sample band transport in capillary electrophoresis. *Anal. Chim. Acta* **2006,** *561* (1), 138-149.

26. Guan, Q.; Noblitt, S. D.; Henry, C. S., Electrophoretic separations in poly(dimethylsiloxane) microchips using a mixture of ionic and zwitterionic surfactants. *Electrophoresis* **2012,** *33* (2), 379-387.

# Chapter 6

# Summary and Future Directions

## 6.1 Conclusions

This dissertation shows the development of electrophoresis methods for the analysis of the opioid peptide dynorphin A (1-17) and its metabolites. Dynorphins (Dyn) are neuropeptides that have one or more basic amino residues such as Lys and Arg in their chemical structure, in addition to an ionizable nitrogen atom at the peptides N-terminal[1].

One of the research objectives focused on the development of an analytical method towards a capillary electrochromatography (CEC) separation method of dynorphins. CEC with UV detection (214 nm) was used to separate and detect several metabolites of Dyn A (1-17). Fused-silica capillaries were coated with gold nanoparticles stabilized with a positvily chagred polymer polydiallyldimethylammonium chloride (pDDA-GNPs). These capillary coated polycationic nanoparticals were used to minimize the undesirable adsorption of the positively charged dynorphin peptides to the surface of negatively charged fused-silica capillaries. PDDA-GNPs coated capillaries were also compared to pDDA coated capillaries on the resolution of separation. The pDDA-GNPs coated capillary was able to separate a peptide mixure of dynorphins fragments with the advantage of providing a 20% greater anodal EOF (EOF = $-6.3 \times 10^{-4}$ $cm^2/V.s$) compred to pDDA (alone) coated capillary (EOF = $-5.2 \times 10^{-4}$ $cm^2/V.s$) The GNPs coated capillaries were then used for the separation of Dyn A (1-17) and seven of its key metabolites, Dyn A (2-17), Dyn A (1-13), Dyn A (1-11), Dyn A (1-8), Dyn A (1-7), Dyn A (1-6) and Leu-enkephalin (Leu-ENK). Evaluated parameters for the separation of fragments of Dyn A included the effect of the capillary length, changes in the separation voltage and the adjustment of the ionic strength of the background electrolyte (BGE). The best separation of all eight peptides was found to be 40 mM sodium acetate buffer (pH 5) containing 5% GNP, and a field strength of $-306$ $Vcm^{-1}$. This method was used for

the separation of peptide mixtures of Dyn fragments arising from tryptic digestion Dyn A (1-17) over a nine-hour study.

Capillary coating with positively charged materials was found to mask the electrostatic adsorption of dynorphins to the negatively charged capillary surface. However, to achieve the limits of detection necessary for the detection of Dyn metabolites in a biological sample, laser induced fluorescence (LIF) was used. Because dynorphins are not intrinsically fluorescence when excited by a 442 nm laser, four fragments of Dyn A were derivatized with the fluorogenic agent naphthalene-2,3-dicarboxaldehyde (NDA) in the presence of sodium cyanide (CN) and produced a fluorescent 1-cyanobenzoic[f]isoindole derivatives. The fluorescent CBI derivatives were separated using a pDDA coated capillary ($L_T$: 75 cm, $L_D$:60 cm), phosphate buffer (pH 6.8) as the BGE, and operated under reverse polarity (applied voltage: −20 kV), and then detected by an external LIF detector (λex: 442nm, λem: 490nm). The effect fo BGE ionic strength on migration time and efficiency of each of the separated peptides was investigated.

Finally, efforts were made to develop a microchip electrophoresis (ME)-LIF system for the separation of dynorphin, for the ultimate goal is developing an on-line microdialysis(MD)-ME-LIF for measuring levels of dynorphins *in vivo*. For ME analysis, two type of microchips were fabricated. The first was polydimethylsiloxane (PDMS)/glass microchip and the second was borosilicate glass microchip. The opioid peptides were derivatized with either fluorescein isothiocyanate (FITC) and excited using 488 nm laser or derivatized with NDA/CN excited using 445 nm laser. The use of NDA/CN for the fluorescent derivatization of Dyn was found to be a more favorable choice compared to FITC. When excess of the fluorescent agent FITC is added to the dervtization mixture, unreacted FITC was found to interfered with separation. Also, the

derivatization of peptides with FITC requires several hours, which may not be ideal for the development of an on-line sampling system to obtain high temporal resolution.

## 6.2 Future directions

### 6.2.1 Future directions in the development of a MD-ME-LIF method for the study of dynorphins

Concerning the MD-ME-LIF system for the analysis of dynorphins in MD samples, changes in the BGE, materials used for microchip fabrication or the modifications microchip design could potentially improve separation. Our group as previously developed an on-chip derivatization microchip that was used for amino acid analysis [Figure 1][2-4]. In addition, a search for a newer fluorescent derivatization agent such as o-phthalaldehyde/ SAMSA fluorescein may improve LODs[5].

### 6.2.2 Development of an analytical method for the investigation of the metabolism of dynorphin A using CEC coupled to mass spectrometry

UV detection systems are the most used detection systems in both CE and CEC commercial systems. However, for peptide analysis using CE with UV detection, UV is restricted by its poor limits of detection. LIF detection is a more sensitive detection method that can also be found to be coupled to CE systems. However, peptide detection using LIF may require derivatization with a fluorescent tag. The advantage of the use of mass spectrometry (MS) in CE and CEC analysis is MS is a known to be a sensitive detection method, which can provide structural information of the

detected peptides. As mentioned previously, Dynorphins are peptides that have high pIs, making them difficult to analysis using CE. In our lab efforts are being made towards the development of CEC capillaries that are coated with the multicharged pDDA polymer and pDDA-GNPs. The coated capillary would then be connected to the electrospray ionization (ESI) interface of a Thermo Fisher LTQ XL® Linear Ion Trap Mass Spectrometer.

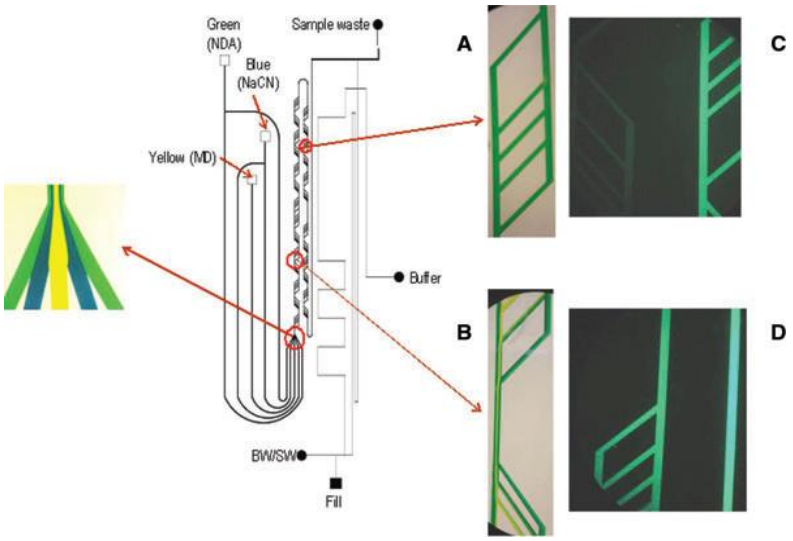


**Figure 1:** Design of on-chip derivatization microchip for amino acid analysis[2]

### 6.2.3 The development of glass microfluidic device coupled to ESI-MS for neuropeptides involved in pain signaling pathways

Several endogenous neuropeptides are relased in response to pain stimulation[6], among these neuropeptides are dynorphin A, substance P[7] and β-endorphin[8] [Table 1]. Studies of the relationship between these neuropeptides under pain stimuli or chronic pain have been reported, for example in the peripheral nervous system β-endorphin is known to inhibit the release substance

P a peptide that is associated with transmission pain[9]. A microfluidic chip "pain chip" can be fabricated in which microfluidic chip performed as the electrospray source. Ramsey's[10-11] group have reported the development of a ME-ESI-MS system for protein and peptide separation. The use of MS as the selective detection method can offer structural information of the analyte. In addition, it does not require the additional derivatization step that may be necessary for analytes that are not natively fluorescent for LIF detection. Furthermore, fluorescent tagging may complicate the development of a separation method, due to the changes in charge/size ratio of analytes after tagging. Similar to ME-ESI-MS microchip that was developed by Ramsey's group [Figure 2], a borosilicate chip would be fabricated to include a 300 μm thick electrospray tip and a single corner of a rectangular glass chip, which forms the ESI interface.

| Peptide | Structure |
|---|---|
| Dynorphin A | YGGFMTSEKSQTPLVTLFKNAIIKNAYKKGE |
| Substance P | RPKPQQFFGLM |
| β-endorphin | YGGFMTSEKSQTPLVTLFKNAIIKNAYKKGE |

**Table 1:** Structure of three neuropeptides that are involved in pain signaling.

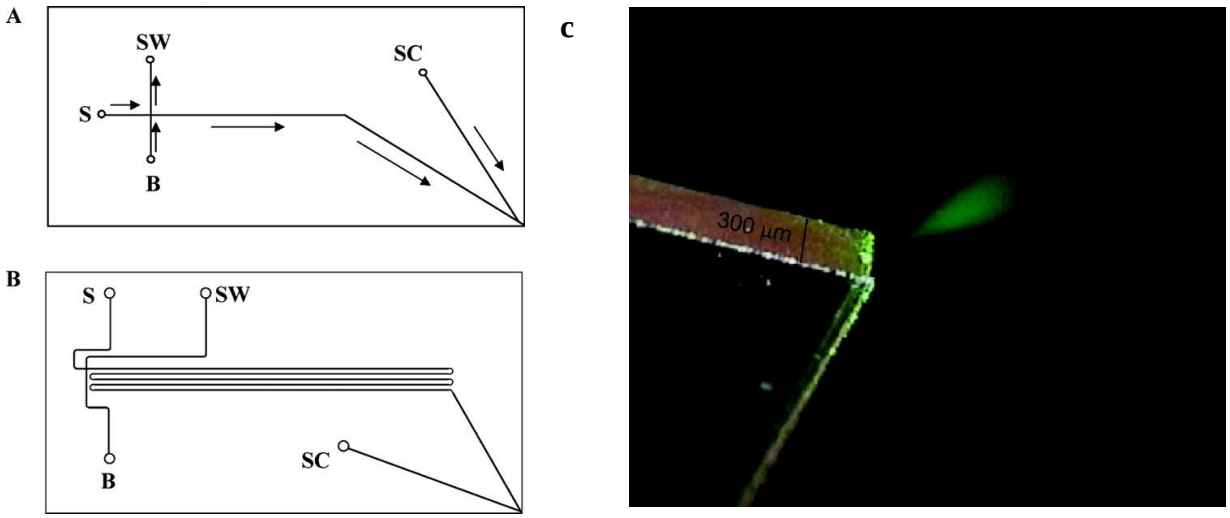


**Figure 2:** Schematic of the CE-ESI-MS chips (A) short-channel (B) long-channel (C) image of the electrospray of ME-ESI-MS[10].

## 6.3 References


1. Kuhnline, C. D.; Lunte, S. M., Evaluation of an on-capillary copper complexation methodology for the investigation of in vitro metabolism of dynorphin A 1–17. *J. Sep. Sci.* **2010,** *33* (16), 2506-2514.

2. Nandi, P.; Scott, D. E.; Desai, D.; Lunte, S. M., Development and optimization of an integrated PDMS based-microdialysis microchip electrophoresis device with on-chip derivatization for continuous monitoring of primary amines. *Electrophoresis* **2013,** *34* (6), 895-902.

3. Huynh, B. H.; Fogarty, B. A.; Martin, R. S.; Lunte, S. M., On-Line Coupling of Microdialysis Sampling with Microchip-Based Capillary Electrophoresis. *Anal. Chem.* **2004,** *76* (21), 6440-6447.

4. Huynh, B. H.; Fogarty, B. A.; Nandi, P.; Lunte, S. M., A microchip electrophoresis device with on-line microdialysis sampling and on-chip sample derivatization by naphthalene 2,3-dicarboxaldehyde/2-mercaptoethanol for amino acid and peptide analysis. *J. Pharm. Biomed. Anal.* **2006,** *42* (5), 529-534.

5. Hapuarachchi, S.; Aspinwall, C. A., Design, characterization, and utilization of a fast fluorescence derivatization reaction utilizing o-phthaldialdehyde coupled with fluorescent thiols. *Electrophoresis* **2007,** *28* (7), 1100-1106.

6. Riedel, W.; Neeck, G., Nociception, pain, and antinociception: current concepts. *Z. Rheumatol.* **2001,** *60* (6), 404-15.

7. Stewart, J. M.; Getto, C. J.; Neldner, K.; Reeve, E. B.; Krivoy, W. A.; Zimmermann, E., Substance P and analgesia. *Nature* **1976,** *262* (5571), 784-785.

8. Bach, F. W., Beta-endorphin in the brain. A role in nociception. *Acta Anaesthesiol. Scand.* **1997,** *41* (1 Pt 2), 133-40.

9. Sprouse-Blum, A. S.; Smith, G.; Sugai, D.; Parsa, F. D., Understanding Endorphins and Their Importance in Pain Management. *Hawaii Med. J.* **2010,** *69* (3), 70-71.

10. Mellors, J. S.; Gorbounov, V.; Ramsey, R. S.; Ramsey, J. M., Fully Integrated Glass Microfluidic Device for Performing High-Efficiency Capillary Electrophoresis and Electrospray Ionization Mass Spectrometry. *Anal. Chem.* **2008,** *80* (18), 6881-6887.

11. Redman, E. A.; Batz, N. G.; Mellors, J. S.; Ramsey, J. M., Integrated Microfluidic Capillary Electrophoresis-Electrospray Ionization Devices with Online MS Detection for the Separation and Characterization of Intact Monoclonal Antibody Variants. *Anal. Chem.* **2015,** *87* (4), 2264-2272.

# Appendix

## An *in situ* Study of the Effect of Dynorphin A (1-6) on the Integrity of the Blood-Brain Barrier

## A.1. Introduction:

### A.1.1 The blood-brain barrier and its function

The blood-brain barrier (BBB) is composed of brain endothelial cells that form the vascular endothelial capillary wall[1] of the BBB. The supporting structure of the BBB includes astrocytes, pericytes, and the basement membrane [Figure 1][2-4]. The main functions of the BBB are to regulate the entry of ions, macromolecules, and nutrients that are required by the CNS and protect the nervous tissues from neurotoxins[5]. The BBB acts as a physical barrier due to the presence of tight junctions (TJ) between endothelial cells that reduces the influx of harmful substances into the brain. It also acts as a metabolic barrier[6] due to the present various metabolic enzymes such as aminopeptidase A, aminopeptidase M, glutamyl aminopeptidase, endopeptidase[7] and cytochrome P-450[8] at the BBB. The transport of nutrients, cells components, and toxins across the BBB is affected by the physiological and pathological states[9-10] of the organism.

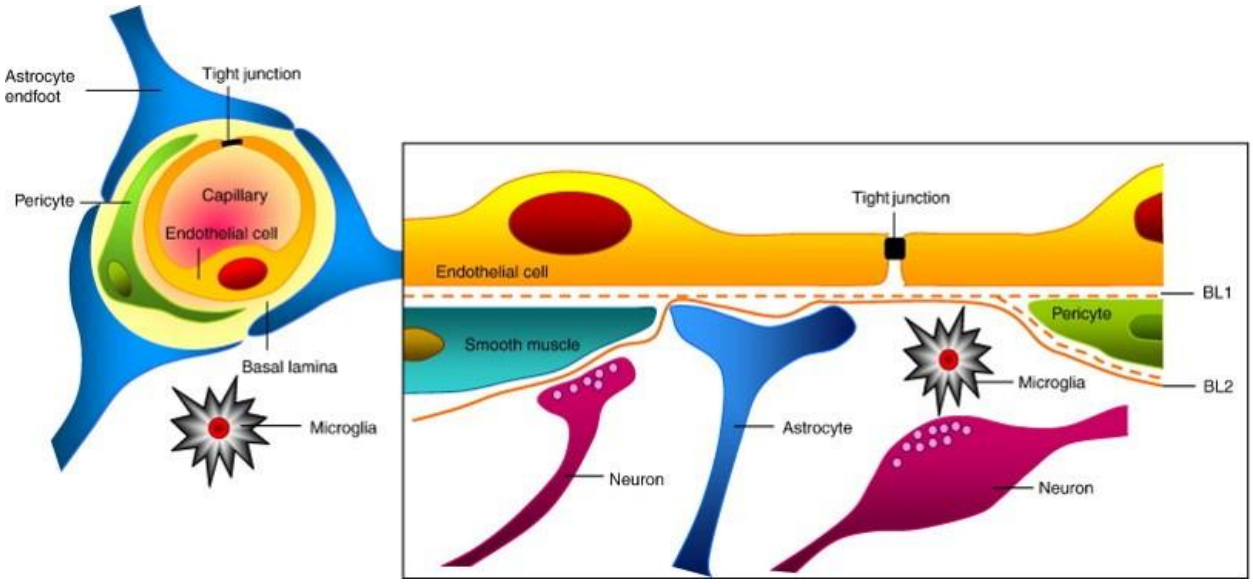


**Figure 1:** Structure of the blood brain barrier.[10] *(Reprinted with permission)*

### A.1.1.1 Transport across the BBB

The pathway that a molecule takes to cross the BBB is based on the molecule's charge, size, the degree of lipophilicity or availability of specific carriers at the luminal of the BBB for the substance. There are five basic mechanisms for the transport of molecules across the BBB. These are paracellular diffusion, transmembrane diffusion, adsorptive mediated endocytosis, receptor-mediated endocytosis and a carrier-mediated transport [Figure 2].

#### A.1.1.1.1 Paracellular diffusion

A very limited number of molecules may be transported to the brain via the paracellular pathway. Small polar molecules, such as ethanol and mannitol, can pass from the blood into the brain through openings in the TJ of the BBB endothelial cells[11]. The opening of the TJ is highly regulated by constituent proteins including occludin, claudin-5, junctional adhesion molecules, and cadherins[12]. An irregular increase in paracellular diffusion can occur due to diseases such as multiple sclerosis[13], HIV[14], and cancer[15]. In addition, the administration of drugs, such as hyperosmotic mannitol, can cause shrinkag of the endothelial cell of the BBB and opening of the TJ, that can lead to the entry of molecules into the brain by the paracellular diffusion pathway that would normally be restricted[16].

#### A.1.1.1.2 Transmembrane passive diffusion

Small molecular weight lipid soluble molecules are generally able to cross the BBB by transmembrane passive diffusion. Factors that can restrict molecules from being transported across

the BBB via transmembrane passive diffusion include, low lipophilicity, size (larger than 400-500 Da) [10, 17], affinity to plasma proteins (high-affinity plasma proteins can reduce BBB permeability)[18], and the number of hydrogen bonds (H-Bonds) that the molecule can form (the formation of more than eight H-bonds increases the free energy requirements to transfer from the polar phase to the nonpolar phase)[10, 19]. Examples of compounds that can passively diffuse across the membrane of endothelial cells of the brain are CNS drugs including fluoxetine and sertraline.

#### A.1.1.1.3 Adsorptive mediated endocytosis

This is a nonspecific mechanism of transport of molecules across the BBB. Due to the anionic nature of the cerebral endothelial cells, cationic molecules are first electrostatically adsorbed onto the cell's membrane and then undergoes endocytosis through the formation of vesicles[20] and are transported into the cell. Examples of molecules that are transported by this mechanism include arginine-containing peptides and polycationic proteins such as β-endorphin-cationized albumin complex[21].

#### A.1.1.1.4 Receptor-mediated endocytosis

Specific receptors within the brain endothelial cells can bind to ligands in the blood side and form a receptor-ligand complex[7]. This is then followed by to the formation of transport vesicles, and the complex is transported across the cell to the brain, where the ligand is then released. An example of compounds that are carried by this method includes peptides and proteins such as insulin[22] and leptin[23].

### A.1.1.1.5 Carrier-mediated transport

Essential polar molecules such as glucose[24], vitamins[25], amino acid[26], and certain peptides are all examples of ligands that are carried by structural specific carrier-mediated transporters from the blood to the brain[11]. GLUT-1[27], and (PTS)-4[28] are examples of carrier transporters for glucose and luteinizing hormone-releasing hormone respectively. Some of these specific transport systems, such as glucose or amino acid transporters, have been explored to improve drug design and enhance permeability across the BBB for poor CNS permeability drugs.[21]

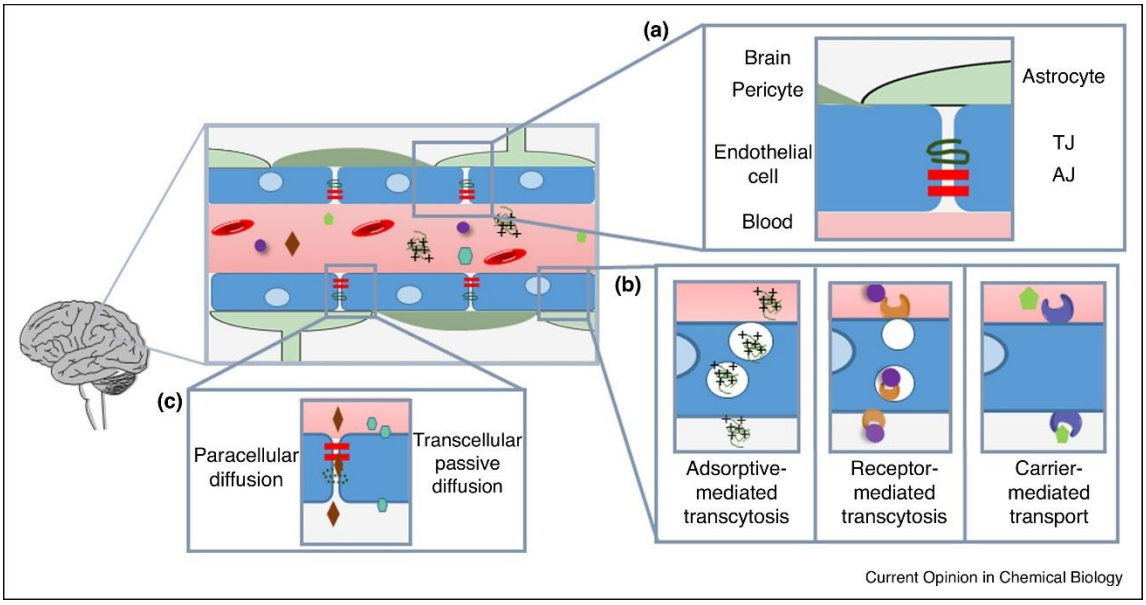


**Figure 2:** Transport pathways of molecules across the blood-brain barrier (BBB)[29]. (*Reprinted with permission*)

#### A.1.1.1.6 Methods used to study the transport of substances across the BBB

Various *in vitro* and *in vivo* experimental methods have been reported for the study of the transport of substances across the BBB and to investigate the effect of these substances on the integrity of the BBB. Examples of the application of these techniques include the study of the disturbance to BBB due to neurological diseases such as Alzheimer's disease and the investigation of CNS drugs transport mechanisms at the BBB.

##### A.1.1.1.6.1 *In vitro* methods for the study of the BBB

Some of the advantages of using *in vitro* models to study the BBB are that many of the physical characteristics and cell biological processes of the BBB, such as the presence of low pinocytic activity, and low fenestrations and presence of efflux carriers such as p-glycoprotein[30] can be found in this model. These similarities make the *in vitro* models of the BBB a convenient technique to be used as a first-pass compound screening method[11]. Several cell lines have been reported as *in vitro* models of the BBB. These include microvessels endothelial cells isolated from porcine[31], bovine[30] or human autopsy brains[32]. In addition, other cell lines, such as epithelial cells from Madin–Darby canine kidney epithelial cells[33] and BBB models generated from human pluripotent stem cells have been used[31]. Although these *in vitro* models are useful for probing the BBB, they have limitations including the isolation of the brain microvesicle cells, which can be challenging and labor-intensive and exhibit poor viability[34]. In addition, these *in vitro* models may not completely represent *in vivo* conditions due to the difference in the barrier tightness and expression of specific transporters of the BBB[32].

#### A.1.1.1.6.2 I*n vivo and in situ* methods for the study of the BBB

The intravenous injection (IV) method can be considered as the "gold standard" for BBB brain uptake studies[35] because the physiological conditions of the test animal are intact. This approach can provide the most accurate picture of the state and amount of a substance that is transported to the brain[32, 35]. Substances are administered by IV to the animal model and samples can be collected from plasma, cerebrospinal fluid (CSF) or the brain and at different time points. A limitation of the IV method is that, in most cases, it does not provide information about the specific activity of ions, hormones, peptides, and proteins on the transport of the studied substances at the BBB. This requires the performance of multiple studies with a large number of test animals. In addition, a large number of test animals may also be required to provide statistical significance due to the larger animal-to-animal variability that is mostly seen with animal models.

The *in situ* perfusion method is similar to the IV method for the investigating BBB permeability, where the *in situ* method uses the same *in vivo* structure of the BBB. However, in this method. the circulating blood of the animal is substituted with a solution that contains the study compounds dissolved within a perfusion solution. The solution's composition can also be modified and delivered directly to the brain[35-36]. The use of an *in situ* model also has the advantage of that both the studied substance and perfusion solution can be delivered to the brain at levels that are usually not tolerable *in vivo*[35]. In addition, the *in situ* perfusion method can eliminate the effect of metabolism by the liver or other organs of the studied compounds, and thus an intact compound can reach the BBB without any change in its structure due to first pass metabolism by the liver[32, 35]. However, a limitation of this method includes that it is harder to perform than IV methods[32]. Also, analogous to IV methods, a large number of animals may be required for *in situ* perfusion studies due animal-to-animal variability[11].

### A.1.1.2 Dysfunction of the BBB in disease

Several diseases have been reported to cause the dysfunction of the BBB. This can be due to downregulation of the transport of specific molecules such as glucose (Alzheimer disease)[10], reduction of the activity of P-glycoproteins in the endothelial cells at the BBB (Parkinson's disease)[37], or the disruption of the BBB tight junctions (HIV)[38-39] or breakdown of the BBB (multiple sclerosis)[38].

Various markers have been used to study the integrity of the BBB in both *in vivo* and *in vitro* models. Examples of these markers used include Evans blue[40], sodium fluorescein[41], fluorescein-labeled dextran and radiolabeled markers (sucrose, inulin or mannitol)[42]. The characteristics of an ideal marker should include that the molecule is non-toxic, metabolically stable, non-binding to tissue or plasma proteins, and easily quantifiable[43].

### A.1.2 Dynorphin A(1-6) effect in the BBMEC monolayer permeability

The study of the metabolism of dynorphin A (Dyn) by enzymes in both blood and tissues of the CNS has been reported by several research groups (see Chapter 2). Our group previously studied the transport of the peptide Dyn A(1-6) across a monolayer of bovine brain microvascular endothelial cells (BBMEC) as an *in vitro* model of the BBB[44]. The effect of preincubation of the cells with Dyn A(1-6) on the permeability of fluorescein was also studied. Fluorescein was used as a low molecular weight permeability marker to monitor the integrity of a monolayer of BBMEC. Isolated microvascular endothelial cells from gray matter of bovine brain were grown on a polycarbonate membrane and placed in a Side-by-Side® diffusion chamber [Figure 3]. For

transport studies of Dyn A(1-6), the peptide was added at the donor side, and at different time points, aliquots were taken from the receiver side. Once the transport studies were completed, fluorescein was added to the donor side, and aliquots were collected from the receiver side at different time points to assess the permeability of BBMECs.

In these studies, Dyn A(1-6) was found to permeate at the BBMECs layer in both apical-to-basolateral and basolateral-to-apical directions (37 ℃). It also showed reduced permeation at a low temperature (4 ℃) [Figure 4A] suggesting the transport of the peptide is by a carrier-mediated transport system[44]. Also, preincubation of Dyn A(1-6) with the BBMECs led to an increase of the transport of fluorescein across the monolayers (37 ℃) and a lower level of fluorescein transport was observed at the lower temperature (4 ℃) [Figure 4B]. These findings were similar to those reported by Thompson et.al. concerning the transport of fluorescein, $^{14}$C-sucrose or $^{3}$H-mannitol across the BBMEC due to the effect of [Leu]-enkephalin (Leu-ENK). They also reported the effect of the transport of $^{14}$C-sucrose at the BBMEC was lowered by the presence of the opioid receptor antagonist naloxone with Leu-ENK, indicating that effect of the peptide may be due to activation of opioid receptors (μ or δ)[45-46].

Dyn A(1-6) has an affinity to all three of the known opioid receptors (μ, δ, and κ) and may cause the opening of the BBB by activation of these receptors. Dyn A(1-6) YGGFLR shares structural similarities to Leu-ENK (YGGFL), Thompson et.al hypothesized that the enhancement in the permeability of low molecular weight molecules is possibly due to an alteration of the TJ or due to the formation of small pores in the monolayer of BBMEC or both. This may be similar to how Dyn A(1-6) causes an enhancement of the permeability of fluorescein seen with the *in vitro* studies of the peptide. It is also possible that Dyn A (1-6) not only affects the permeability of low molecular weight molecules at the BBB, but it may also play a role in increasing the permeability

of the parent peptide Dyn A(1-17) or other harmful substances into the CNS. These findings lead us to further investigate the effect of Dyn A(1-6) on BBB using Sprague-Dawley® (SD) rats as *in situ* animal model.

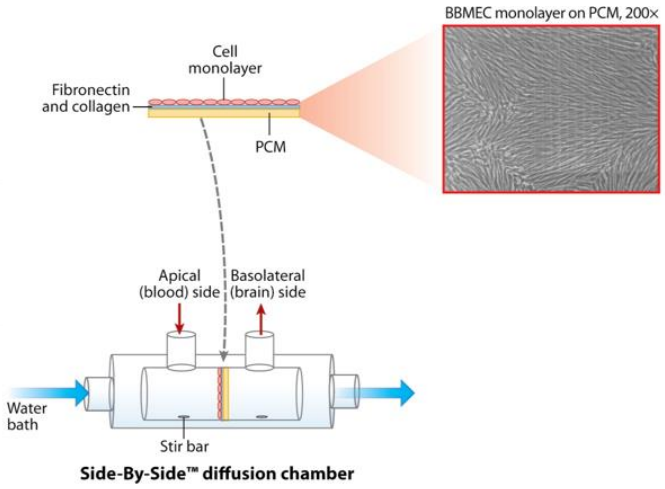


**Figure 3:** Side-by-Side® diffusion chamber used for monitoring *in-vitro* transport across the BBMECs[11]. *(Reprinted with permission)*

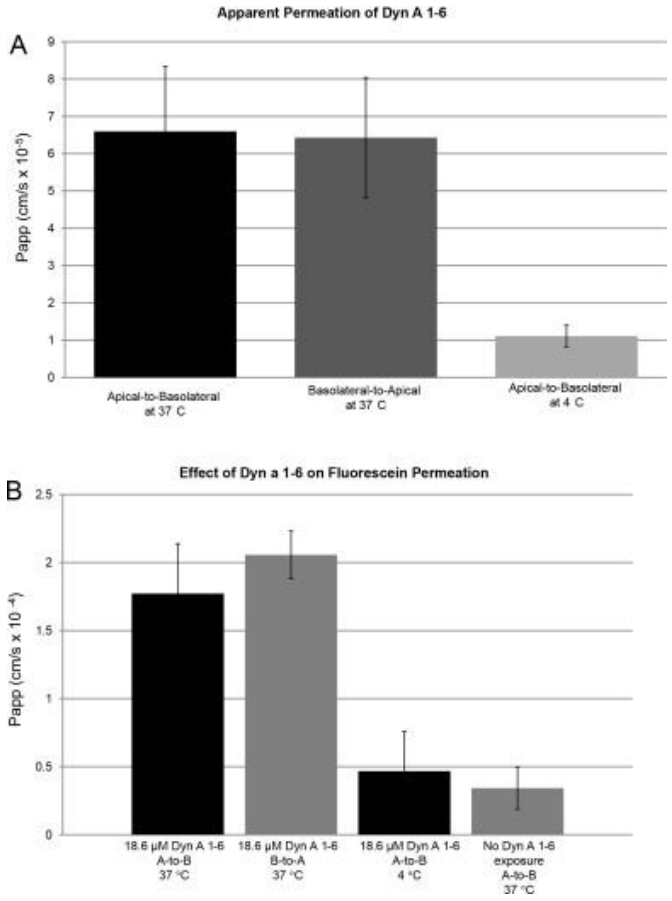


**Figure 4:** A) Bi-directional apparent permeability coefficients ($P_{app}$) of Dyn A(1–6) and the temperature dependence of the A-to-B transport of Dyn A(1–6). (B) Effect of pretreatment with Dyn A(1–6) on the BBB permeability of fluorescein[44]. *(Reprinted with permission)*

## A.2 Materials and methods

### A.2.1 Peptide and buffer saline solutions

Dyn A(1-6) (Shanghai MoCell Biotech; Shanghai, China), or scrambled peptide (GLYRFG) (Shanghai MoCell Biotech; Shanghai, China) with DMSO were each dissolved in a

bicarbonate buffer physiological saline containing 0.5% v/v tween 20. The bicarbonate-buffer physiological saline was prepared with NaCl (142 mmol/L), $NaHCO_3$ (28 mmol/L), $KH_2PO_4$ (4.2 mmol/L), $CaSO_4$ (1.7 mmol/L), $MgSO_4$ (1 mmol/L) and D-glucose (6 mmol/L). The solution was filtered through a sterile 0.2 μm cellulose nitrate filter (Nalgene®) and incubated with 5% $CO_2$ in 95% humidity before the experiment at 37°C. Radiolabeled $^{14}$C-mannitol (Moravek Biochemicals Inc; Brea, CA) was dissolved within the perfusion bicarbonate-buffered physiological saline solution, to be then used as the permeability marker.

### A.2.2 *In situ* rat brain perfusion

A modification of the *in situ* brain perfusion technique developed by Y. Takasato[36] was performed to study the effect of Dyn A(1-6) on the integrity of the BBB. Briefly, the animal surgeries were conducted on two groups of male SD rats (weight 250-350 g). All animal experiments were carried out in accordance with regulations of the Institutional Animal Care and Use Committee (IACUC) at the University of Kansas. Each rat used in the perfusion experiments was initially anesthetized by IP administration of 100 mg/kg ketamine and 5 mg/kg xylazine and a heat lamp was used to maintain the animals body temperature. This was followed by insertion of a cannula into the left common carotid artery (LCCA) with a polyethylene catheter (PE-50) containing heparinized saline (100 I.U./mL) and then following ligation of the external branches of the artery using surgical thread. This was then followed by cardiac puncture under anesthesia and immediately after was then followed by 20s pre-perfusion with perfusion solutions.

Rats were perfused with 10 mL of either a perfusion solution (control solution) or peptide dissolved in the perfusion solution (peptide solution), which was then followed by perfusion of a

solution of $^{14}$C-mannitol, followed by a 5 s post-perfusion wash with saline. Finally, while still under anesthesia the procedure was terminated by decapitation of the animal and the brain tissue was harvested.

## A.3 Results and discussion

### A.3.1 Comparison of the effect of dynorphin A 1-6 to control

The activity of the peptide Dyn A(1-6) regarding the opening of the blood-brain barrier was investigated. Two different concentrations of Dyn A (1-6) 0.75 mM (n=3) and 1.0 mM (n= 3) were compared to the control (n=5). The results show an effect of the Dyn A(1-6) on the permeability of $^{14}$C-mannitol compared to the control [Figure 5]. However, there was no statistically significant difference between all the groups (p-value > 0.05). This is most likely due to the animal-to-animal variability as well as the relatively small sample size (n=3) used for each of the peptide groups.

### A.3.2 Comparison of the effect of dynorphin A (1-6) to a scrambled peptide on BBB transport

The effect of the scrambled peptide (GLYRFG) on the permeability of $^{14}$C-mannitol at the BBB was also investigated. It was hypothesized that this peptide would not open the BBB due to weak binding to opioid receptors. A concentration of 0.75 mM of the scrambled peptide perfusion solution containing 0.17% v/v DMSO was prepared. DMSO was added due to the perfusion solution because of the low solubility of the peptide GLYRFG in the bicarbonate buffer saline solution. The control solution was made using the same volume of DMSO added to the perfusion

solution. Figure 6 shows a comparison of the effect of the scrambled peptide (n= 3) to its control (n= 1) within the same day. The scrambled peptide did not show an increase in permeability of $^{14}$C-mannitol compared to its control.

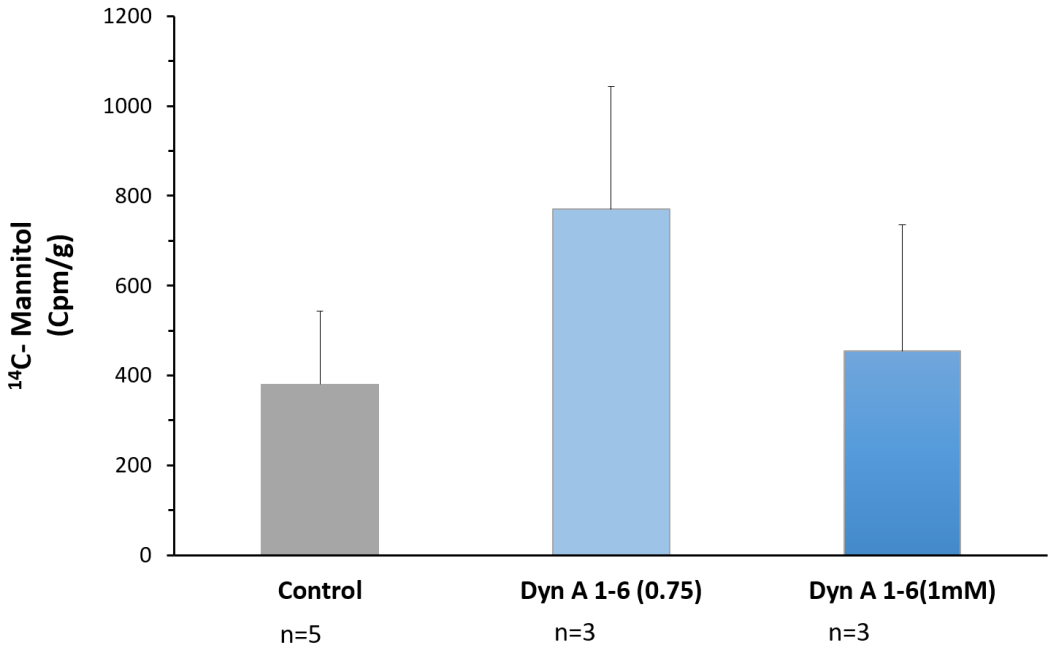


**Figure 5:** Comparison of the effect of the dynorphin A(1-6) on the BBB permeability of $^{14}$C-mannitol (p-value > 0.05).

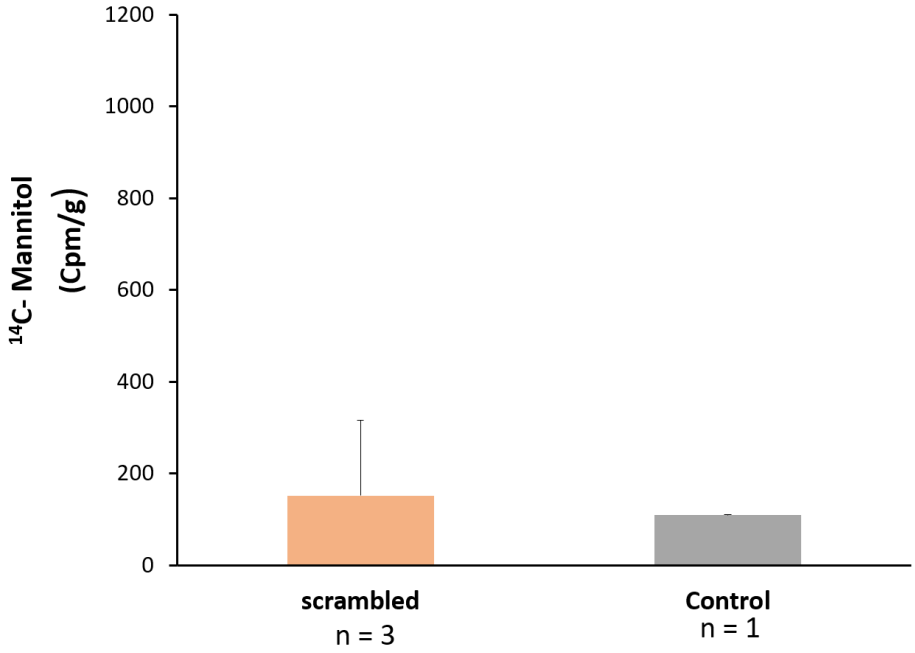


**Figure 6**: Comparison of the effect of the scrambled peptide (GLYRFG) vs. control on the permeability of $^{14}$C-mannitol.

## A.4 Conclusions

The result of *in situ* perfusion study indicate that the neuropeptide Dyn A(1-6) has activity at the BBB. Although the results of the *in situ* perfusion study are not statistically significant, there is a trend of the effect of the neuropeptide on the BBB. We believe, based on previous *in vitro* experimental results performed by our lab, and the *in situ* rat experiments carried out on SD rats, that the peptide may activate opioid receptors. The activation of opioid receptors leads to the enhancement of the transport of low molecular weight permeability markers that may be due to the opening the TJ of the brain endothelial cells, an increase in the formation of small pores at the BBB, or combination of both permeation pathways. A larger sample size is needed to confirm the initial *in situ* perfusion study results and then to determine the mechanism responsible for increasing the BBB permeability by the neuropeptide.

## A.5 Reference


1. Zheng, K.; Trivedi, M.; Siahaan, T. J., Structure and function of the intercellular junctions: barrier of paracellular drug delivery. *Curr. Pharm. Des.* **2006,** *12* (22), 2813-24.

2. Abbott, N. J.; Friedman, A., Overview and introduction: the blood-brain barrier in health and disease. *Epilepsia* **2012,** *53 Suppl 6*, 1-6.

3. Abbott, N. J.; Rönnbäck, L.; Hansson, E., Astrocyte-endothelial interactions at the blood-brain barrier. *Nature Reviews Neuroscience* **2006,** *7* (1), 41-53.

4. Schmitt, G.; Parrott, N.; Prinssen, E.; Barrow, P., The great barrier belief: The blood–brain barrier and considerations for juvenile toxicity studies. *Reprod. Toxicol.*

5. Persidsky, Y.; Ramirez, S. H.; Haorah, J.; Kanmogne, G. D., Blood–brain barrier: structural components and function under physiologic and pathologic conditions. *J. Neuroimmune Pharmacol.* **2006,** *1* (3), 223-236.

6. Pardridge, W. M., Transport of small molecules through the blood-brain barrier: biology and methodology. *Adv. Drug Del. Rev.* **1995,** *15* (1), 5-36.

7. Davis, T. P.; Abbruscato, T. J.; Egleton, R. D., Peptides at the blood brain barrier: Knowing me knowing you. *Peptides* **2015,** *72*, 50-56.

8. Laksitorini, M. D.; Kiptoo, P. K.; On, N. H.; Thliveris, J. A.; Miller, D. W.; Siahaan, T. J., Modulation of Intercellular Junctions by Cyclic-ADT Peptides as a Method to Reversibly Increase Blood-Brain Barrier Permeability. *J. Pharm. Sci.* **2015,** *104* (3), 1065-1075.

9. Abbott, N. J., Astrocyte-endothelial interactions and blood-brain barrier permeability. *J. Anat.* **2002,** *200* (6), 629-38.

10. Abbott, N. J.; Patabendige, A. A.; Dolman, D. E.; Yusof, S. R.; Begley, D. J., Structure and function of the blood–brain barrier. *Neurobiol. Dis.* **2010,** *37* (1), 13-25.

11. Kuhnline Sloan, C. D.; Nandi, P.; Linz, T. H.; Aldrich, J. V.; Audus, K. L.; Lunte, S. M., Analytical and biological methods for probing the blood-brain barrier. *Annu. Rev. Anal. Chem. (Palo Alto Calif.)* **2012,** *5*, 505-31.

12. Sandoval, K. E.; Witt, K. A., Blood-brain barrier tight junction permeability and ischemic stroke. *Neurobiol. Dis.* **2008,** *32* (2), 200-219.

13. Minagar, A.; Alexander, J. S., Blood-brain barrier disruption in multiple sclerosis. *Mult. Scler.* **2003,** *9* (6), 540-9.

14. Buckner, C. M.; Luers, A. J.; Calderon, T. M.; Eugenin, E. A.; Berman, J. W., Neuroimmunity and the Blood–Brain Barrier: Molecular Regulation of Leukocyte Transmigration and Viral Entry into the Nervous System with a Focus on NeuroAIDS. *J. Neuroimmune Pharmacol.* **2006,** *1* (2), 160-181.

15. Martin, T. A.; Jiang, W. G., Loss of tight junction barrier function and its role in cancer metastasis. *Biochim. Biophys. Acta* **2009,** *1788* (4), 872-891.

16. Stamatovic, S. M.; Keep, R. F.; Andjelkovic, A. V., Brain Endothelial Cell-Cell Junctions: How to "Open" the Blood Brain Barrier. *Curr. Neuropharmacol.* **2008,** *6* (3), 179-192.

17. Pardridge, W. M., The Blood-Brain Barrier: Bottleneck in Brain Drug Development. *NeuroRx* **2005,** *2* (1), 3-14.

18. Tanaka, H.; Mizojiri, K., Drug-Protein Binding and Blood-Brain Barrier Permeability. *J. Pharmacol. Exp. Ther.* **1999,** *288* (3), 912-918.

19. Pardridge, W. M., Drug transport across the blood–brain barrier. *J. Cereb. Blood Flow Metab.* **2012,** *32* (11), 1959-1972.

20. Hervé, F.; Ghinea, N.; Scherrmann, J.-M., CNS Delivery Via Adsorptive Transcytosis. *The AAPS Journal* **2008,** *10* (3), 455-472.

21. Tsuji, A.; Tamai, I., Carrier-mediated or specialized transport of drugs across the blood–brain barrier. *Adv. Drug Del. Rev.* **1999,** *36* (2), 277-290.

22. Banks, W. A.; Jaspan, J. B.; Huang, W.; Kastin, A. J., Transport of Insulin Across the Blood-Brain Barrier: Saturability at Euglycemic Doses of Insulin. *Peptides* **1997,** *18* (9), 1423-1429.

23. Jones, A. R.; Shusta, E. V., Blood-Brain Barrier Transport of Therapeutics via Receptor-Mediation. *Pharm. Res.* **2007,** *24* (9), 1759-1771.

24. McAllister, M. S.; Krizanac-Bengez, L.; Macchia, F.; Naftalin, R. J.; Pedley, K. C.; Mayberg, M. R.; Marroni, M.; Leaman, S.; Stanness, K. A.; Janigro, D., Mechanisms of glucose transport at the blood-brain barrier: an in vitro study. *Brain Res.* **2001,** *904* (1), 20-30.

25. Spector, R.; Johanson, C. E., REVIEW: Vitamin transport and homeostasis in mammalian brain: focus on Vitamins B and E. *J. Neurochem.* **2007,** *103* (2), 425-438.

26. Gardiner, R. M., Transport of amino acids across the blood-brain barrier: implications for treatment of maternal phenylketonuria. *J. Inherit. Metab. Dis.* **1990,** *13* (4), 627-33.

27. Deng, D.; Xu, C.; Sun, P.; Wu, J.; Yan, C.; Hu, M.; Yan, N., Crystal structure of the human glucose transporter GLUT1. *Nature* **2014,** *510* (7503), 121-125.

28. Brasnjevic, I.; Steinbusch, H. W. M.; Schmitz, C.; Martinez-Martinez, P., Delivery of peptide and protein drugs over the blood–brain barrier. *Prog. Neurobiol.* **2009,** *87* (4), 212-251.

29. Sánchez-Navarro, M.; Giralt, E.; Teixidó, M., Blood–brain barrier peptide shuttles. *Curr. Opin. Chem. Biol.* **2017,** *38*, 134-140.

30. Audus, K. L.; Borchardt, R. T., Bovine brain microvessel endothelial cell monolayers as a model system for the blood-brain barrier. *Ann. N. Y. Acad. Sci.* **1987,** *507*, 9-18.

31. Helms, H. C.; Abbott, N. J.; Burek, M.; Cecchelli, R.; Couraud, P. O.; Deli, M. A.; Forster, C.; Galla, H. J.; Romero, I. A.; Shusta, E. V.; Stebbins, M. J.; Vandenhaute, E.; Weksler, B.; Brodin, B., In vitro models of the blood-brain barrier: An overview of commonly used brain endothelial cell culture models and guidelines for their use. *J. Cereb. Blood Flow Metab.* **2016,** *36* (5), 862-90.

32. Bickel, U., How to measure drug transport across the blood-brain barrier. *NeuroRx* **2005,** *2* (1), 15-26.

33. He, Y.; Yao, Y.; Tsirka, S. E.; Cao, Y., Cell-Culture Models of the Blood–Brain Barrier. *Stroke; a journal of cerebral circulation* **2014,** *45* (8), 2514-2526.

34. Ruck, T.; Bittner, S.; Meuth, S. G., Blood-brain barrier modeling: challenges and perspectives. *Neural Regeneration Research* **2015,** *10* (6), 889-891.

35. Smith, Q. R., A Review of Blood-Brain Barrier Transport Techniques. In *The Blood-Brain Barrier: Biology and Research Protocols*, Nag, S., Ed. Humana Press: Totowa, NJ, 2003; pp 193-208.

36. Takasato, Y.; Rapoport, S. I.; Smith, Q. R., An in situ brain perfusion technique to study cerebrovascular transport in the rat. *American Journal of Physiology - Heart and Circulatory Physiology* **1984,** *247* (3), H484-H493.

37. Bartels, A. L.; Willemsen, A. T.; Kortekaas, R.; de Jong, B. M.; de Vries, R.; de Klerk, O.; van Oostrom, J. C.; Portman, A.; Leenders, K. L., Decreased blood-brain barrier P-glycoprotein function in the progression of Parkinson's disease, PSP and MSA. *J Neural Transm (Vienna)* **2008,** *115* (7), 1001-9.

38. Weiss, N.; Miller, F.; Cazaubon, S.; Couraud, P.-O., The blood-brain barrier in brain homeostasis and neurological diseases. *Biochim. Biophys. Acta* **2009,** *1788* (4), 842-857.

39. Ivey, N. S.; MacLean, A. G.; Lackner, A. A., AIDS and the blood-brain barrier. *J. Neurovirol.* **2009,** *15* (2), 111-122.

40. Morrey, J. D.; Olsen, A. L.; Siddharthan, V.; Motter, N. E.; Wang, H.; Taro, B. S.; Chen, D.; Ruffner, D.; Hall, J. O., Increased blood-brain barrier permeability is not a primary determinant for lethality of West Nile virus infection in rodents. *J. Gen. Virol.* **2008,** *89* (Pt 2), 467-73.

41. Kaya, M.; Ahishali, B., Assessment of permeability in barrier type of endothelium in brain using tracers: Evans blue, sodium fluorescein, and horseradish peroxidase. *Methods Mol. Biol.* **2011,** *763*, 369-82.

42. Ziylan, Y. Z.; Robinson, P. J.; Rapoport, S. I., Differential blood-brain barrier permeabilities to [14C]sucrose and [3H]inulin after osmotic opening in the rat. *Exp. Neurol.* **1983,** *79* (3), 845-57.

43. Saunders, N. R.; Dziegielewska, K. M.; Mollgard, K.; Habgood, M. D., Markers for blood-brain barrier integrity: how appropriate is Evans blue in the twenty-first century and what are the alternatives? *Front. Neurosci.* **2015,** *9*, 385.

44. Sloan, C. D. K.; Audus, K. L.; Aldrich, J. V.; Lunte, S. M., The permeation of dynorphin A 1–6 across the blood brain barrier and its effect on bovine brain microvessel endothelial cell monolayer permeability. *Peptides* **2012,** *38* (2), 414-417.

45. Thompson, S. E.; Audus, K. L., Leucine enkephalin effects on brain microvessel endothelial cell monolayer permeability. *Pharm. Res.* **1994,** *11* (9), 1366-9.

46. Thompson, S. E.; Cavitt, J.; Audus, K. L., Leucine enkephalin effects on paracellular and transcellular permeation pathways across brain microvessel endothelial cell monolayers. *J. Cardiovasc. Pharmacol.* **1994,** *24* (5), 818-25.